12-2011

Identification and Behavior of Collapsible Soils

Alain El Howayek
Purdue University, ahowayek@purdue.edu

Pao-Tsung Huang
Purdue University, huang69@purdue.edu

Rachael Bisnett
Purdue University, rbisnett@gmail.com

Maria C. Santagata
Purdue University, mks@purdue.edu

JOINT TRANSPORTATION RESEARCH PROGRAM

INDIANA DEPARTMENT OF TRANSPORTATION
AND PURDUE UNIVERSITY

IDENTIFICATION AND BEHAVIOR OF COLLAPSIBLE SOILS

Alain El Howayek
Graduate Research Assistant
School of Civil Engineering
Purdue University

Pao-Tsung Huang
Graduate Research Assistant
School of Civil Engineering
Purdue University

Rachael Bisnett
Graduate Research Assistant
School of Civil Engineering
Purdue University

Maria Caterina Santagata
Associate Professor of Civil Engineering
Purdue University
Corresponding Author

SPR-3109
Report Number: FHWA/IN/JTRP-2011/12
DOI: 10.5703/1288284314625

This page intentionally left blank.

RECOMMENDED CITATION

Howayek, A. E., P. T. Huang, R. Bisnett, and M. C. Santagata. *Identification and Behavior of Collapsible Soils*. Publication FHWA/IN/JTRP-2011/12. Joint Transportation Research Program, Indiana Department of Transportation and Purdue University, West Lafayette, Indiana, 2011. doi: 10.5703/1288284314625

CORRESPONDING AUTHOR

Professor Maria Caterina Santagata
School of Civil Engineering
Purdue University
(765) 494-0697
mks@purdue.edu

JOINT TRANSPORTATION RESEARCH PROGRAM

The Joint Transportation Research Program serves as a vehicle for INDOT collaboration with higher education institutions and industry in Indiana to facilitate innovation that results in continuous improvement in the planning, design, construction, operation, management and economic efficiency of the Indiana transportation infrastructure.
https://engineering.purdue.edu/JTRP/index_html

Published reports of the Joint Transportation Research Program are available at: http://docs.lib.purdue.edu/jtrp/

NOTICE

This page intentionally left blank.

TECHNICAL REPORT STANDARD TITLE PAGE

1. Report No.	2. Government Accession No.	3. Recipient's Catalog No.
FHWA/IN/JTRP-2011/12		

4. Title and Subtitle	5. Report Date
Identification and Behavior of Collapsible Soils	2011
	6. Performing Organization Code

7. Author(s)	8. Performing Organization Report No.
Alain El Howayek, Pao-Tsung Huang, Rachael Bisnett, Maria Caterina Santagata	

9. Performing Organization Name and Address	10. Work Unit No.
Joint Transportation Research Program Purdue University 550 Stadium Mall Drive West Lafayette, IN 47907-2051	
	11. Contract or Grant No. SPR-3109

12. Sponsoring Agency Name and Address	13. Type of Report and Period Covered
Indiana Department of Transportation State Office Building 100 North Senate Avenue Indianapolis, IN 46204	
	14. Sponsoring Agency Code

15. Supplementary Notes

Prepared in cooperation with the Indiana Department of Transportation and Federal Highway Administration.

16. Abstract

.

Loess is a soil that can exhibit large deformations upon wetting. Cases of wetting induced collapse in loess have been documented for natural deposits and man-made fills. These issues are of concern to the Indiana DOT due to the growth of the state's infrastructure in regions with significant loess deposits.

The research reviewed the existing literature on loess, focusing on index properties, structure, mineralogy, criteria used for quantifying collapsibility, methods for measuring collapse potential, and, in particular, the collapsibility of compacted loess. Additionally, available documentation on loess deposits in Indiana was reviewed and summarized.

This research also included experimental work conducted on two loess samples, obtained in one in Daviess (Soil A) and in Tippecanoe (Soil B) county. The soils have similar characteristics, with close to 70% silt content and plasticity characteristics that classify both of them as CL (USCS) and A-6 (AASHTO).

Experiments performed on the two soils included index tests, standard Proctor compaction tests, and an extensive program of double odeometer tests to measure the wetting induced strains as a function of stress level. Specimens of soils A and B were compacted over a wide range of values of relative compaction (from 75% to close to optimum) and of water contents (from 5-6% points dry of optimum to optimum). The collapse potential of each specimen was quantified using the ASTM D5333 criterion. All specimens but one (compacted at close to optimum conditions) showed some wetting induced collapse. The collapse strains increased with decreasing relative compaction and decreasing compaction water content, in some cases exceeding 10%. In some tests significant wetting induced strains were measured under relatively small stresses (50-100 kPa), indicating that this problem may require consideration even for small fill heights.

The results of the experiments were compared to literature data for other soils, and overall found to be consistent with previously reported behavioral trends. Based on the results of the testing, recommendations are made for field compaction specifications.

17. Key Words	18. Distribution Statement
Loess, collapsibility, double oedometer, collapse potential, wetting	No restrictions. This document is available to the public through the National Technical Information Service, Springfield, VA 22161

19. Security Classif. (of this report)	20. Security Classif. (of this page)	21. No. of Pages	22. Price
Unclassified	Unclassified		

Form DOT F 1700.7 (8-69)

This page intentionally left blank.

CONTENTS

LIST OF TABLES

LIST OF FIGURES

EXECUTIVE SUMMARY

IDENTIFICATION AND BEHAVIOR OF COLLAPSIBLE SOILS

Introduction

Collapsible soils are soils susceptible to large volumetric strains when they become saturated. Numerous soil types fall in the general category of collapsible soils, including loess, a well-known aeolian deposit, present throughout most of Indiana. Loess is characterized by relatively low density and cohesion, appreciable strength and stiffness in the dry state, but is susceptible to significant deformations as a result of wetting.

Cases of wetting induced collapse in loess type soils have been documented in natural deposits and in man-made fills. In the latter case they can often cause large differential settlements that reduce the serviceability of the structure, and raise the frequency and cost of rehabilitation. These issues are especially of concern to the Indiana DOT due to the growth of the infrastructure in regions with significant loess deposits. This was the motivation for the research presented in this report.

The research reviewed the existing literature on: loess, on criteria used for quantifying the degree of collapsibility, on methods for measuring collapse potential in the laboratory and in the field, and on the collapsibility of compacted soils Additionally, available documentation on loess deposits in Indiana was summarized.

This research also included experimental work conducted on two natural loess samples: one (Soil A) obtained in Daviess county, an area of Indiana overlain by medium to thick natural loess deposits, and one (Soil B) from Tippecanoe county. The two soils have similar characteristics, with close to 70% silt content and plasticity characteristics that classify both of them as CL (USCS) and A-2-6 (AASHTO).

Experiments performed on the two soils included index tests (particle size analysis, Atterberg limits and specific gravity determination), standard Proctor compaction tests, and an extensive program of double odeometer tests to measure the wetting induced collapse strains as a function of stress level (12.5 kPa to 2760 kPa). Specimens of soils A and B were compacted over a wide range of values of relative compaction (from 75% to close to optimum) and of water contents (from 5–6% points dry of optimum to optimum). The collapse potential was quantified using the criterion in ASTM D5533, which uses the collapse index I_e, the collapse strain measured under a stress of 200 kPa. This criterion allows for distinction between severe, moderately severe, moderate, slight and no degree of collapsibility.

Findings

Loess deposits are common throughout Indiana and based on the existing literature concerns on the use of these materials in compacted fills and embankments were legitimate given the lack of data prior to this study on the wetting induced collapse of compacted loess.

The experimental work conducted as part of this research has demonstrated that if relative compaction and compaction water content are not appropriately controlled, subsequent wetting can cause significant collapse strains. For the soils and compaction conditions tested in this research the degree of collapsibility was found in all but one of the specimens to vary from slight ($I_e<1\%$) to severe ($I_e>11\%$). The collapse was found to increase with decreasing relative compaction, compaction water content and degree of saturation. Significant wetting induced strains were observed even for specimens compacted around 90% RC, in the case of water contents significantly on the dry side of optimum.

While the collapse strains were typically observed to decrease with stress level, in some cases significant collapse strains were observed at relatively low stresses (25–100 kPa), indicating that wetting induced collapse may require consideration even for small fill thicknesses.

For the soils examined in this research elimination of wetting induced collapse required compaction to over 100% RC. Based on this result it is suggested that a minimum relative compaction of 105% be specified for the compaction of loess in the field.

Compaction on the wet side of optimum eliminates the issue of wetting induced collapse. However, the collapsibility of the soil is very sensitive to small reductions in compaction water content. It is suggested that compaction specifications for loess do not allow for compaction at water contents lower than w_{opt}-1.5%.

While the behavioral trends observed in this study are generally consistent with the data presented in the literature, the measured values of the collapse strains exceed previous data for Indiana loess.

Existing criteria for estimating collapse potential do not completely capture the collapse behavior of the soils examined in this research. They may be used to gain an initial assessment of the degree of collapsibility of a soil but cannot be considered a substitute for laboratory determination of the collapse potential. For this purpose the double oedometer test has been found to be an effective method for measuring the collapse potential of compacted soils, and it is recommended that a battery of such tests be required whenever a loess soil is being considered for use in a fill or embankment.

Implementation

The research performed has reviewed the existing literature on loess soils; has examined existing criteria for estimating the degree of collapsibility of soils, and currently employed methods used for measuring the collapse potential in the laboratory; has highlighted the significance of loess deposits in Indiana; has developed a data base on the collapse properties of two soils representative of typical loess deposits in Indiana, that may be used as a starting point when evaluating a similar soil as a candidate material for a fill or embankment; has drawn conclusions on compaction conditions that reduce or eliminate problems of wetting induced collapse; has provided suggestions for compaction specification to be used for these soils and for laboratory methods to be use in evaluating the collapse potential of a given soil.

These suggestions can find immediate implementation in INDOT practice and specifications. Further evaluation on a broader range of soils is recommended.

CHAPTER 1 INTRODUCTION

1.1 Problem Statement

"Large areas of the Earth's surface, particularly in the Midwest and Southwest United States, parts of Asia, South America, and Southern Africa, are covered by soils that are susceptible to large decreases in bulk volume when they become saturated. Such materials are termed ***collapsible soils****" (Mitchell and Soga 2005).*

Collapsible soils are generally associated with an open structure formed by sharp grains, low initial density, low natural water content, low plasticity, relatively high stiffness and strength in the dry state, and often by particle size in the silt to fine sand range (Mitchell and Soga 2005). As their name indicates these soils can exhibit a large volume change upon wetting, with or without extra loading, thus posing ***significant challenges to the geotechnical profession.*** Numerous soil types can fall in the general category of collapsible soils, including aeolian deposits, alluvial deposits, colluvial deposits, residual deposits, and volcanic tuff. A well-known aeolian deposit, known to often exhibit collapsing behavior, is loess, a yellow to reddish brown silt size soil, which is characterized by relatively low density and cohesion, but appreciable strength and stiffness in the dry state. Aeolian deposits with significant tendency to collapse are often found in arid regions where the water table is low. However, even in environments with medium rainfall, such as the Midwestern United States, fine aeolian deposits can still present high collapsible potential (Clemence and Finbarr 1981), particularly if an impermeable surface crust has protected them from water infiltration.

In view of the above, collapsible soils can be considered a critical issue for construction in Indiana, particularly as the infrastructure network within the state continues to grow, as is forecasted for the next 10–15 years. For example, the extension of Highway I-69 from Indianapolis to Evansville, crosses along its alignment regions characterized by significant loess deposits. In these areas loess deposits are likely to often be several meters thick (and possibly a few tens of meters locally).

Collapsible soils are characterized by very distinct geotechnical properties that include high void ratio, low initial bulk density and water content, great dry strength and stiffness, high percentage of fine grained particles and zero or slight plasticity. In most cases they contain over 60% of fines and have a porosity of 50% to 60%, liquid limit of about 25 and plastic limit ranging from 0 to 10.

As mentioned above, the main geotechnical problem associated with these soils is the significant loss of shear strength and volume reduction occurring when they are subjected to additional water from rainfall, irrigation, broken water or sewer lines, moisture increase due to capillarity or "pumping" as a result of traffic loading, ground water rise, etc. Generally, collapsible soils are under unsaturated conditions in the dry state, with negative pore pressure resulting in higher effective stresses and greater shear strength. Additionally, cementing agents such as $CaCO_3$ can also contribute to maintaining an open "honeycombed" structure. Upon wetting, the pore pressure become less negative and the effective stresses are reduced causing a decrease in shear strength. Additionally, the water can dissolve or soften the bonds between the particles, allowing them to take a denser packing.

This mechanism, referred to as wetting-induced collapse, or hydrocompression, can take place with or without extra loading.

Pereira et al. (2000) summarize the factors that produce collapse as follows: "*1) an open, partially unstable, unsaturated fabric, 2) a high enough net total stress that will cause the structure to be metastable, 3) a bonding or cementing agent that stabilizes the soil in the unsaturated condition, and 4) the addition of water to the soil, which causes the bonding or cementing agent to be reduced and the interaggregate or intergranular contacts to fail in shear, resulting in reduction in total volume of the soil mass.*"

Collapsible soils present significant challenges to the engineering profession during construction, during the service life and, to a lesser degree, during design. Numerous case histories pertaining to the problems caused by collapsible soils have been reported in the literature (see more on this point in Chapter 2). Since the mid 1950's cases of collapse in loess have been documented extensively in the United States (e.g. Peck and Ireland (1958), Holtz and Hilf (1961)) as well as around the world.

In addition to the problems posed to buildings and embankments, challenges related primarily to differential settlements are encountered also in the construction of roads on collapsible soils. Differential collapse settlement across roadway sections comes from two major factors: non-homogenous subgrades that encompass materials with different degree of collapse potential, and non-uniform distribution of wetting in subgrades materials (Houston et al. 2002). Often the latter can be originated by upward "pumping" of the water as a result of traffic loading. In loess this effect is enhanced by the fact that, unlike what is observed for most other geomaterials, the hydraulic conductivity in the vertical direction exceeds the value in the horizontal direction.

Differential settlements cause a rough and bumpy surface; reduce the serviceability, and raise the frequency and cost of rehabilitation.

Preventing the problems induced by collapsible soils requires consideration of the following four important issues: 1) identification and characterization of collapsible soils, 2) assessment of collapse potential and settlement; 3) estimation of the distribution and the degree of wetting in the deposit; and 4) evaluation of design alternatives and mitigation strategies.

While the literature on collapsible soils is quite extensive, there are significant voids that still need to be filled. An area that appears to require further work pertains to the (rapid) identification and characterization

of these soils. From a more fundamental point of view, much still is to be learned on the mechanism(s) responsible for the collapse. Finally, a more general approach for the selection of mitigation/improvement methods to deal with these soils is also needed. From a local perspective, despite the extension of loess deposits in the State of Indiana (see more on this point in Chapter 3), comparatively limited research has been performed on these geomaterials. Given the specific interest of the State DOT of utilizing these materials in compacted fills, there is the need to establish the compaction requirements that need to be met to limit the collapse potential of these soils. This is the main focus of the research performed as part of this project.

As part of this project, informal conversations via phone and e-mail were conducted with DOT engineers and geologists from five neighboring states (Kansas, Ohio, Illlinois, Minnesota and Iowa) to get their perspectives on the following issues: a) experiences with problems of wetting induced collapse in compacted loess in these States b) tests and/or methods used to assess the potential for wetting induced collapse; c) specifications—if any—adopted for use of loess in compacted fills/embankments; d) mitigation methods applied for dealing with problems of wetting induced collapse. These interactions (see Appendix A for a summary of the contents) indicated the following: i) while there is some awareness of the problem of wetting induced collapse in compacted loess, observations of these problems in the field seem to have been limited; ii) there are no standard methods or tests used to assess collapse potential; iii) there are no loess-specific compaction specifications related to eliminating collapse (there are instead restrictions on the use of loess in embankments or in some portions of the embankments, as well as limitations on the maximum value of the water content); iv) because of (i), experience with mitigation methods is limited, although it appears recognized that a key strategy is limiting the access of water to the soil.

Overall, these conversations suggest that an investigation into the susceptibility of compacted Indiana loess to wetting induced collapse is timely and opportune.

1.2 Project Scope and Research Objectives

The overall scope of the project is to contribute to develop a knowledge base within INDOT for dealing with collapsible soils used in compacted fills.

The specific objectives of the research are to:

- Summarize the current knowledge on the collapse of compacted fills;
- Recommend test procedures for identifying and testing these soils to measure their collapse potential;
- Compare the collapse potential of typical Indiana loess to that previously measured on other similar geomaterials

These objectives were pursued through:

- An in depth review of the literature on collapsible soils, with focus on the collapse of compacted loess;
- Sampling of two loess representative of typical deposits occurring in the State of Indiana;
- An experimental program involving double oedometer tests on samples of the two soils compacted over a range of water contents and dry densities

1.3 Organization of the Report

This report is organized in six chapters. Chapter 1 provides a brief introduction of the problem investigated and summarizes the objectives of the research conducted to address it. Chapter 2 summarizes the existing literature on collapsible soils. A number of topics are covered including: the definition and the different types of collapsible soils, the methods used to measure collapse potential and the criteria used for identifying collapsible soils. The emphasis of this chapter is on loess, its index properties, genesis, structure, mineralogy, and, in particular, the collapsibility of compacted loess. Chapter 3 reviews the areas within the State of Indiana where there are significant loess deposits. Chapter 4 focuses on the materials and experimental methods employed in this research project. In particular, it includes a discussion of the sampling procedures, of the index properties of the samples, and of the methods used to prepare the laboratory compacted specimens and to measure their collapse potential. The results of the collapse measurements performed on both soils are presented in Chapter 5, which also includes a comparison of these results to data available in the literature on loess from other regions of the US. Finally, Chapter 6 presents the conclusions of the work and provides recommendations for future research in the field and for implementation.

CHAPTER 2 BACKGROUND

2.1 Collapsible Soils

2.1.1 Definition

Collapsible soils have been widely studied for more than 70 years resulting in a broad literature. As their name indicates, these soils can exhibit large volume change upon wetting, with or without extra loading, thus posing significant challenges to the geotechnical profession. Rogers (1994) provided a compilation of the major characteristics of collapsible soils:

1) *"……a soil that undergoes an appreciable amount of volume changes upon wetting, load application, or a combination of both." (Sultan 1969)*
2) *"…….any unsaturated soil that goes through radical rearrangement of particles and great loss of volume upon wetting with or without additional loading." (Dudley 1970)*
3) *"…..additional settlement…. due to the wetting of a partially saturated soil, normally without any increase in applied pressure." (Jemings and Knight 1975)*

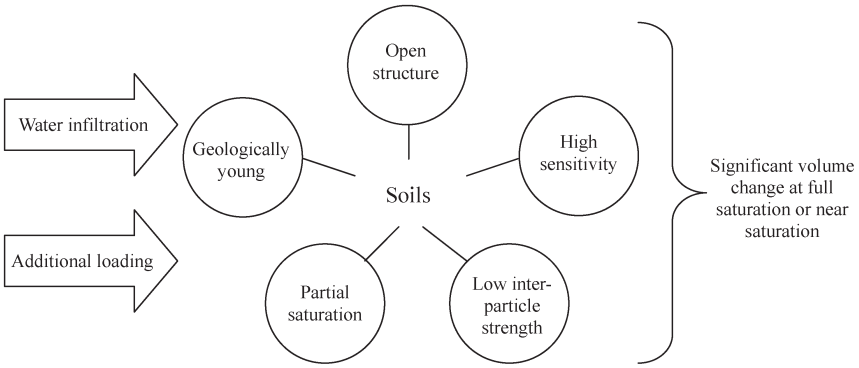

Figure 2.1 Schematic view of key characteristics of collapsible soils

4) *"…..a state of underconsolidation related to apparent cohesive strength of unsaturated soils." (Booth 1977*

Based on the characteristics of collapsible soils found in literature, it can be concluded that collapsible soils are soils which remain at a stable state in unsaturated conditions but are susceptible to appreciable volume change induced by water infiltration alone or water infiltration in combination with external loading (including self-weight) and dynamic force at full saturation or near saturation. However, in general, the study of collapsible soils is limited to collapse produced by static external loading, while the collapse dincued by dynamic forces is usually studied in the context of liquefaction phenomena. In addition to the basic definition of collapsible soils above, collapsible soils have typical features that contribute to collapse including: an open (metastable) structure which results in low bulk density, high void ratio and high porosity, geologically young deposit, lately altered deposit, significant sensitivity, and weak inter-particle bonding (Rogers 1994). Figure 2.1 gives a schematic of the characteristics of collapsible soils.

2.1.2 Classification

Numerous soil types can fall in the general category of collapsible soils, including compacted soils and natural soils such as aeolian deposits, alluvial deposits, colluvial deposits, residual deposits, and volcanic tuff as shown in Figure 2.2. A well-known aeolian deposit, known to often exhibit collapsing behavior, is loess, a yellow to reddish brown silt size soil, which is characterized by relatively low density and cohesion, but appreciable strength and stiffness in the dry state. Aeolian deposits with significant tendency to collapse are often found in arid regions where the water table is low. However, even in environments with medium rainfall, such as the Midwestern United States, fine aeolian deposits can still present high collapsible potential (Clemence and Finbarr 1981), particularly if an impermeable surface crust has protected them from water infiltration.

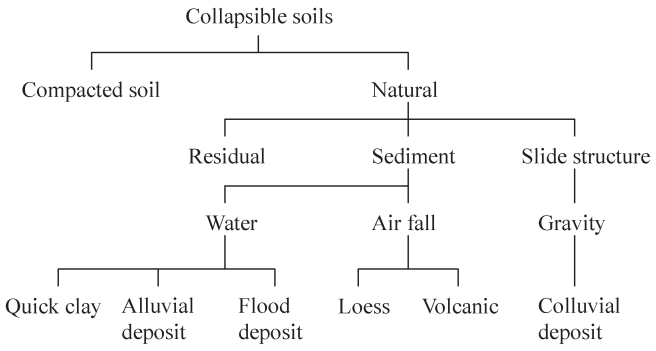

Figure 2.2 A family of collapsible soils (Rogers 1994)

Collapsing behavior has also been reported for some alluvial deposits, specifically water deposited loose sediments. Alluvial-type collapsible soils are mainly formed by flash flood or mudflows (debris flows) which come from huge precipitation in irregular intervals. Under these conditions, loose and metastable structures are induced due to particles which are deposited suddenly and locally. In addition, alluvial deposits are poorly graded and may contain a considerable amount of clay, which plays an important role in binding particles in the dry state.

High void ratio unstable structures can be also generated in colluvial deposits, i.e. deposits which have been formed in place and then transported by gravity. Collapsible colluvial and alluvial soil deposits are common in desert portions of the southwestern U.S, where collapse settlements of two to three feet are common, and settlements up to 15 feet have been reported.

In residual soils, which can contain particle size fractions varying from clays and silts to large fragments of rock, an unstable and high void ratio structure can alternately be formed by leaching of the soluble and fine material which is between large particles and provides cementation. Other types of soils that can present collapsible behavior upon wetting are "*those derived from volcanic tuff, gypsum, loose sands cemented by soluble salts, dispersive clays, and sodium-rich montmorillonite clays*" (Clemence and Finbarr 1981).

2.1.3 Measurement of Collapse Potential

Collapse potential is an indication of the degree of bulk volume change soils exhibit due to load and water infiltration. In a semi-infinite field (i.e. one dimensional condition), the collapse potential is expressed by the change in height after wetting and an applied load. The following equation shows a typical engineering definition of collapse potential in terms of change in void ratio which is associated with the difference in height (Lutenegger and Hallberg 1988).

$$CP = \frac{\Delta e}{1 + e_o}$$

where: Δe = decrease in void ratio due to wetting, and e_o is the initial void ratio.

There are a variety of approaches to measure the collapse potential of soils including laboratory methods and field methods. The most common way is to conduct laboratory tests using the oedometer test or triaxial test. The main advantage of laboratory tests is that the three most important factors which affect collapse potential: degree of saturation, dry density, and overburden stress, can be controlled and measured (Lawton et al. 1992). Typically, results of oedometer tests are used for one-dimensional analysis and results of triaxial tests are employed for three-dimensional analysis. Lawton (1989) showed that little additional information on collapse is gained from triaxial tests, so oedometer tests are recommended.

Two types of oedometer tests can be employed to determine collapse potential: the single-oedometer test and the double-oedometer test. The single-oedometer test is conducted based on the "*soaked-after-loading method*" (Lawton et al. 1992), where the soil is placed in the oedometer, and an overburden stress is gradually applied until strain equilibrium is achieved in the sample. After that, the soil sample is flushed with water under the applied stress. The collapse measured after water infiltration is termed collapse potential. The principle of the double-oedometer test is different. It is based on an assumption that "*the deformations induced by wetting are independent of the loading-wetting sequence*" (Lawton et al. 1992). The test is conducted using two identical samples: one is tested as in a typical oedometer test at the original water content, while the other specimen is loaded after flushing with water at a low stress level. The difference in the deformations measured from the two tests is the collapse due to wetting. The advantage of the double-oedometer test is that through a single test one can obtain a large amount of data without repeating single oedometer tests at different stress levels. Figure 2.3 presents a typical result of a double-oedometer test. ASTM D5333 describes the procedure for the single odeometer test to measure the collapse potential of soils. The standard also introduces the collapse index (I_c), which is the wetting induced strain measured at a reference stress level of 200 kPa. Based on the value of the collapse index, the degree of specimen collapse (or collapse potential) can be classified as none ($I_c \sim 0$), slight ($0.1\% < I_c < 2\%$), moderate ($2.1\% < I_c < 6\%$), moderately severe ($6.1\% < I_c < 10\%$), and severe ($10\% < I_c$).

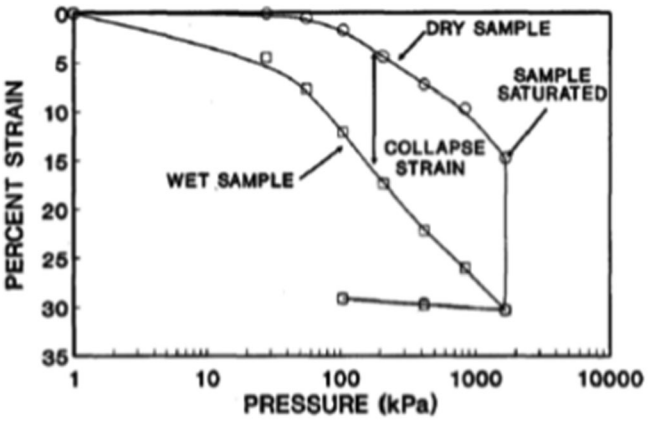

Figure 2.3 Typical result of a double-oedometer test (Rollins 1994)

Some field tests are available to determine collapse potential. However most, of them are not a direct measurement of collapse potential. For example, the level of collapse potential can be correlated to the SPT N-values and CPT tip resistance. Additionally, empirical equations have been proposed to determine the collapse potential based on the soil's dry density and water content, which can be obtained in the field, for example, using time domain reflectometry (TDR) or the nuclear density gage. In addition to these correlations, Mahmoud and Houston et al. (1995) proposed an in-situ collapse test using soil boxes on a concrete pad, as shown in Figure 2.4. The soils boxes filled on top of the footing provide the desired overburden pressure, and once the pressure is reached, water is added to the

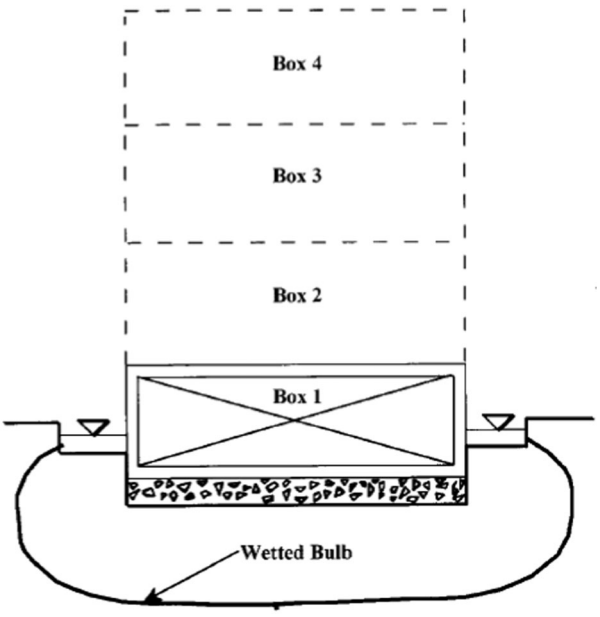

Figure 2.4 A plate load test for in-situ collapse potential (Houston 2001)

pit to increase the moisture under the footing. The disadvantage of this type of test is the applied stress is limited to a shallow depth of only two to three meters (Mahmoud et al. 1995). In other words, this test only provides collapse potential measurements for surface soils.

2.1.4 Criteria for Estimating Collapse Potential

In order to classify the collapsibility of soils, a variety of criteria for collapse potential have been proposed in the literature. Most of these criteria determine the critical condition of collapse based on void ratio, dry unit weight, degree of saturation, Atterberg limits, natural water content, and percentage of fine grain soils.

Russia is a country where collapsible soils, especially loess, are widely spread. Numerous research and criteria of collapse potential can be found in the Russian literature, although for the most part written in the native language. Das (2007) summarized some major criteria from Russia as follows. The criterion proposed by Denisov (1951) uses the coefficient of subsidence, which is the ratio of the void ratio at the liquid limit over the in situ void ratio. According to this criterion, if this ratio is 0.5–0.75, soils are likely to be highly collapsible. If the ratio is larger than 1.5, soils are not expected to collapse. Priklonski's (1952) criterion utilizes the liquidity index to estimate the degree of collapsibility. Specifically, if the liquidity index is less than zero, soils have a high collapsibility because they are in a very dry state and thus susceptible to water infiltration. When the liquid index is larger than 0.5, soils are not likely to collapse. The Soviet Building Code measures collapse potential based on a parameter L that depends on in-situ void ratio and void ratio at the liquid limit (see Table 2.1). For a natural degree of saturation less than 60%, if $L > -0.1$, soils are considered collapsible.

In addition to the criteria proposed in Russian literature, Clevenger (1956) proposed the criterion for

TABLE 2.1
Criteria for collapse potential (Das 2007; Lutenegger 1988)

Investigator	Year	Criteria
Denisov	1951	Coefficient of subsidence: $K = \frac{e_{LL}}{e_0}$ K=0.5–0.75→highly collapsible K=1.0→noncollapsible loam K=1.5–2.0→ noncollapsible soil
Clevenger	1958	If dry unit weight is less than 12.6 kN/m^3 (80 lb/ft^3)→large settlement If dry unit weight is larger than 14 kN/m^3 (90 lb/ft^3)→small settlement
Priklonski	1952	$K_D = \frac{\omega_n - PL}{PI}$ K_D<0→highly collapsible soils K_D>0.5→non-collapsible soils K_D>0→swelling soils
Gibbs	1961	Collapse ratio $R = \frac{\omega_{sat}}{LL}$ This was put into graph form
Soviet Building Code	1962	$L = \frac{e_o - e_{LL}}{1 + e_o}$ For natural degree of saturation <60%, if L>−0.1, the soil is a collapsing soil
Feda	1964	$K_L = \frac{(\omega_n/S) - PL}{PI}$ For S<100%, if K_L>0.85, the soil is considered collapsible
Benites	1968	A dispersion test in which 2g of soil are dropped into 12 ml of distilled water and specimen is timed until dispersed; dispersion times for 20 to 30s were obtained for collapsing Arizona soils
Handy	1973	Iowa loess with clay (<0.002mm) contents: <16%: high probability of collapse 16–24%: probability of collapse 24–32%: <50% probability of collapse >32% usually safe from collapse
South Africa Criteria (Brink 1958)	n/a	Aeolian sand: $CP = \frac{1672 - \gamma_d}{22} < 0$ not collapse Mixed origin: $CP = \frac{1590 - \gamma_d}{18.9} < 0$ not collapse
Czechslovak Standard	n/a	Collapse may occur when Silt % > 60% Clay% < 15% S < 60% and LL < 32% n > 40 % Wn < 13%

collapsibility in terms of dry unit weight. Based on research on loess in the Missouri Basin Area, he concluded that upon wetting, soils with unit weight smaller than 80 lb/ft^3 (12.6 kN/m^3) undergo large settlement and have low shear strength, while if the dry density is larger than 90 lb/ft^3 (14.1 kN/m^3), soils are capable of supporting the assigned loads.

Gibbs (1961) proposed a measure of collapse potential, which is displayed in graphical form in Figure 2.5. It depends on the ratio of the water content at full saturation to the liquid limit when this ratio is larger than one (case I), saturation leads to the soil being at its weakest condition as void spaces would be sufficient for collapse of the soil structure. If the ratio is less than one, the voids are less than the amount of water at liquid limit; soils remain in the plastic state and have greater resistance against particle shifting (case III). If the ratio is equal to one, this indicates that the voids are sufficient to hold the liquid limit moisture content (case II). Soils with liquid limit and natural dry density falling in the upper area in Figure 2.5 are associated with case I soils which have high collapse potential. Soils falling in the lower area are termed case III soils and are not expected to experience large collapse.

Feda (1964) applied a criterion similar to that proposed by Priklonski (1952), except that it considers the degree of saturation $K_L = \frac{(\omega_n/S) - PL}{PI}$. Feda proposed that for soils with degree of saturation less than 100%, the potential for collapse is significant if K_L is larger than 0.85 (this usually corresponds to porosity higher than 40%).

To estimate collapse, Benites (1968) used a dispersion test "*in which 2g of soil are dropped into 12 ml of distilled water.*" He finds that for collapsing Arizona soils *dispersion times range between 20 and 30s* (based on Das 2007).

Handy (1973) studied Iowa loess with clay and determined that when clay content is less than 16% soils are subject to a high probability of collapse. For clay content in the 16–24% range, soils are likely to collapse. For clay content in the 24–32% range, the probability of collapse is 50%. If the clay content is greater than or equal to 32%, soils are usually safe from collapse.

The South Africa Criteria (Brink 1985) employed dry density to estimate collapse potential. The criteria are based on numerous testing data in South Africa. For aeolian soils, if the collapse potential, $CP = \frac{1672 - \gamma_d}{22}$, is less than zero, there is no collapse. For soils of mixed origin, if the collapse potential, $CP = \frac{1590 - \gamma_d}{18.9}$, is less than zero, soils do not collapse.

The Czechslovak Standard (Klukanova and Frankovaska 1994) applied six critical conditions to classify the collapse potential. Specifically, the standard defines the following threshold values for collapse: silt content greater than 60%, clay content less than 15%, degree of saturation less than 60%, liquid limit below 32%, porosity greater than 40%, and natural water content less than 13%.

Table 2.1 summarizes the criteria discussed above.

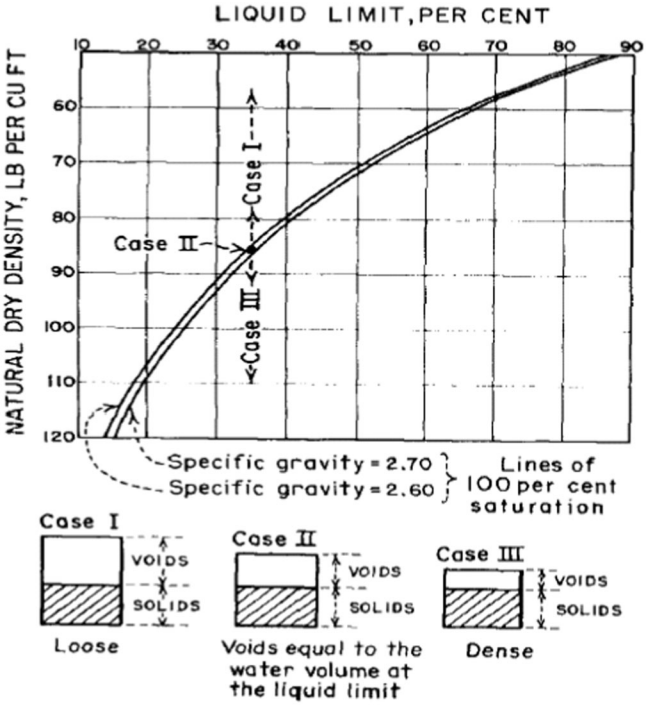

Figure 2.5 Criterion for collapse potential (Gibbs 1961)

2.2 Loess

Loess is the most well-known collapsible soil, covering approximately 10% of the land area of the world. In general, loess is a silt-based soil commonly yellow to buff in color that is wind deposited. The particle size of loess falls in a wide range depending on its composition and the environment, but typically loess has quite uniform particle size in the range of 0.01–0.005 mm. Since loess is wind deposited, stratification is not observed in loess layers. In-situ, loess slopes can stand vertically when in a dry state. However, when it is wetted the slope face is markedly reduced to a 21 to 31 relationship (West 1995). This is associated with the collapsibility of loess upon wetting and is the chief consideration in engineering practice.

2.2.1 Geographic Distribution

Table 2.2 and Figure 2.6 show the wide-spread distribution of loess in the world. In particular, China, Russia, Eastern Europe, U.S.A., South America, and New Zealand, are covered by extensive loess deposits.

In the United States, there are five major regions of significant loess deposits. These regions include (West 1995):

TABLE 2.2
Distribution of loess in the world

Nations	Percentage of area covered by loess (Area)	Reference
Argentinean	39.76% (1,100,000 km^2)	(Smith et al. 2003)
Bulgarian	13% (14,400 km^2)	(Evstatiev 1994)
China	6.6% (631,000 km^2)	(Derbyshire 2001)
New Zealand	10% (27,000 km^2)	(Eden and Hammond 2003)
Poland	6% (18,800 km^2)	(Grabowska-Olszewska 1988)
Romania	11.5% (27,300 km^2)	(Popescu 1986)
Russia	20% (3,500,000 km^2)	(Osipov and Sokolov 1994)
Ukraine	65% (392,000 km^2)	(Rogers et al. 1994)
U.S.A.	46% (4,500,000 km^2)	(Arthur Bettis et al. 2003)

Note: The percentage of area covered by loess is based on the total area of the nation

1) Low Mississippi River section
2) Central U.S. Interior Lowland
3) Great Plains, Nebraska, Kansas, and Eastern Colorado
4) Snake River Plain, South Idaho
5) Palouse Area, Eastern Washington and Northeast Oregon

In addition to above regions, Alaska also has large loess deposits. Figure 2.7 presents the distribution of loess in the contiguous United Sates. It is evident from the map that an understanding of the properties of collapsible soils is critical in the Midwest. Specifically, Southwestern Indiana is a geographic area where collapsible soils are prevalent.

2.2.2 Geological Formation

As mentioned above, loess is a wind-deposited material and is mainly derived from the major valley train of glaciers. Figure 2.8 shows an illustration of the formation of loess. The glacier movement carries different type of materials including coarse-grained and fine-grained soils (Figure 2.8 (a)). The glacier may thaw periodically due to climate cycles, and the outwash is usually not protected by any vegetation, so it is exposed. Therefore, the wind causes both erosion and deposition (Figure 2.8 (b)). The soil particles can be transported along the windward direction for a certain range depending on soil particle size, wind speed, and topography. In the U.S., loess is usually accompanied by some clay and fines and is found leeward of glacier outwash, typically deposited along the east bank of rivers and upland (Figure 2.8(c)).

Based on its observed physical, mineralogical and chemical properties, the loess in the United States was transported by westerly or northwesterly wind during the Last Glacier Period (Muhs and Bettis III 2000). This observation is different from the simulated Palaeo-wind direction under glacial anticyclonic circulation. Figure 2.9 shows the distribution of loess of the U.S. with the direction of Palaeo-wind.

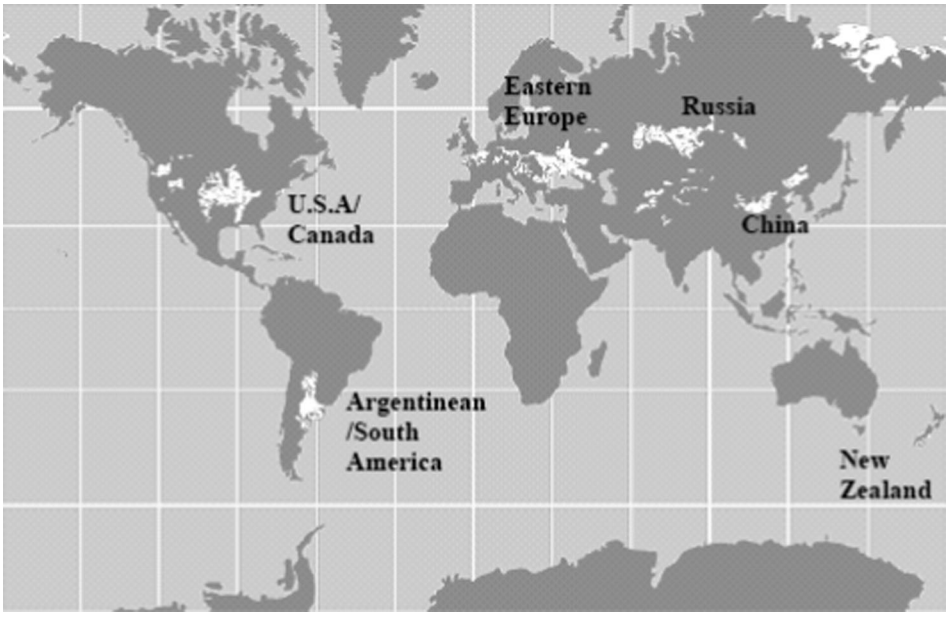

Figure 2.6 Loess distribution in the world Reproduced form www.physicalgeography.net/fundamentals/10ah.html

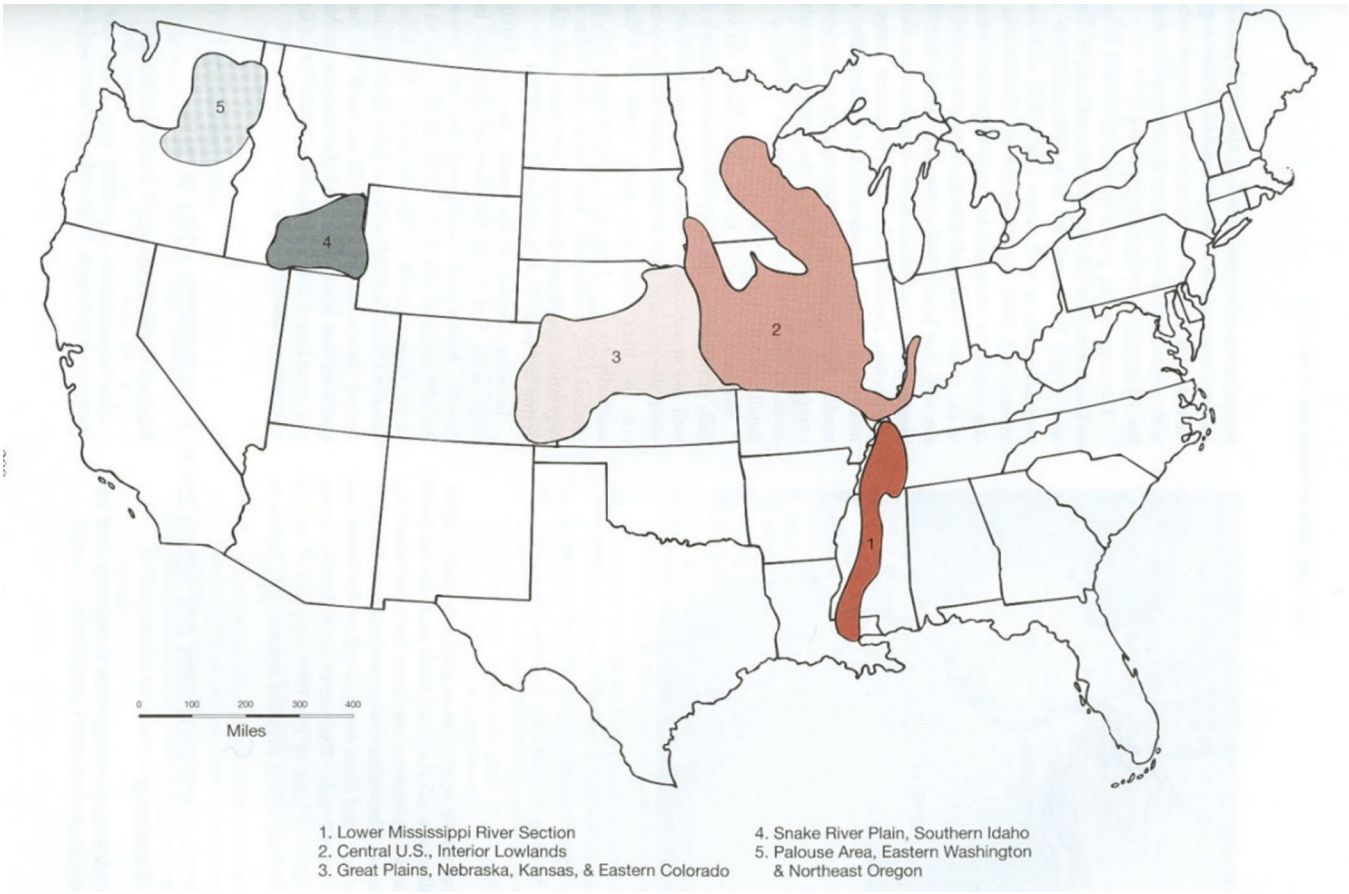

Figure 2.7 Distribution of loess in the United States (West 1995)

Loess is deposited during glacier action. Different glacial periods produced loess of varying age. Figure 2.10 shows the general extent of continental glaciation in the United States. The latest glacial period is the Wisconsin glaciation, and loess formed during this period is termed Wisconsin loess. Two different Wisconsin loesses are recognized: Roxana silt of the Altonian stage (75000 to 28000 years BP) and Peoria loess, mostly of the Woodfordian substage (22000 to 12500 years BP). Illinoian glaciation occurred before the Wisconsin glaciation, and is the second most recent glacial period. Loess formed in this period is named Loveland loess. Between the two latest glaciations, the period is called Sagamon interglacial and the materials formed in this stage are called Sagamon soils. Figure 2.11 presents typical altered deposits of loess. At the top, there is eroded modern soil. Peoria loess formed in Wisconsin glaciation is immediately beneath the eroded modern soil. Between Loveland loess formed in Illinoian glaciation and Peoria loess, there is a layer of interglacial Sagamon soil. At the bottom, Loveland loess is underlain by older loess deposits.

2.2.3 Structure

Loess is constituted of fine-grained materials. From a mineralogical standpoint, the basic unit of the loess structure is formed by a core of quartz, carbonates, and more rarely feldspar. The core is coated by a clay film composed mainly of illite, momtmorillonite, mixed structures, sporadic iron, manganese hydroxides, and finely dispersed quartz and calcite particles as shown in the schematic from Osipov and Sokolov (1994) in Figure 2.12. In this schematic Region 1 (inner part) is the quartz or feldspar nucleus; Region 2 and Region 3 are amorphous SiO gel and a calcite envelopes, respectively; Region 4 is the clay shirt, saturated by FeO. The grain surface is amorphous. Trace calcite etches the surface and the grain is covered by a spotted envelope of calcite. This calcite coat is overlapped by a poly-mineral "shirt" consisting of clay minerals and cemented by fine-dispersed calcite quartz, oxides of iron and amorphous silica. Typically, the calcite envelopes and clay shirt are water resistant.

Loess structure, and therefore the type of loess, also depends on the percentage of sand, silt, and clay present. Klukanova and Frankovska (1994) stated that typical loess (silty loess) is characterized as a skeleton structure, which presents micro-granularity. Silt is the dominant fraction, while clay "bridges" or "buttress" fit between basic structural elements (Figure 2.13). Sandy loess, which has lower clay content and more sand grains, is also characterized as having a skeleton structure. Sandy grains with clay coating dominate,

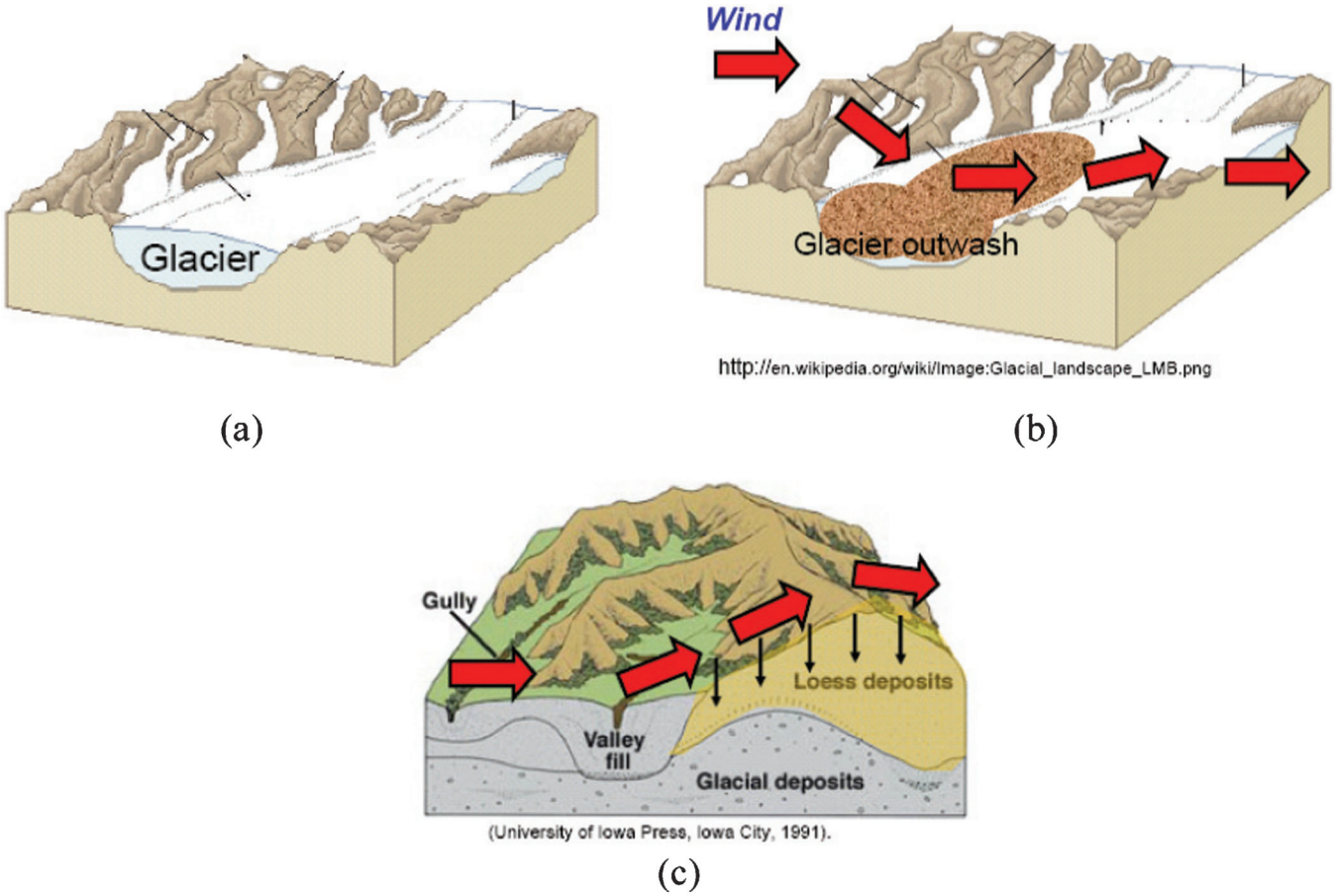

Figure 2.8 Formation of loess: (a) glacial deposition; (b) erosion and deposition by wind, and (c) loess hill formation (Pictures of (a) and (b) are adopted from http://en.wikipedia.org/wiki/File:Glacial_landscape.svg and picture (c) is adopted from http://pubs.usgs.gov/info/loess/)

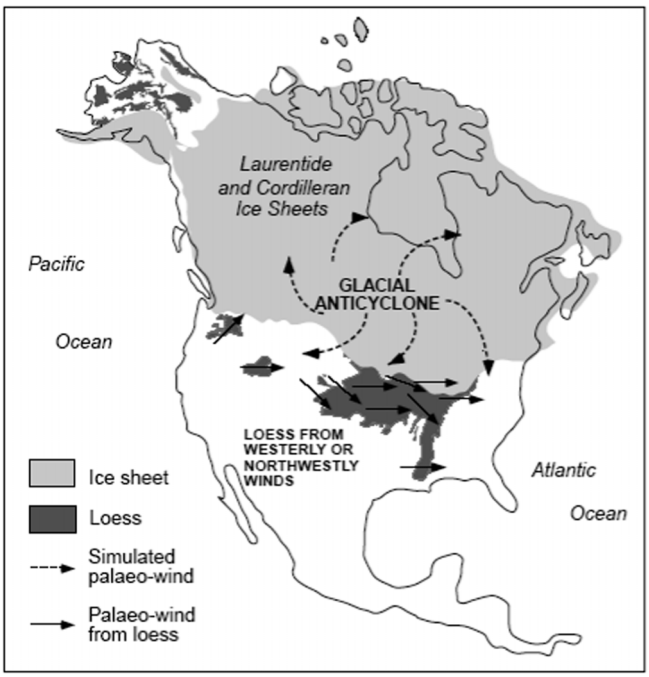

Figure 2.9 The distribution of loess in the U.S. with the direction of Palaeo-wind (Bettis et al. 2003)

but many sand grains are not fully coated by clay films. Particle bonding is again achieved through clay bridges as in typical loess. The sandy loess tends to collapse mainly at the contact of grains with uncompleted coating of clay films. Clayey loess ranges from matrix (higher clay content) to matrix-skeleton microstructure (lower clay content). The matrix microstructure presents a more heterogeneous fabric and the matrix-skeleton microstructure exhibits a fabric that may be either homogeneous or heterogeneous.

2.2.4 Mineralogy

Loess typically contains 40–60 minerals (Egri 1972). The typical and most important minerals are summarized in Table 2.3. In the sand and silt fractions, quartz, feldspar, carbonate, mica, and gypsum are usually present. In the clay fraction hydromica, momtmorillonite, mixed layered kaolinite, and finely-dispersed quartz and calcite dolomite are the major minerals.

These typical minerals can be divided into two groups, based on the role they play in the process of collapse (Egri 1972):

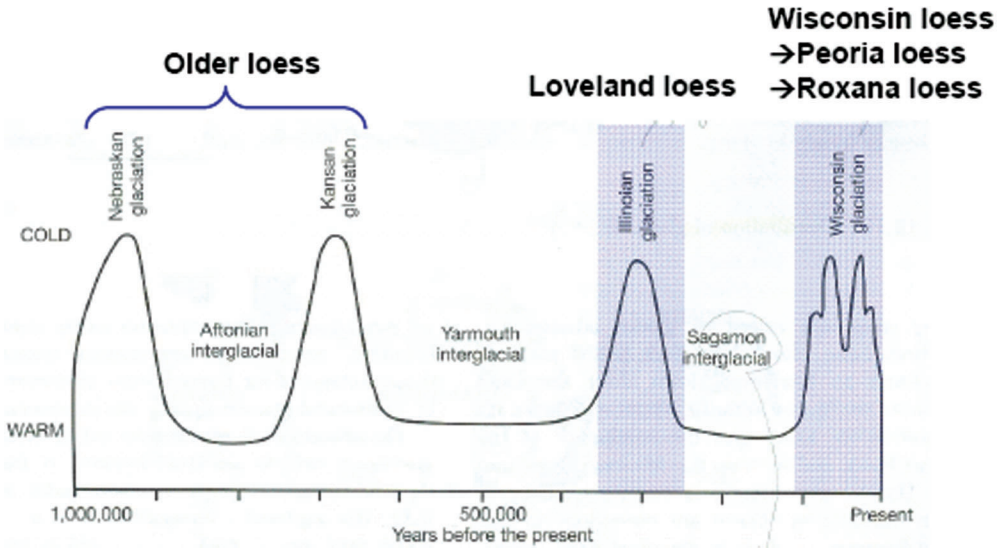

Figure 2.10 Geological periods during which different loess deposits formed (West 1995)

1) Active minerals, which are changed due to the process of collaps, and which include carbonates (mainly calcite), sulphates (gypsum), and salt.
2) Passive minerals, which are not changed due to the process of collapse, and which include quartz, feldspar, and mica.

The composition of clay minerals in loess can vary depending on the origin of the loess. Table 2.4 gives a summary of the mineral composition of loess in the Central Lowland of the United Sates. The term "expandables" in Table 2.4 refers to vermiculite plus montmorillonite.

In addition to the minerals listed above, most loess has "*carbonate content from 1% to 15–25%, medium soluble mineral (gypsum) content 4–10%, readily soluble salts (chloride) content <2%, half soluble oxides and hydroxides <2.4% and humus content 1–2%*" (Osipov and Sokolov 1994). Figure 2.14 shows iron and aluminum content and the mineralogy of the carbonate fraction (i.e. calcite and dolomite) of Peoria Loess from the Central Lowland and Great Plains. Table 2.5 gives the carbonate content of loess from the mid-continental United States.

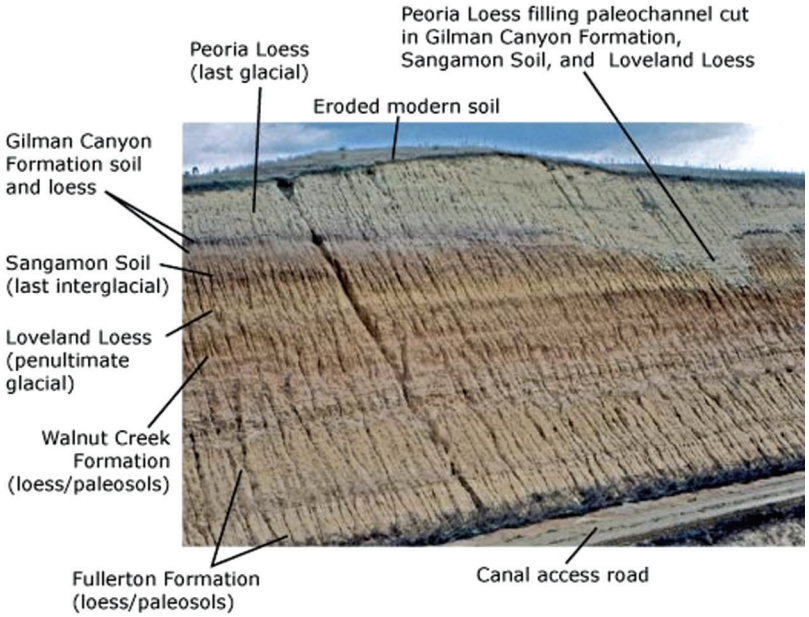

Figure 2.11 Typical altered deposits of loess Adopted from http://esp.cr.usgs.gov/info/eolian/task2.html

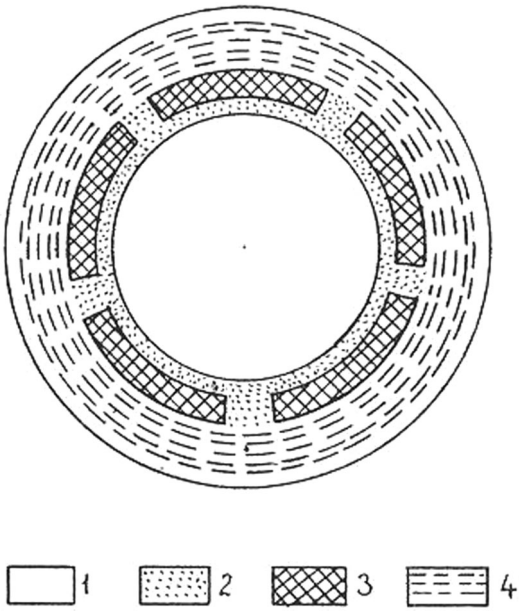

Figure 2.12 A simple schematic of loess (Osipov and Sokolov 1994)

These salts, carbonates, and hydroxides serve critical roles in the bonding system of loess and result in different collapsibility.

TABLE 2.3
Typical mineralogy of loess

Sand fraction	Silt fraction	Clay fraction
Quartz	Quartz	Hydromica
Feldspar	Feldspar	Momtmorillonite
Carbonate	Carbonate	Mixed layered
Mica	Mica	Kaolinite
Gypsum	Gypsum	Fined-dispered quartz and calcite dolomite

2.2.5 Bonding and Collapsing Mechanism

Loess is bonded in many different ways. In an unsaturated condition, the big grains can be held together by capillary tension, and in the fine grains, capillary forces provide silt-silt and silt-sand bonds (Figure 2.15 A and B). Since coarse (sand) grains are usually coated by clays, the bonding can be provided by aggregated clay grains (Figure 2.15 C), by flocculated clay (clay buttress, Figure 2.15 D), or by the combination of silt and clay (Figure 2.15 E). Some loess does not have high clay content, so the coarse grain and silt-size particles are not fully surrounded by clay; however, particles are still bonded by clay bridges (Figure 2.15

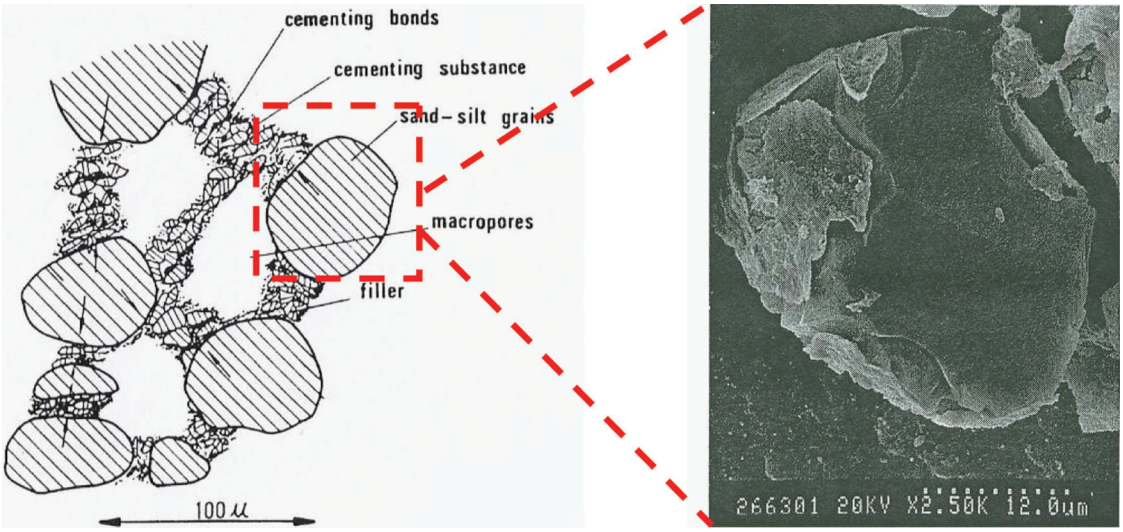

Figure 2.13 A basic unit of loess structure (Left: Rogers (1994), Right: Osipov and Sokolov (1994))

TABLE 2.4
Clay minerals in loess of different origin in the Central Lowland of the U.S. (Table adopted from Ruhe 1984)

Province	Kaolinite (%)	Illite (%)	Expandables (%)	Vermiculite (%)	Montmorillonite (%)
Upper Ohio Valley	13~28	19~37	35~63	27~52	3~29
Wabash Valley	10~22	42~61	27~45	7~24	16~34
Lower Mississippi Valley	3~13	20~45	45~76	2~12	41~75
Upper Mississippi-Missouri Valley	3~11	15~24	66~80	0~10	58~79

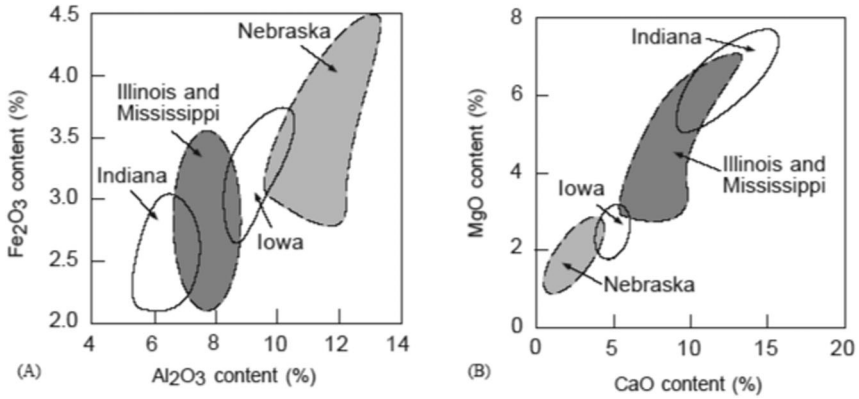

Figure 2.14 Mineralogy of the carbonate fraction of Peoria Loess in the Central Lowland and Great Plains (Table adopted from Bettis et al. 2003; Data from Muhs and Bettis III 2000; Muhs et al. 2001; Pye and Johnson 1988)

TABLE 2.5
Carbonate content of mid-continent United States loess (Table adopted from Bettis et al. 2003)

Source Area	Carbonate Content (%)	Reference
North/South Platte Valley	3~12[a]	Muhs et al., 1999
White River Group	10~18[a]	Swineford and Frye, 1951
Missouri Valley	12~14[a]	Ruhe, 1969
Middle Mississippi Valley	26~30[a]	Grimley et al., 1998
Lower Mississippi Valley	15~30[a]	Miller et al., 1984
Wabash Valley	25~29[a]	Ruhe and Olson, 1978

Note: Bulk loess, determined with Chittick Apparatus

F). Clay bridges are clearly seen the SEM shown in Figure 2.16.

In certain collapsing soils, chemical cementing agents such as iron oxide, calcium carbonate, etc., are critical bonding agents and these are often the main agents in loessial soils. While in many collapsible soils, clay provides the dominant bonding effect, calcium-carbonate cementing can be important in the case of loess. Whatever physical bonding strength these agents provide, they are likely broken down by water infiltration.

Yang (1989) proposed a classification of types of bonds present in loess. The classification considers two types of bonds: hydro-stable cementation and hydro-labile cementation. Hydro-stable cementation occurs when the cementing strength does not visibly decrease

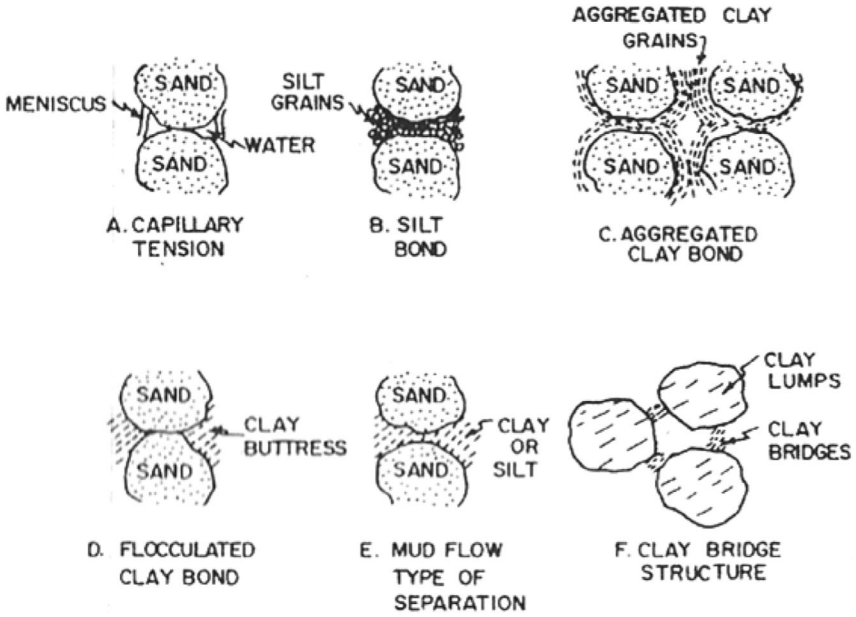

Figure 2.15 Typical bonding structures of collapsible soils (Clemence and Finbarr 1981)

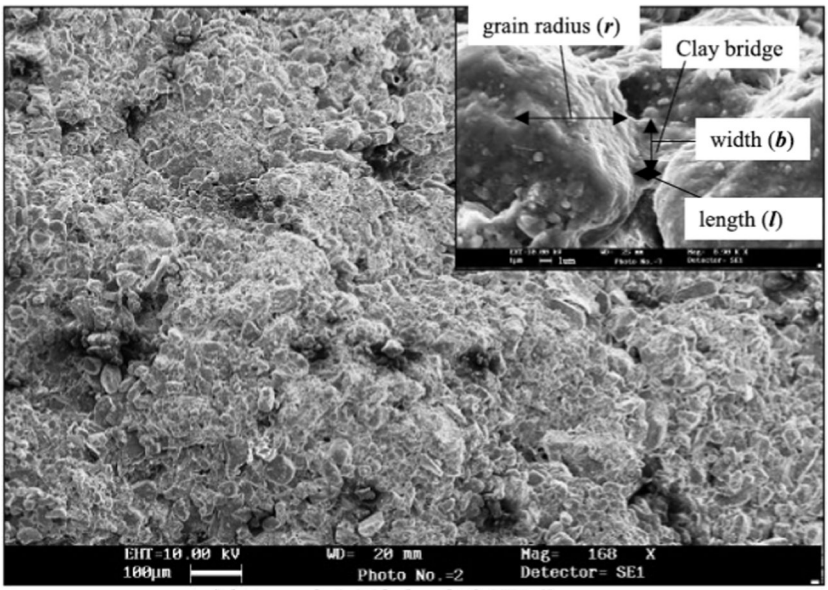

(Photograph A. Milodowski © NERC)

Figure 2.16 SEM photograph of loess (Jackson et al. 2006)

with water, and hydro-labile cementation is easy to break down when in contact with water. Table 2.6 summarizes the most common sources for these two types of bonds forming in loess.

Osipov and Sokolov (1994) studied structural bonds in loess, and Table 2.7 provides a summary of their findings. Molecular forces between particles are the weakest and the strength decreases with an increase in water saturation. The ionic-electrostatic force and capillary force are similar in magnitude, however ionic-electrostatic force is not stable in the presence of water, and capillary forces only exist at degrees of saturation between 0.35 and 0.80. Chemical agents, such as salts, sesquioxides of irons, and aluminums, can form cementation bridges with the strongest force. The water resistance of the chemical bonding forces depends

TABLE 2.6
Classification of bonding types of loess (Yang 1989)

Hydro-stable cementation	Hydro-labile cementation
Calcium carbonate	Strongly soluble salts
Hydrous calcium sulphate	Clay cementing agent
Ferrous oxide and ferrous hydroxides	-Flocculant
Hydro-stable secondary mica	-Non-flocculant
Secondary zeolite	Hydro-labile secondary mica

TABLE 2.7
Structural bonds in loess (Osipov and Sokolov 1994)

Forces	Strength of contact between two particles, N	Resistance to water
Molecular	$5 \times 10^{-10} \sim 10^{-8}$	Gradually decrease with increase of water saturation
Ionic-electrostatic	$5 \times 10^{-18} \sim 4 \times 10^{-7}$	Unstable
Capillary	$6 \times 10^{-10} \sim 10^{-7}$	Only exists at degree of saturation between 0.35–0.8
Chemical	$5 \times 10^{-7} \sim 5 \times 10^{-6}$	Unstable, stable

Stage of hydration	Degree of water saturation	Strength of single contact	Scheme of contact
A	<0.15	$\approx 4\times10^{-7}$ N	
B	0.15-0.8	$10^{-7} - 10^{-8}$ N	
C	>0.8	$10^{-9} - 10^{-10}$ N	

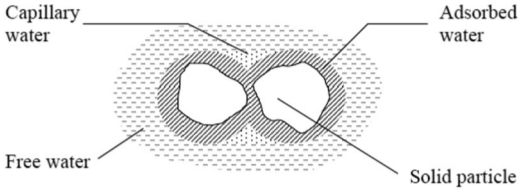

Figure 2.17 Structural bonds transformation in loess under water infiltration (Redrawn from Osipov and Sokolov 1994))

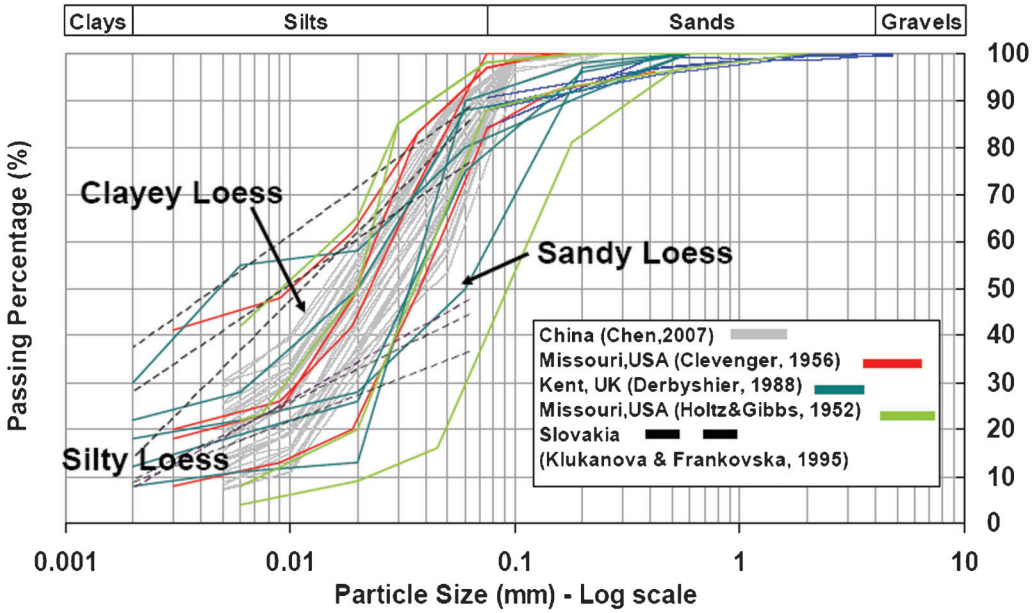

Figure 2.18 Particle size distribution of loess from literature (Data from Chen et al. 2007; Clevenger 1956; Derbyshire and Mellors 1988; Holtz and Gibbs 1956; Klukanova and Frankovaska 1994)

on the types of agents. Figure 2.17 provides a diagram of structural bonds transformation in loess under water infiltration at different degrees of saturation.

Klukanova and Frankovska (1994) suggest that the collapsing mechanism can be divided into three phases according to the loess microstructure and the structural bonds existing:

"Phase 1

1) *initial stage of destruction of the original microstructure due to increasing moisture and external load*
2) *clay films, clay bridges, and buttress start to break*
3) *aggregates, microstructure disintegrate*
4) *intensity of dissolution of carbonate and their migration in the soil increase*

Phase 2

1) *disintegration of microstructure continues – clay particles are water transported in the soil*
2) *content of carbonate decreases*
3) *other fabric elements compress*
4) *total volume of soil decreases*

Phase 3

1) *a new microstructure develops-after collapse*
2) *basic structural units disintegrate, they are no more coated by clay films and have no mutual contacts with clay bridges*
3) *clay films of silty grains were destroyed and removed completely*
4) *clay particles were aggregated and a coherent matrix formed in some place.*
5) *the soil acquires a heterogeneous structure in contrast with the original homogeneous structure*
6) *void ratio is reduced*

2.2.6 Identification

Loess is a silt-type material but not all soils with silt size particles are loess. For this reason, identification of loess requires professional experience. However, there are numerous ways to help screen and identify loess deposits. First of all, geological maps may provide geological information on the location and depth of loess deposits. In the field, the visual-manual classification process can be a useful way to identify loess. As a silt-type material with clay, loess usually has a flour texture when touched. Its color is typically from yellow to buff. Sometimes the carbonate or iron content may change the color slightly. The loess deposit has no stratification and vertical cuts are stable in a dry state. The slope can be reduced to 21 to 31 following wetting. Tubular macro probes due to plant root penetration can be observed in loess deposit when it is thick. In the laboratory, loess can be identified by index properties. Loess usually has sand content less than 15%, clay content not over 25%, dry density less than 1.4 g/cm^3, and low plasticity index with liquid limit usually less than 50%. Figure 2.18 and Figure 2.19 show the particle size distribution and range of Atterberg limits of loess compiled from the literature.

2.3 Compacted Fills

Compacted fills are frequently employed in the construction of roadways, railway embankments and earthen dams. These fills may experience water penetration, and therefore, exhibit problematic volume changes which can trigger direct or indirect damages to the construction. The problematic volume changes can

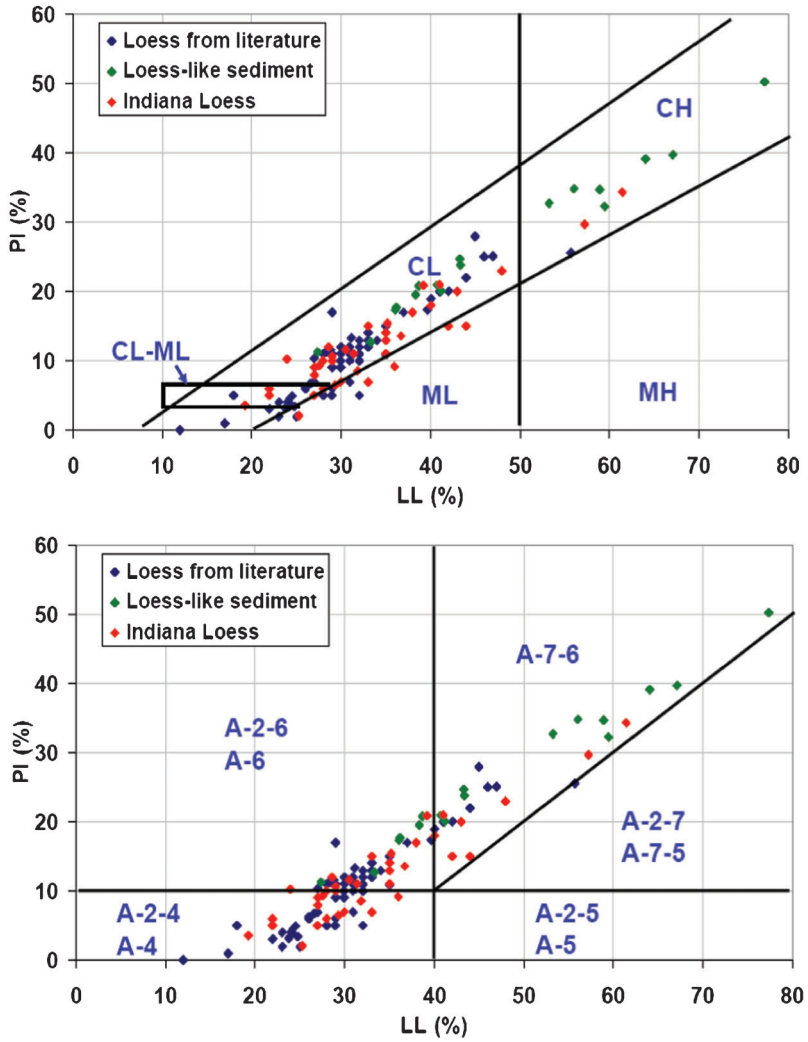

Figure 2.19 Atterberg limits of loess from literature in USCS (top) and AASHTO (bottom) representation.

be subsidence or swelling depending on the pre-wetting conditions (dry density, degree of saturation) and the applied load. In high embankments or earthen dams, appreciable settlement due to wetting (wetting induced settlement) can occur if critical values of as-compacted conditions are not attained.

2.3.1 Collapse Mechanism Overview

The collapse mechanism of compacted fills is similar to the mechanism of natural collapsible soil. The main characteristics shared by compacted fills known to exhibit wetting-induced settlement are a partially saturated, open, unstable structure, under high applied stress, with strong bonding or cementation in partial saturation, and weak bonding and cementing strength in contact with water.

In compacted cohesionless soils, capillarity, i.e. matric suction, dominates the collapsibility. The theory of effective stress can be applied to explain the collapse. The following equation describes the effective stress for partially saturated soils (Bishop 1959),

$$\sigma' = (\sigma - \mu_a) + \chi(\mu_a - \mu_w)$$

where σ' is the effective stress, σ is the total stress, $\mu_a$is the pressure of pore air, μ_w is the pressure of pore water, and χ is an empirical coefficient. The first term, $(\sigma - \mu_a)$, refers to the net normal stress, and the second term, $\chi(\mu_a - \mu_w)$ represents the matric suction. The empirical coefficient is one when soils are fully saturated and zero when soils are completely dry. In a partially saturated soil, the matric suction provides capillary tensile stress to bond particles. Once the degree of saturation gradually increases, the matric suction decreases. The strength of holding particles reduces as well and results in collapse under the applied load.

In compacted cohesive soils, capillary force is only one of the mechanisms controlling the collapse.

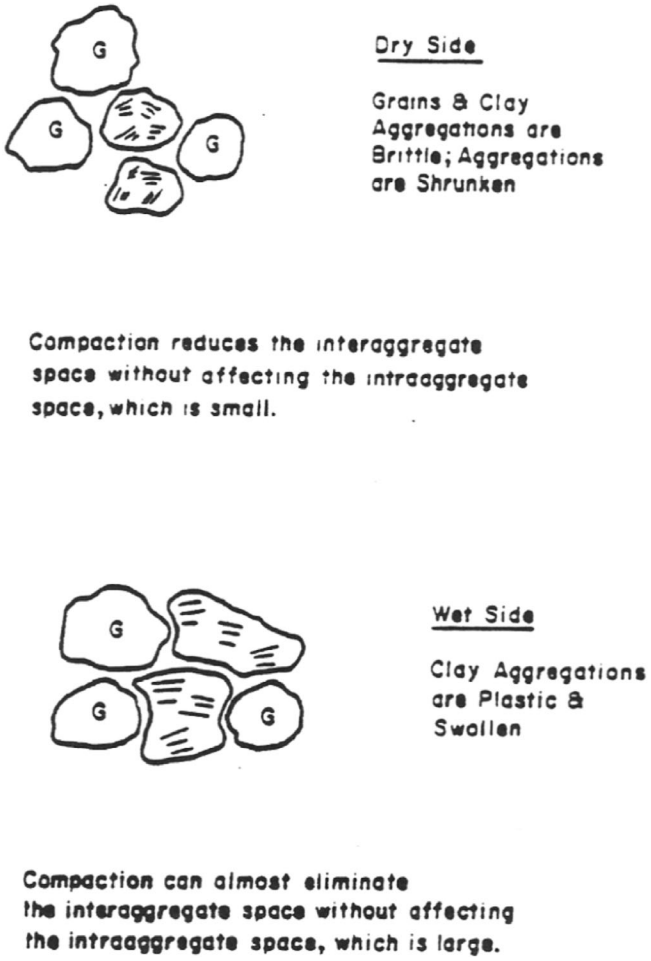

Figure 2.20 Hodek and Lovell's schematic of compaction effect on pores (Steadman 1987)

However, the net normal force acting at the particle contacts is also due to the different types of bonding structures and cementations formed between particles. These bonding structures and cementations have been discussed in Section 2.2.5. In addition, the collapsibility of compacted cohesive soils also depends on the distortion and size of the inter-aggregate and intra-aggregate pores. Hodek and Lovell (1979) proposed a physical model to describe the soil structure of compacted fills. This model consists of coarse particles and aggregates of fine particles. Two types of pores exist in this model, inter-aggregate and intra-aggregate pores. Inter-aggregate pores are much larger than intra-aggregate pores, and their size can be easily reduced with compactive energy. Conversely, the size of intra-aggregate pores is not highly affected by compaction efforts; however, the size of intra-aggregate pores varies depending on the as-compacted water content. Generally, dry side compaction produces smaller intra-aggregate pores whereas wet side compaction increases the intra-aggregate pores due to the swelling aggregate. Figure 2.20 shows a schematic of the effect of compaction on pores. Figure 2.21 presents Hodek and Lovell's model of the effect of saturation on the aggregate skeleton. In Figure 2.21, (a) is the as-compacted state, (b) is the state of collapse only, (c) is the state of swelling only, and (d) is the combination of collapse and swelling where swelling controls. Typically, the total final volume change (i.e. swelling or collapse of compacted soil mass) depends on the as-compacted water content which controls the initial size of inter-particles and affects water absorption in combination with the magnitude of shrinkage of inter-particle pores and the magnitude of swelling of intra-particle pores upon wetting.

2.3.2 Wetting-Induced Subsidence of Compacted Fills

For compacted fills, four main factors affect the magnitude of wetting-induced subsidence: applied stress, clay content, dry density and as-compacted water content (or, perhaps, more appropriately, degree of saturation). Other influencing factors include compactive prestress, principal stress ratio, and sample disturbance. These topics have been studied by various researchers within a wide range of scopes.

Lawton (1986) (see also Lawton et al. 1989) performed over 150 laboratory tests to characterize wetting-induced collapse in compacted soil. One-dimensional tests were completed using oedometers to simulate plane strain conditions in a fill, and three-dimensional tests were conducted using a triaxial apparatus to evaluate the effect of the minor principal stress. The soil used was a natural, expansive soil from Southern California, with 62% sand (by weight), 23% silt, 15% clay-sized particles, plastic limit of 19, liquid limit of 34, plasticity index of 15, and specific gravity of 2.73. It was a tan clayey sand with a USCS classification of SC and an AASHTO classification of A-6(2).

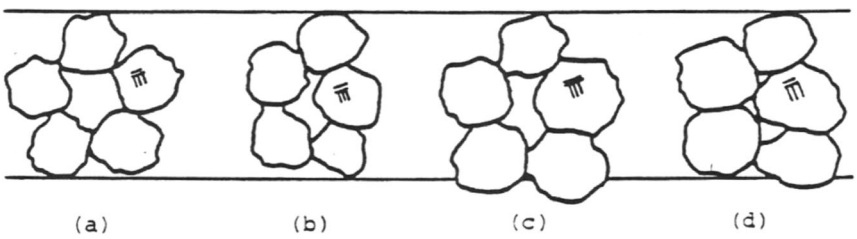

Figure 2.21 Hodek and Lovell's model of the effect of saturation on the aggregate skeleton (a) as-compacted state, (b) state of collapse only, (c) state of swelling only, and (d) combination of collapse and swelling with swell controlling (Steadman 1987)

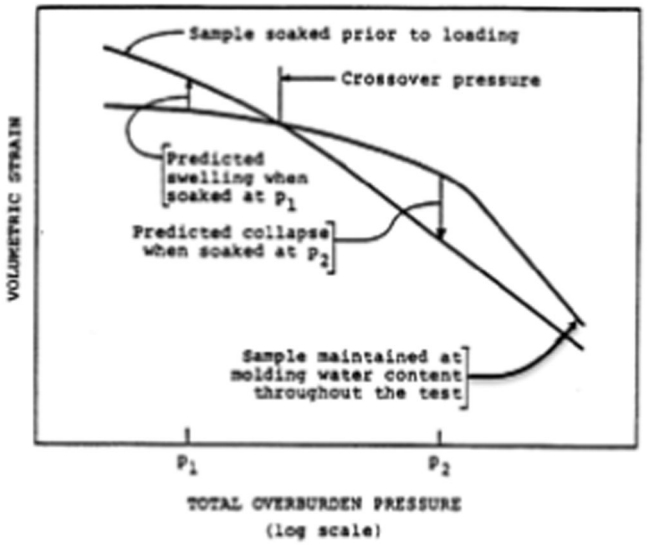

Figure 2.22 Typical double-oedometer test result on compacted fill (Lawton 1986)

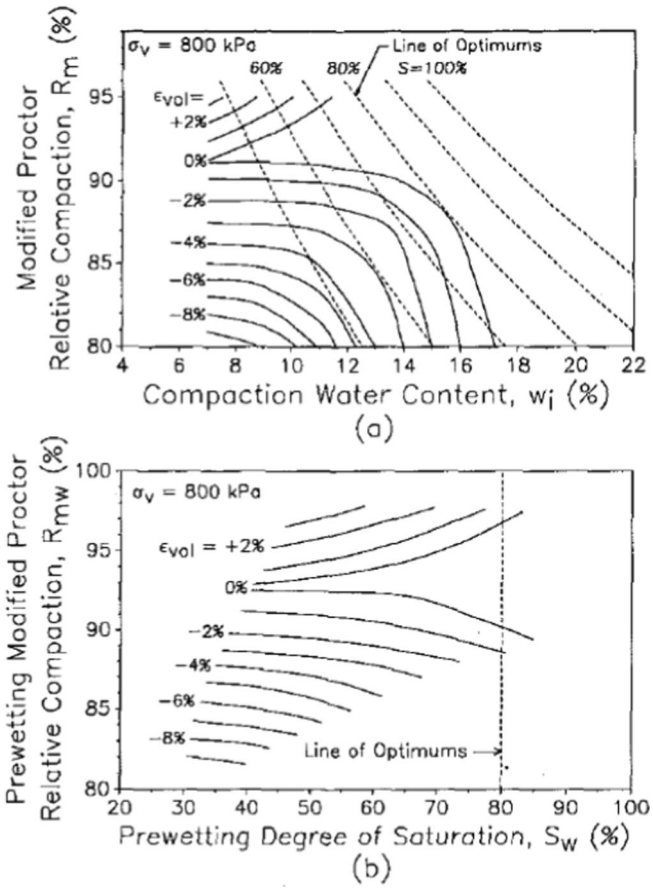

Figure 2.23 An example of isogram of wetting-induced volume change in terms of (a) as-compacted density and water content and (b) prewetting density and saturation under an overburden pressure (Lawton et al. 1992)

Modified and Standard Proctor tests yielded the following results: maximum dry density = 2.025 Mg/m^3 (Mod.) and 1.815 Mg/m^3 (Std); optimum water content = 10% (Mod.) and 15% (Std.). For this soil the line of optimum occurred at approximately 80% saturation.

Three different types of compaction were studied including impact, kneading, and static compaction. Lawton found a negligible difference in laboratory collapse measurements due to different compaction techniques. Tests were conducted at nominal relative compaction levels of 95%, 90%, 85%, and 80% (all references to Modified Proctor) and for nominal molding (as-compacted) water contents of 7%, 10%, 13%, 16%, and 19%.

Figure 2.22 shows a typical double-oedometer test result for the compacted soil. For the same relative compaction, collapse due to wetting tends to increase as water content is decreased. Tests conducted at water contents very wet of optimum (19% and 22%) showed negligible volumetric strain at all overburden pressures and were not included in plots of the results. As compaction water content increases, less swelling occurs at low overburden pressures. The curve crosses the plane of zero axial strain at a "crossover pressure" where the as-compacted curve falls below the saturated curve. At overburden pressures below this crossover, swelling occurs, and at values above the crossover, collapse occurs. The collapse strain increases up to a certain stress level, after which the collapse decreases. Lawton concluded that "for any given relative compaction and molding water content, there is a critical overburden pressure at which the magnitude of collapse is a maximum." This critical overburden pressure is equal to the compactive prestress developed in the soil during compaction and decreases as water content increases for a constant relative compaction. For constant water content, as relative compaction increases, less collapse occurs.

Lawton (1986) compiled collapse data in plots such as the one shown in Figure 2.23, which shows isograms of wetting-induced volume change in terms of (a) as-compacted density and water content, and (b) prewetting density and saturation under an overburden pressure. The data pertain to one particular value of the overburden stress. (Note that, contrary to the usual sign convention used in geotechnical engineering, in this figure, as well in some additional figures obtained from this same reference, collapse strains are plotted as negative, while swelling strains are plotted as positive). It is found that the contours of equal volumetric strain have two unique characteristics. First, the zero volumetric strain contour does not intersect the line of optimums (S $\sim$ 80%) in the collapse region (Figure 2.23(a)). Therefore, if a soil is compacted on or to the right of the line of optimum, no collapse will occur if the soil becomes saturated in the future. Secondly, there is a range of relative compaction where little to no collapse will occur regardless of water content or degree of saturation. For example, in

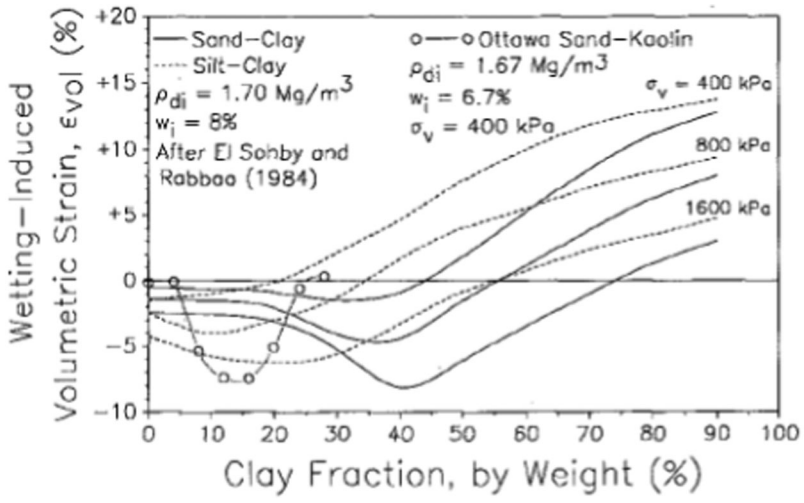

Figure 2.24 Influence of clay fraction on collapse potential (Lawton et al. 1992)

Figure 2.23 the contours indicate that for values of relative compaction above 91%, negligible collapse occurs for all values of molding water content. Further, at these high values of relative compaction, the samples increased in volume, then decreased and increased again to produce a net volumetric strain near zero; hence the negligible volume change is due to the fact that swelling and collapse cancel each other.

Lawton et al. (1992) remarked on the effects of the principal stress ratio and stated that "*the magnitude of wetting-induced volumetric collapse is independent of principal total stress ratio (σ_1/σ_3). However, the individual component of volumetric strain – axial and radial strain – depends significantly on principal total stress ratio.*" This is supported by results showing the equilibrium value of the coefficient of lateral earth pressure, K_0, approaching the full passive condition after substantial collapse occurs. On the effects of stress ratio see also Lawton et al. (1991).

Lawton et al. (1992) also provided a review of soil types susceptible to collapse, primarily focusing on the effect of clay content on collapsibility based on work done by El Sohby and Rabbaa (1984). Figure 2.24 shows the influence of clay fraction on collapse potential. The solid line pertains to results for "sand-clay" type materials, while the dotted line pertains to data for a "silt-clay" type material. For "sand-clay" type materials, the collapse potential first increases with an increase in clay content. This is due to the fact that clay expands during wetting and reduces the frictional shear resistance between the sand particles. However when the clay content dominates in the material (i.e. clay content over 40%), the clay swelling controls the behavior and reduces the subsidence caused by the softening and distortion of the macropeds. For a "silt-clay" type material, the effect of clay content is similar, but the critical clay content is smaller, around 10–25%. Also shown in Figure 2.24 are data for the "Ottawa sand-kaolin" mixture tested by Lawton et al. (1992). For these specimens (ρ_{di} = 1.67 Mg/m^3, w_i = 6.7%), which were flushed at σ_v = 400 kPa, the maximum collapse occurs at clay fractions between 12% and 16%. Further, for clay between 5% and 25%, the Ottawa sand-kaolin mix collapsed much more than either the silt-clay or sand-clay mixes shown in Figure 2.24.

Steadman (1987) followed the work of Lawton and also studied the effect of percentage of fines on collapse potential as well as the effect of compactive effort. This work made use of a laboratory fabricated soil comprised of oven-dried sand (C_u=2.67, C_c=1.19, USCS SP, AASHTO A-3, G = 2.66, only ≥#200 used), silt (tan-brown with 8.8% clay, PL=22, LL=27,

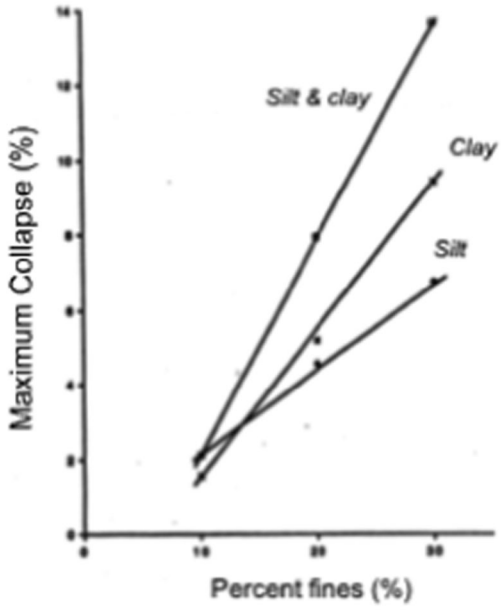

Figure 2.25 Influence of fines composition on collapse potential (Steadman 1987)

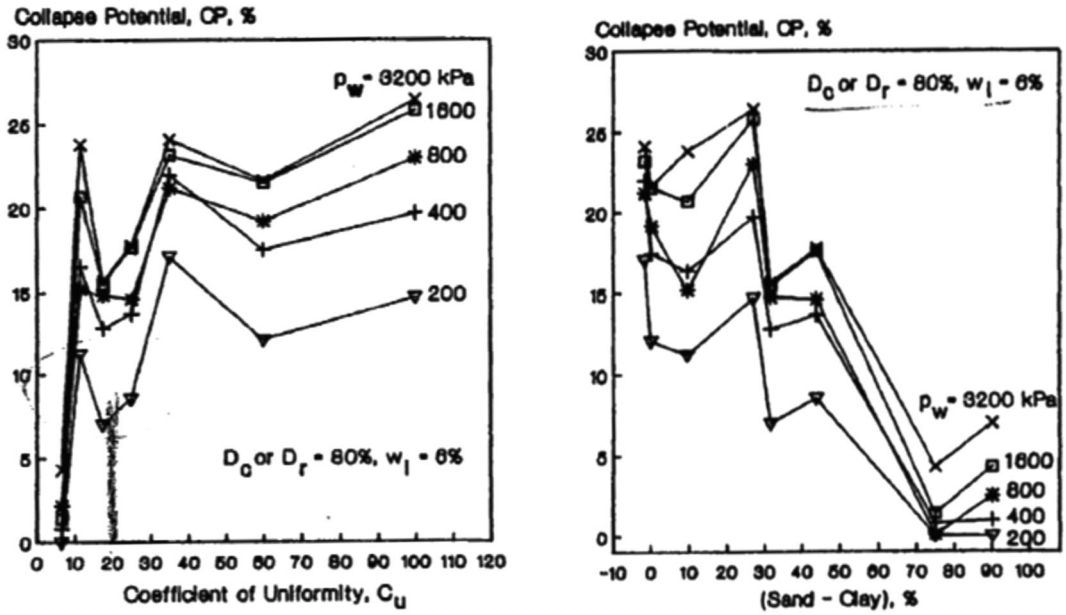

Figure 2.26 Influence of (a) Coefficient of Uniformity and (b) Sand-Clay Value on Collapse Potential (Basma and Tuncer (1992)

USCS ML, AASHTO A-4, G = 2.71, only <#200 used), and kaolinite clay (PL=27, LL=49, USCS CL, AASHTO A-6, G=2.61). Varying compositions of the soil were tested at relative compaction levels of 85% and 90% and at water content 3% below optimum.

Based on these tests, Steadman (1987) found that for low fines contents (approx. 10%), the maximum collapse was very small for all soils, in the range of 0.8 to 2.1%. For increasing percentages of fines (20% and 30%), collapse increased substantially. Additionally, as shown in Figure 2.25, the type of fines also played an important role. Soils containing equal parts of silt and clay collapsed more than the soil containing only clay or silt as the fine material. Further, soils containing only clay fines collapsed more than soils containing only silt fines.

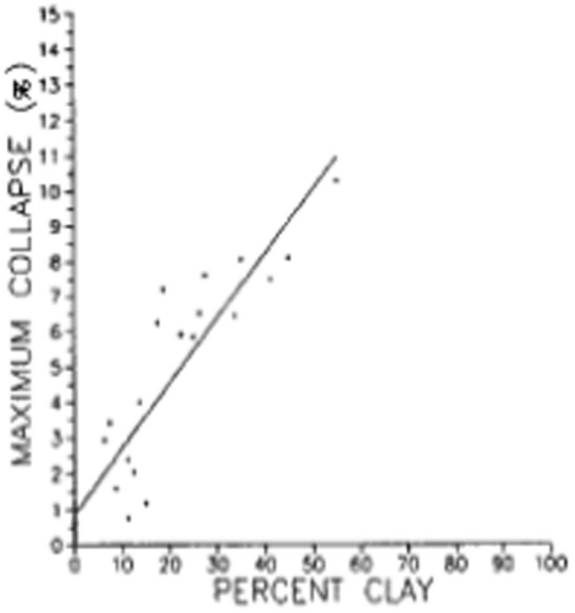

Figure 2.27 Maximum collapse as a function of percent clay (Alwail et al. 1994)

As expected, Steadman (1987) also found that as compactive effort decreases, the magnitude of collapse increases. Relating this result to the effect of fines, Steadman found a unique relationship between maximum collapse and compactive energy, which is soil dependent, and particularly influenced by the fines present.

Basma and Tuncer (1992) researched similar factors relating to collapse; they investigated the effect of initial dry unit weight and water content, then expanded the study to include the effects of soil type and the coefficient of uniformity, C_u. They used eight sets of native soils from Jordan classified as CL, CH, ML-CL, ML, SM, or SP-SC found in the vicinity of damaged structures with the following range of soil properties: C_u from 3.4 to 100.0, LL from 25.0 to 57.2, PI from 3.0 to 28.9, γ_{dmax} from 16.3 to 19.3, w_{opt} from 13.5 to 21.0, and G from 2.63 to 2.77. Single oedometer tests were conducted because they most closely replicated the field conditions of soaked-after-loading. These authors used the results of the testing to develop a model for predicting collapse from the following properties of a soil: coefficient of uniformity, initial water content, compaction dry-unit weight, and pressure at wetting. They evaluated this model for their own data, as well as for data available in the literature, including from the work by Houston et al. (1988) and Lawton et al. (1989).

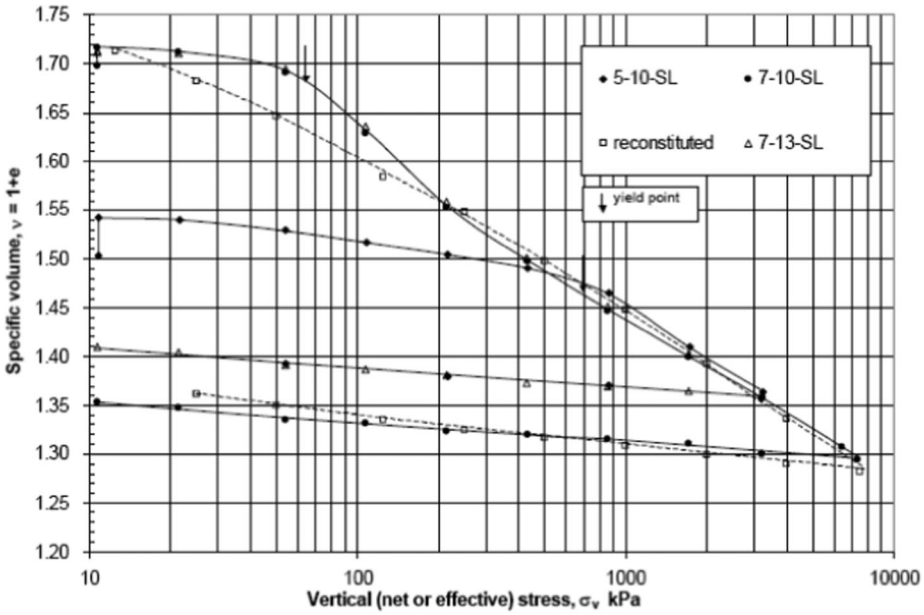

Figure 2.28 Compression curve for fully saturated oedometer tests (Jotisankasa 2005)

Similar to Lawton and Steadman, Basma and Tuncer (1992) concluded that higher initial values of dry unit weight and water content lead to a lower collapse potential. With regard to soil type, they found that a higher difference between percentage of sand and clay in the soil lowers the collapse potential at a specific stress level. Likewise, a higher C_u indicates a higher collapse potential. Figure 2.26 plots these relationships.

Alwail et al. (1994) further investigated the effect of clay fraction on collapse. These researchers created 25 soil combinations by varying the percentage of fines (15, 25, 35, 45, and 55 percent) and clay to silt ratio (01, 13, 11, 31, and 10) then tested them using the double oedometer technique. Their major finding was a linear relationship between maximum collapse and percentage of clay as shown in Figure 2.27. These authors also observed that soils with a higher clay/silt ratio experienced greater magnitude of collapse than soils with a lower clay/silt ratio.

Jotisankasa (2005) (see also Jotisankasa et al. 2007) ran a battery of suction-monitored tests on a compacted silty clay obtained mixing 70% of a silt size material consisting mainly of angular quartz grains with 20% kaolin, and 10% London clay. The resulting mixture had 26% clay content, 52% silt content, 22% sand content, liquid limit of 29%, and plastic limit of 18%. Three series of specimens were prepared: 7–10, 7–13, and 5–10, where the first number indicates the nominal as-compacted void ratio (i.e. for 7–10, e = 0.700) and the second number indicates the nominal as-compacted water content (i.e. for 7–10, w ~ 10%). Different tests were performed on the specimens varying the wetting and loading histories, in all cases loading the specimens beyond yielding, with the goal of confirming the uniqueness of the loading-collapse surface. Figure 2.28 portrays the compression curves for the tests involving soaking of the specimens at a low stress (~11 kPa) prior to loading. The figure highlights the different degree to which the three specimens swell as a result of soaking, and how they appear to follow the same normal compression line.

Houston et al. (1988) were amongst the first to devise combined field and laboratory measurements of collapse. To measure field collapse, they constructed a full-scale footing and loaded it to 66.3 kPa to simulate the conditions under a small commercial/industrial structure. Water was then ponded around the footing to saturate the underlying soil. By the end of the 12 day test, the water had infiltrated 2.3 m deep into the ground and 90 mm of collapse were measured. Double oedometer tests in the lab were performed on soil from the site to correlate the testing and predict field collapse; the predicted value of the field collapse was 91.7 mm, very close to the actual measured collapse. Additional contributions to the collapsible soils literature by Houston and co-workers include: Houston and Houston (1997) and Houston et al. (2001) which focus on engineering issues of collapsible soils and provide general guidelines for the identification of collapsible soils, the estimation of collapse potential and the effectiveness of mitigation methods.

Another case history is documented by Rollins et al. (1994). It pertains to the construction of a cement plant in Utah on an alluvial deposit (groundwater level about 30.5m below the ground surface, S=20–40%). At this site collapse settlements exceeding 100 mm (~ 4in) were observed to be caused by an increase in water content associated with poor surface drainage, a broken water line, percolation from the plant, as well as from unusually high precipitation.

Rollins et al. (1994) discuss also a second case history, this time dealing with the effects of wetting induced collapse on an embankment. This case history pertains to a storage reservoir in Nevada, constructed on an alluvial fan slope using materials excavated within the reservoir area. In this case, it was found that, despite the fact that the core materials were well compacted and protected by a liner, the settlement due to infiltration and leakage was close to 0.6 m(~23 in) leading to severe cracking of the embankment.

Pereira and Fredlund (2000) tested a residual silty sand at an initial water content of 10.5% and an initial dry unit weight of 14.75 kN/m^3 (93.9 lb/ft^3) using the double oedometer test with vertical stress up to 800 kPa. These testing conditions were intended to replicate the conditions existing at the first filling of a small dam. What they found was no collapse for $\sigma_v < 50$ kPa, 3% collapse for $\sigma_v = 100$ kPa, and 7.2% collapse for $\sigma_v = 200$ kPa. The soil exhibited low compressibility when loaded in the as-compacted condition. When inundated with water at higher stresses, the collapse was greater; for inundation at $\sigma_v = 400$ kPa, the collapse strain exceeded 11%, and inundation at $\sigma_v = 800$ kPa generated a similar response.

Miller et al. (2001) also examined collapse problems in their investigation of the effects of the as-compacted water content and dry unit weight on wetting-induced collapse. Their work included single and double oedometer tests complemented by centrifuge tests to model a 20 m high embankment. All tests were performed using a CL-ML (A-4) soil with liquid limit of 30%, plastic limit of 22%, fines content of 73%, clay fraction (<0.002 mm) of 20%, optimum moisture content of 14.6%, and maximum dry unit weight of 17.7 kN/m^3 (112.7 lb/ft^3). Three centrifuge tests were performed compacting the soil to: a relative compaction of 95% and w = 12.5%; a relative compaction of 90% and w = 10.6%; and a relative compaction of 95% and w = 9.6%. They found substantial agreement between single and double oedometer tests, and values of the collapse index varying between 0.4% and 1.8%, depending on the compaction conditions, and indicating a slight degree of collapse according to ASTM D5333, They found that the wetting-induced settlements mesured in the embankment tested in the centrifuge were underpredicted by a factor of 2.2 by the oedometer tests. Their work also confirmed that collapse potential increases as molding water content and dry density decrease.

Kropp et al. (1994) report a case study of collapse settlement of a deep compacted fill. At the site al old quarry, about 25 m deep, was filled using interbedded layers of GM, GW, GP, SM, SP, and ML soils, placed at 1–3% below optimum (with some layers at 5–7% below optimum) and compacted to 92–96% relative compaction. Condominiums were built on the site. Over time significant differential settlements were observed at the site, and attributed to wetting of the fill. Two full scale wetting tests and laboratory tests were conducted to better understand the phenomenon. The laboratory tests on soil (that, however, did not include the large rock fragments present at the site) compacted to 90% R.C. and water content 2–3% dry of optimum showed 3–5% collapse at 400 kPa, no collapse at 100 kPa and slight swelling at 25 kPa. Additional flushing of the previously wetted specimens under high gradients (4–320) led to an additional settlement of 0.5% to 1.5%. The large-scale field wetting tests involved wetting under controlled conditions at depth through piezometers, and resulted in a maximum settlement of 100 mm under the center of the load, with the settlement decreasing radially outward. The lower 9 m of fill settled 98 mm with the deepest 3 m causing half of the total surface settlement and exhibiting an average collapse strain of 1.5%. Based on these results, the authors recommend pre-wetting of the fill combined with mud-jacking of the floor slabs to minimize differential movements.

TABLE 2.8
Collapse measurements on Indiana loess (adapted from Kim et al. 2007)

Clay (%)	20	20	20	10	25	30
R.C. (%)	100	90	80	80	80	80
w (%)	16.2	9.5	7.2	7.0	7.1	7.6
I_c (%)	0.16	0.19	3.83	4.33	3.5	3.2

Kim et al. (2008) investigated the collapse behavior of an Indiana loess (LL=32.2%, PL=22.9%, Gs=2.65, ~92% finer than 0.075 mm, and ~20% finer than 0.002 mm) for use as fill in highway embankments. The soil was tested both alone and with the addition of 5–10% clay (LL=46%. PL=20%). In addition, controlled sieving of the loess was used to produce a soil with 10% clay. The experimental program included compaction tests and single oedometer tests (with wetting at 100 kPa) on the soils with 4 different clay contents (10, 20, 25, and 30%). The results of the collapse potential measurements are summarized in Table 2.8. As expected, increasing the degree of compaction greatly decreases the collapse potential and total compression of the soil. These authors also found an increase in collapse potential with a decrease in the clay fines.

CHAPTER 3 LOESS IN INDIANA

Indiana loess originated from glacial deposition and loess is distributed across Indiana, with large concentrations in southwest Indiana. The Illinois ice entered Indiana from the north and northeast and flowed south from Lake Michigan containing deposits of silt, sand, and gravel. The melting water carried the deposits and left them as outwash along valleys across Indiana. The strong westerly winds blew the silt and dumped it across Indiana with the most significant deposits occurring downwind of large rivers e.g. the

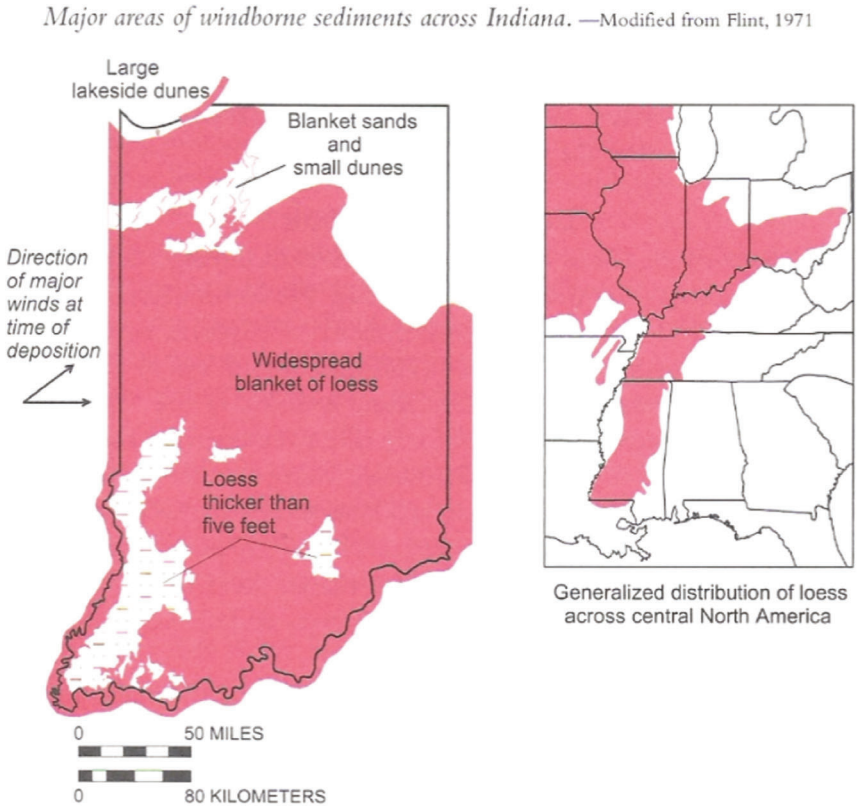

Figure 3.1 Maps of loess distribution in Mid-West and Indiana (Camp and Richardson 1999)

Wabash River. This is evident by the varying thicknesses of loess across Indiana; near the Wabash River deposits are close to 25 feet thick, and they decrease to a few inches along the eastern side of Indiana. The following sections discuss the distribution of Indiana loess.

3.1 Roadside Geology of Indiana (Camp and Richardson 1999)

Camp and Richardson (1999) described the geology near the roadsides in Indiana. They found that the entire state of Indiana is covered by loess deposits with thicknesses of a few inches to a couple feet, except the northeast part of Indiana. Figure 3.1 shows a general distribution of loess in the Midwest and Indiana. The southwest region of Indiana and a small area in the southeast near the Ohio River have the most appreciable loess deposits with thicknesses potentially over 25 feet. In Indiana, loess underlies major highways such as I65, I64, I70, US31, US41, US50, US40, and IN64. This book does not provide more detailed information such as thickness and properties. Figure 3.2 show the roadside geology of I65, I64, I70, US31, US41, US50, US40, and IN64. The loess area mapped in the figure is for deposits thicker than 5 feet; these are underlain by Illinoian till in many places.

3.2 Quaternary Geology Map of Indiana (Hester 1997)

Figure 3.3 shows the Quaternary Geology Map of Indiana. In this map, the pink area under "Wisconsin Deposits" with a symbol, "lo", is the major loess area (typically over 3 feet thick). It can be seen that the thick loess deposits mainly distribute along the East bank of Wabash River. In addition to the major loess area, the areas with symbols "tv", "ta", "ϕ", "T", "TR", "Rs", and "R1" all contain surface layers of loess. Figure 3.4 presents a map of major highway routes in combination with the geological map of Indiana. From this map it can be seen that deformations due to wetting induced collapse of loess deposits may potentially be a concern for the following routes: I-70, I-64, I-164, US50, and US41. Figure 3.5 shows the quaternary geological map with the Interstate 69 extension from Indianapolis, IN to Evansville, IN superimposed. The new constriction of the I-69 extension clearly crosses the major loess area in southwest part of Indiana. With that in mind, the potential for collapse should be considered for this construction.

3.3 Map of Indiana Soil Regions (Purdue University, USDA, and Indiana Soil Conservation Service 1977)

Purdue University, USDA, and Indian Soil Conservation Service provided a soil map (Figure 3.6)

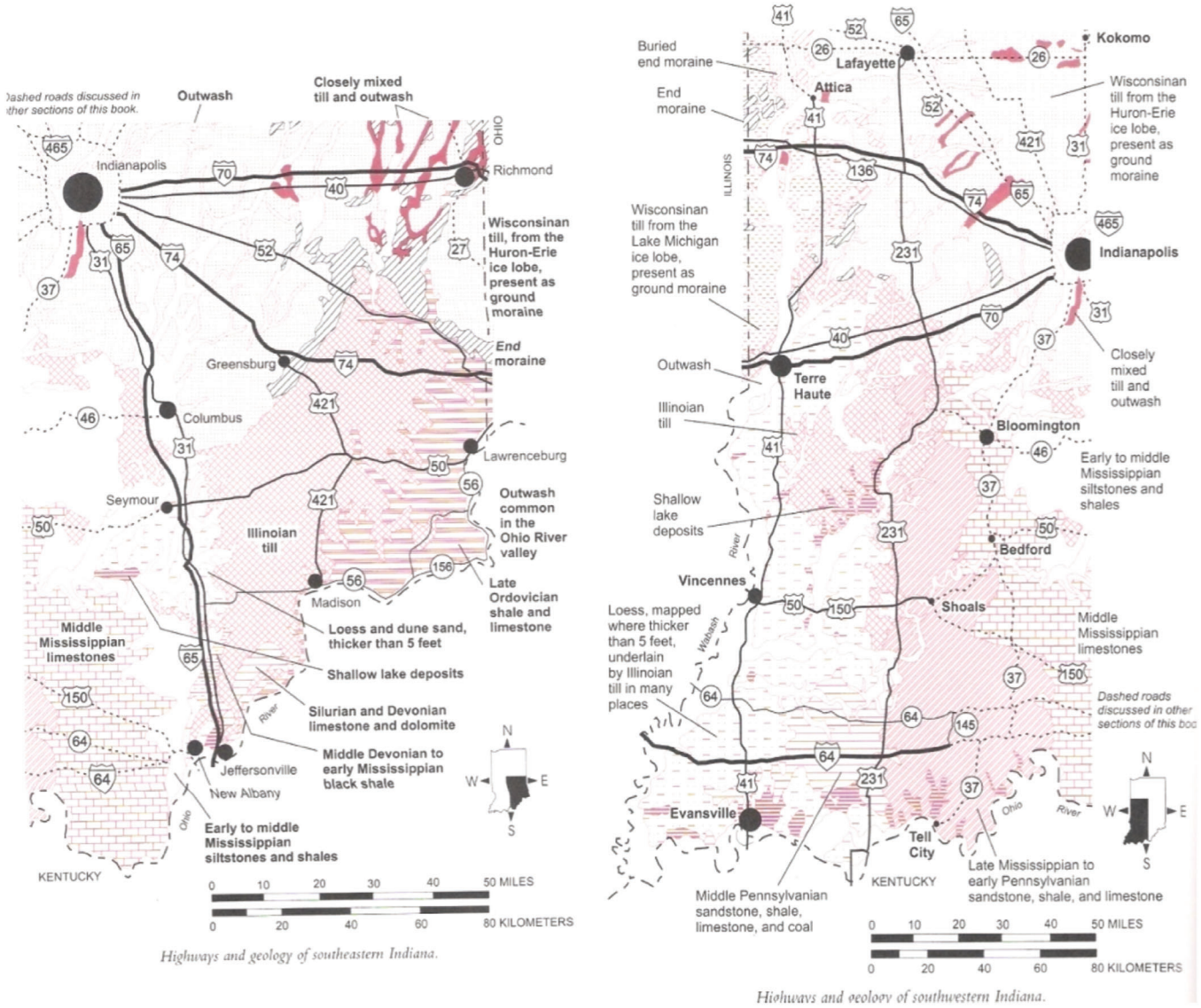

Figure 3.2 Maps of roadside geology in southern Indiana (Camp and Richardson 1999)

to classify Indiana soils into 13 soil regions. Most of the regions are covered by a surface layer of loess with varying thickness. Figure 3.7 is the map showing the thickness of loess deposits after the soil map. The thickest loess deposits are located in the southwest part of Indiana; this is consistent with information provided above. Central and southeast Indiana contain thin and moderately thick loess deposits, respectively. South-central Indiana is covered by some discontinuous loess.

3.4 Engineering Soil Maps of counties in the Indiana State (JHRP reports)

Since the 1970s, the Indiana Department of Transportation in conjunction with Purdue University has taken on through the Joint Highway Research Program (JHRP), now Joint Transportation Research Program (JTRP), the development of engineering soils maps of each county in the State of Indiana. The distribution of loess in several countries in southwest Indiana, where the most substantial deposits are located, is summarized in the following sections, based on these reports.

3.4.1 Knox County

Figure 3.8 is a isogram (contour) map of loess thickness in Knox County. The west side of Knox County is the Wabash River. Loess is deposited in large portions of this county and distributed from West to East, mantling the Illinoian drift on the upland areas. The thickest deposit in Knox County is about 200

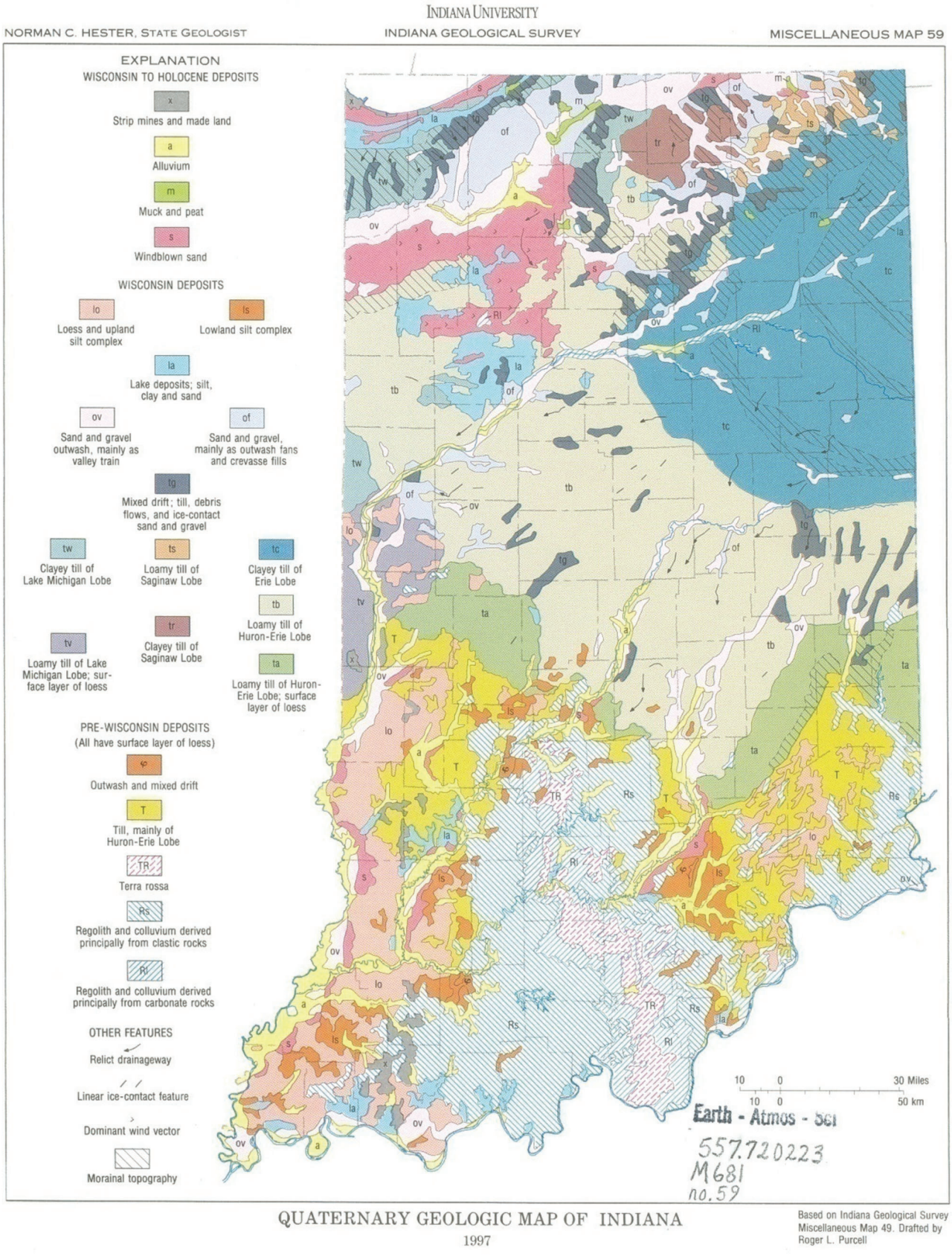

Figure 3.3 Quaternary Geology Map of Indiana (Indiana Geological Survey, Miscellaneous Map 59)

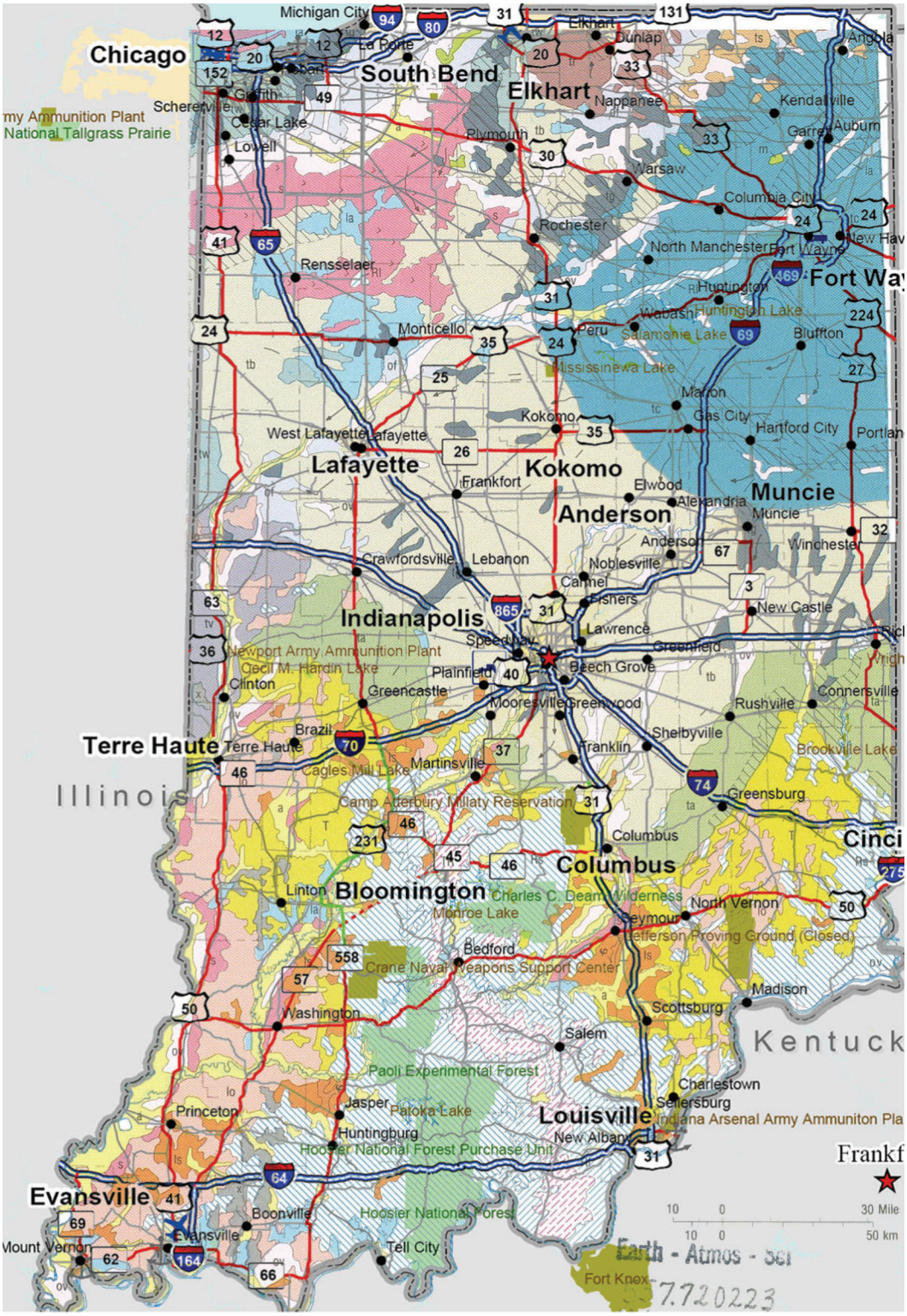

Figure 3.4 Quaternary Geology Map of Indiana with major highway routes (Indiana Geological Survey, Miscellaneous Map 59 and www.indot.gov)

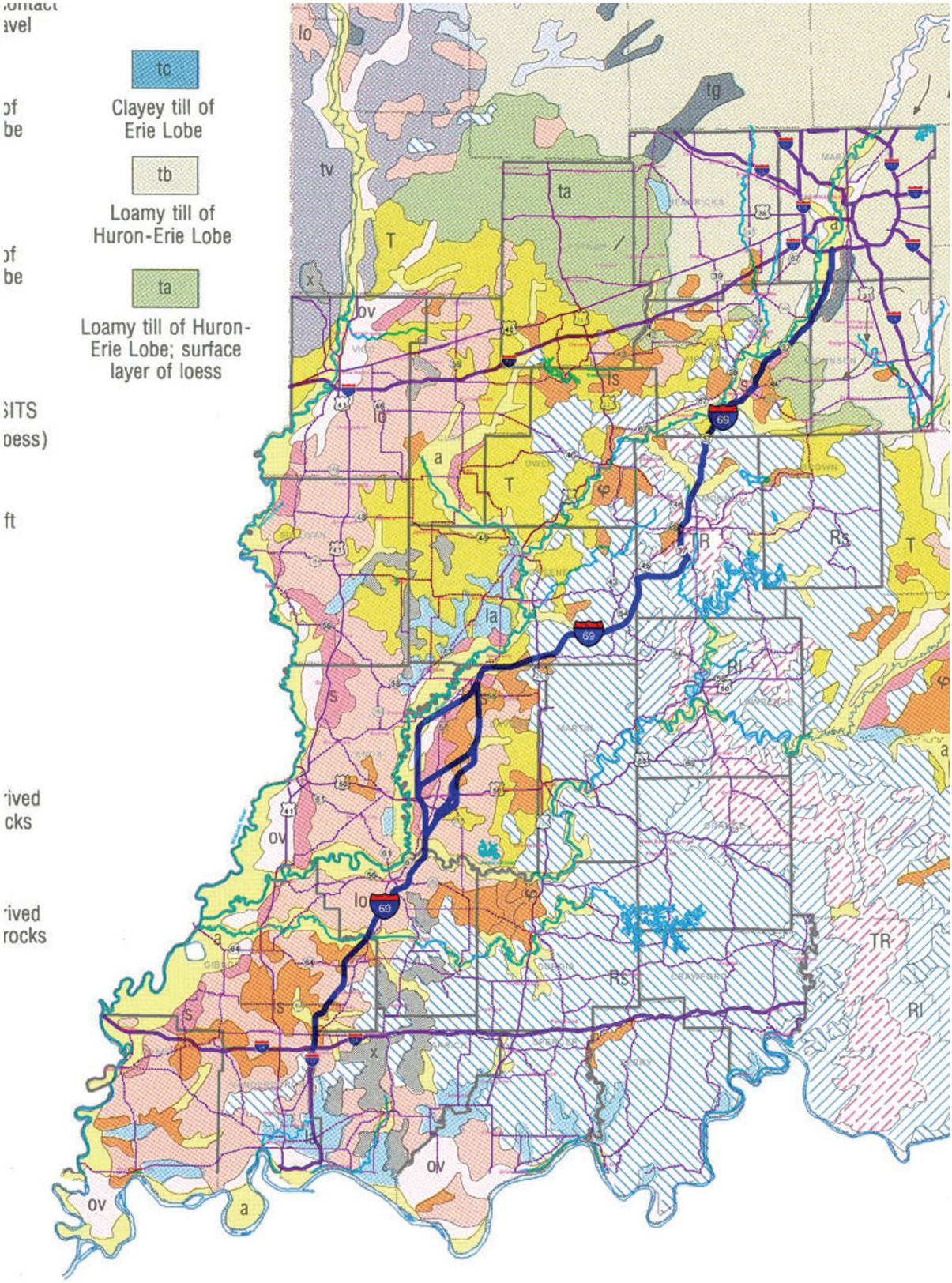

Figure 3.5 Quaternary Geology Map of Indiana with I-69 extension from Indianapolis to Evansville (Indiana Geological Survey, Miscellaneous Map 59 and www.i69indyevn.org)

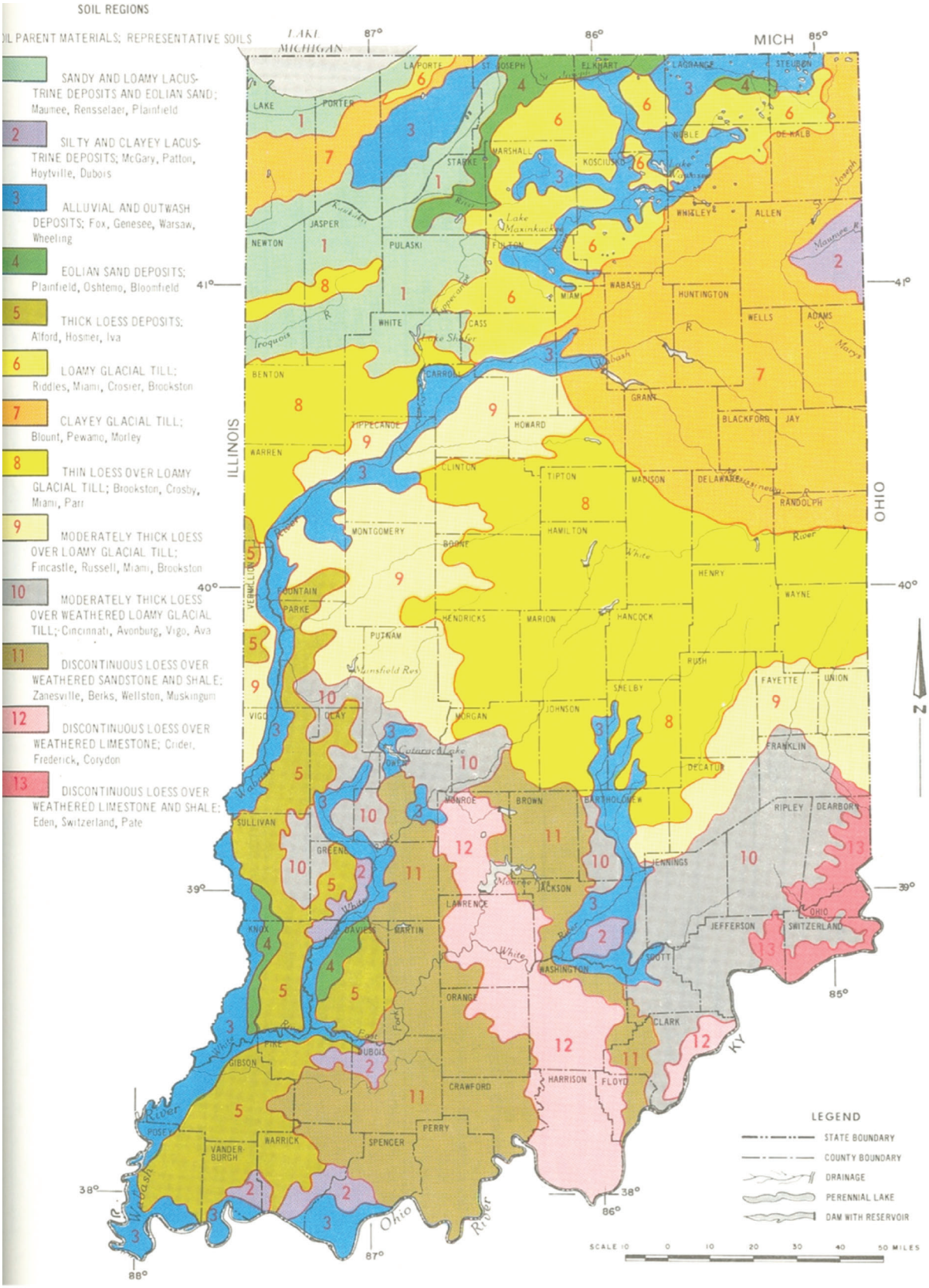

Figure 3.6 Map of Indiana Soil Regions (Purdue University, USDA and Indiana Soil Conservation Service)

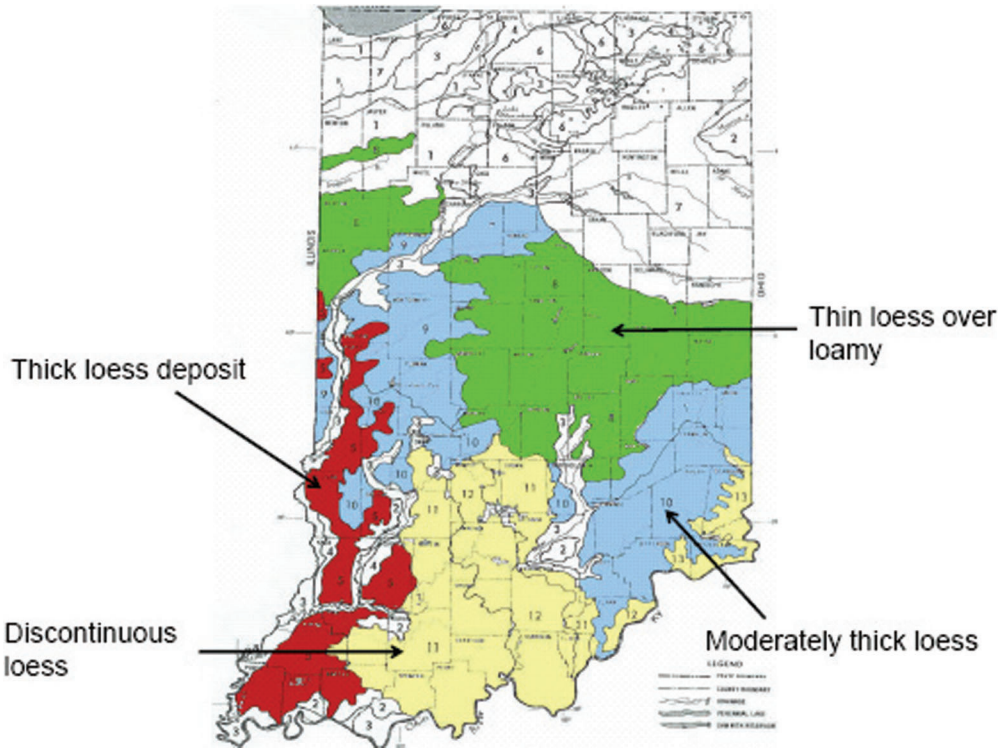

Figure 3.7 Map of loess deposits in Indiana (After Map of Indiana soil regions by Purdue University, USDA and Indiana Soil Conservation Service)

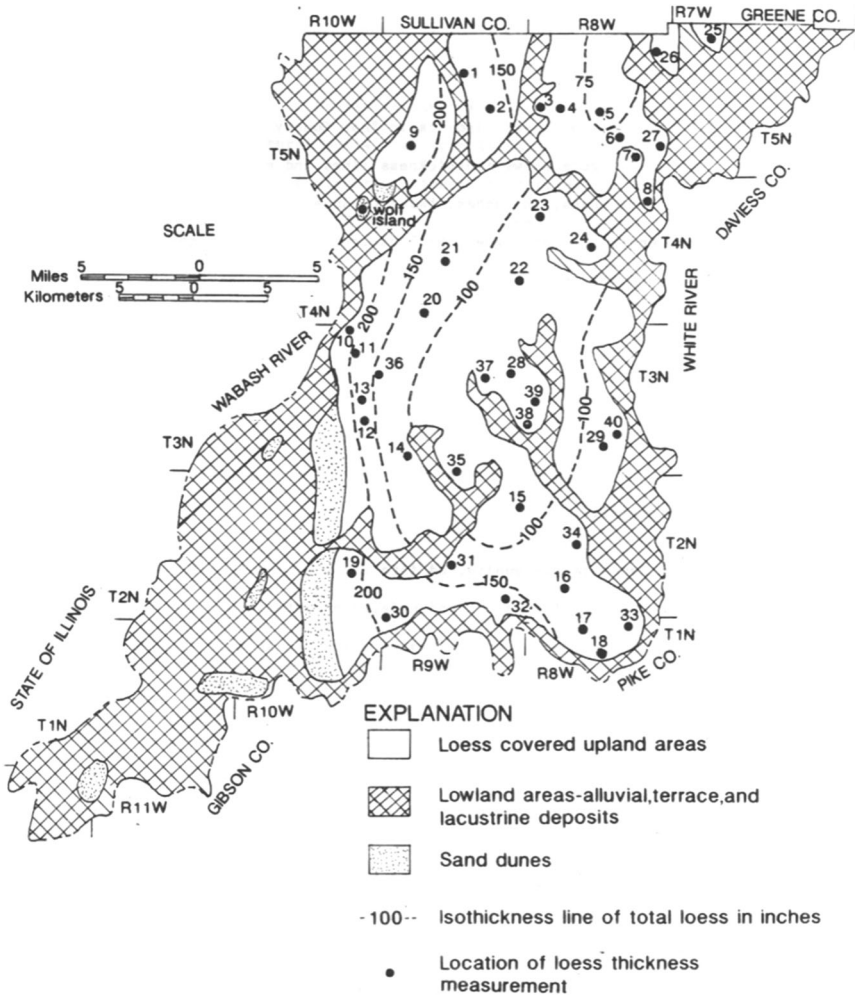

Figure 3.8 Isograms of loess thickness in Knox County (Johnson 1988)

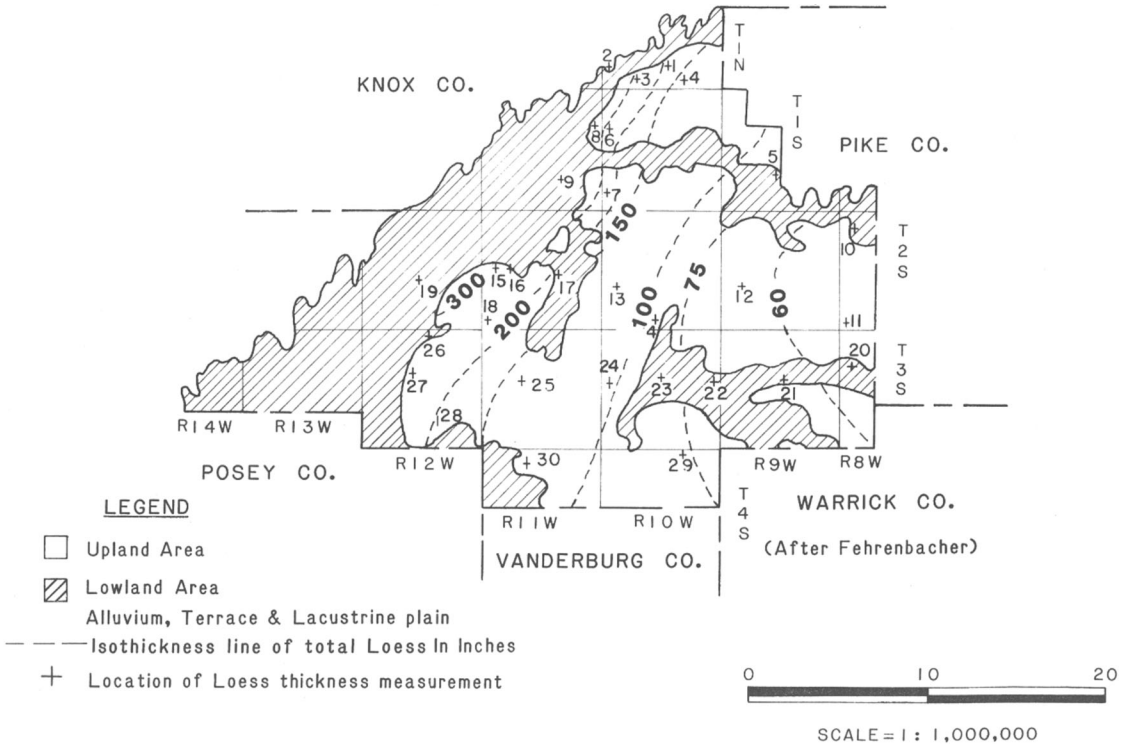

Figure 3.9 Isograms of loess thickness in Gibson County (Huang 1984)

inches and the thickness generally decreases toward the northeast of the county reaching a thickness of only 25 inches near the border with Greene County.

3.4.2 Gibson County

Figure 3.9 is the isogram map of loess thickness in Gibson County. It shows that one-third of the total area of Gibson County is covered by moderately deep loess deposits (5–25 feet). The west-central part has the thickest loess deposits and there is a decrease in thickness in the East. The thickest loess deposits occur on all the ridge tops where erosion is minimal, and the thickness quickly decreases in the nearby streams and gullies.

3.4.3 Posey County

Figure 3.10 is the isogram map of loess thickness in Posey County where all the upland area of Posey County is mantled by windblown silt or loess deposits. The thickest loess deposits are around 300 inches located at the west-central and south-east portion of the county. The thinnest loess deposits are to the East near the border with Vanderburgh County. The thick loess deposits are underlain by Illinoian drift in the northern half and inter-bedded by sandstone and shale bedrock in the southern half of the county.

3.4.4 Vanderburgh County

Figure 3.11 is the isogram map of loess thickness in Vanderburgh County. Approximately half of the upland area in Vanderburgh County is covered by moderately deep loess deposits (6–15 feet). The thickest loess deposits are about 300 inches and are located in the southwest portion of the county. The thickness tends to decrease toward the northeast.

3.4.5 Warrick County

Figure 3.12 is the isogram map of loess thickness in Warrick County showing that about one-seventh of the county is covered by moderately deep loess deposits. The thickest loess deposits are about 200 inches in the Southwestern corner of the county, and the Northeastern corner of the county has the thinnest loess deposits of about 50 inches. The general distribution is from the Southwestern portion of the county near the Ohio River toward the Northeast.

3.4.6 Spencer County

Figure 3.13 is the isogram map of loess thickness in Spencer County. Almost one-sixth of Spencer County is covered by moderately deep loess deposits (3–15 feet). The distribution of the loess is similar to that of Warrick County. The Southwestern corner has the thickest loess deposits of over 200 inches, while the

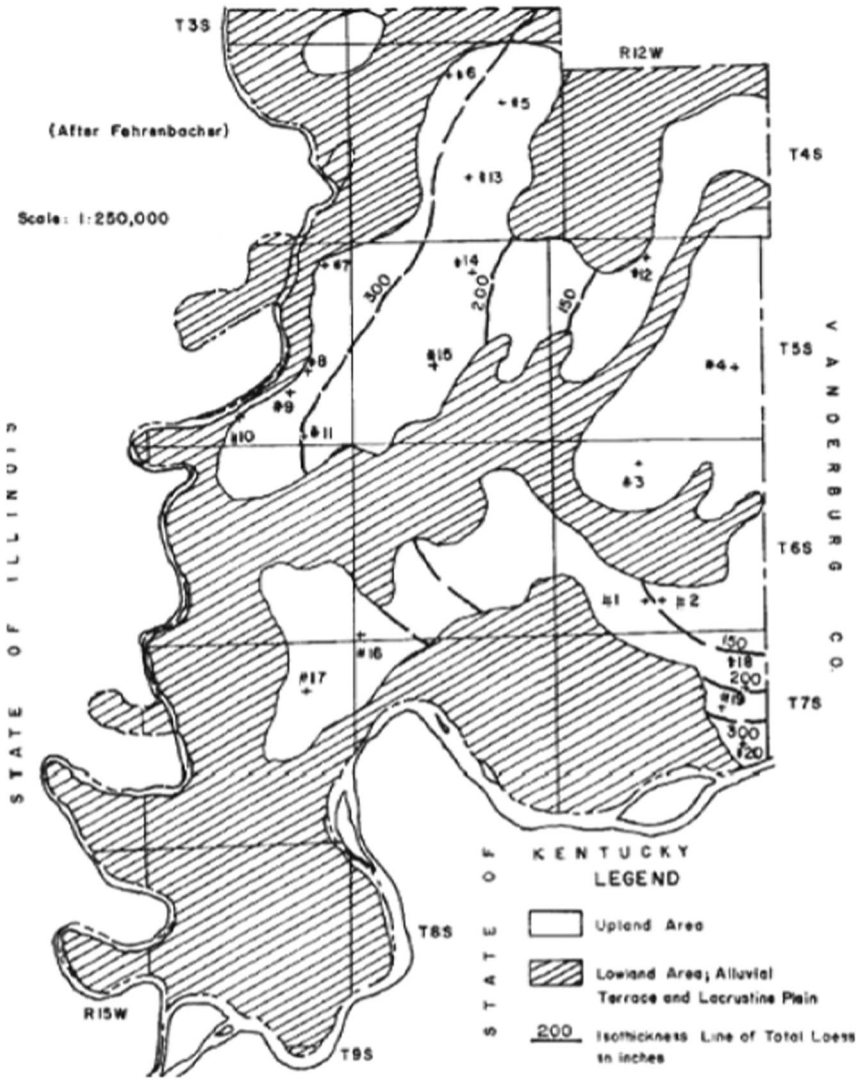

Figure 3.10 Isograms of loess thickness in Posey County (Yeh 1982)

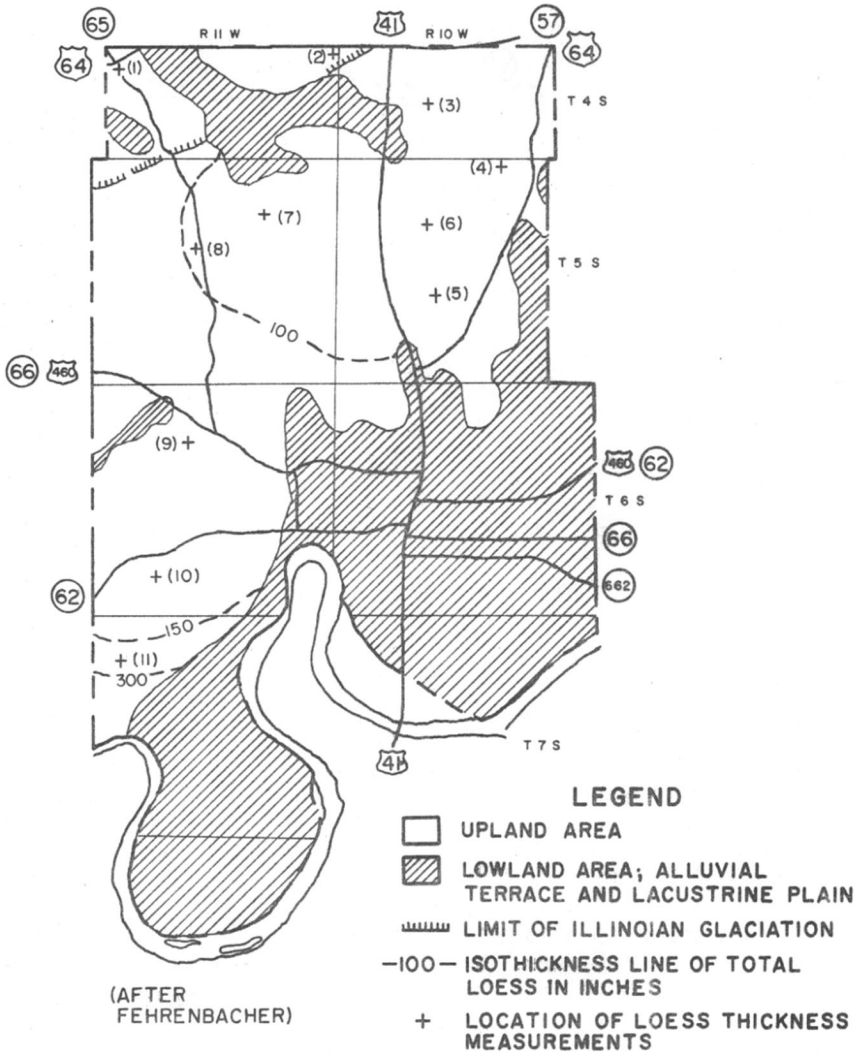

Figure 3.11 Isograms of loess thickness in Vanderburgh County (Yeh 1975)

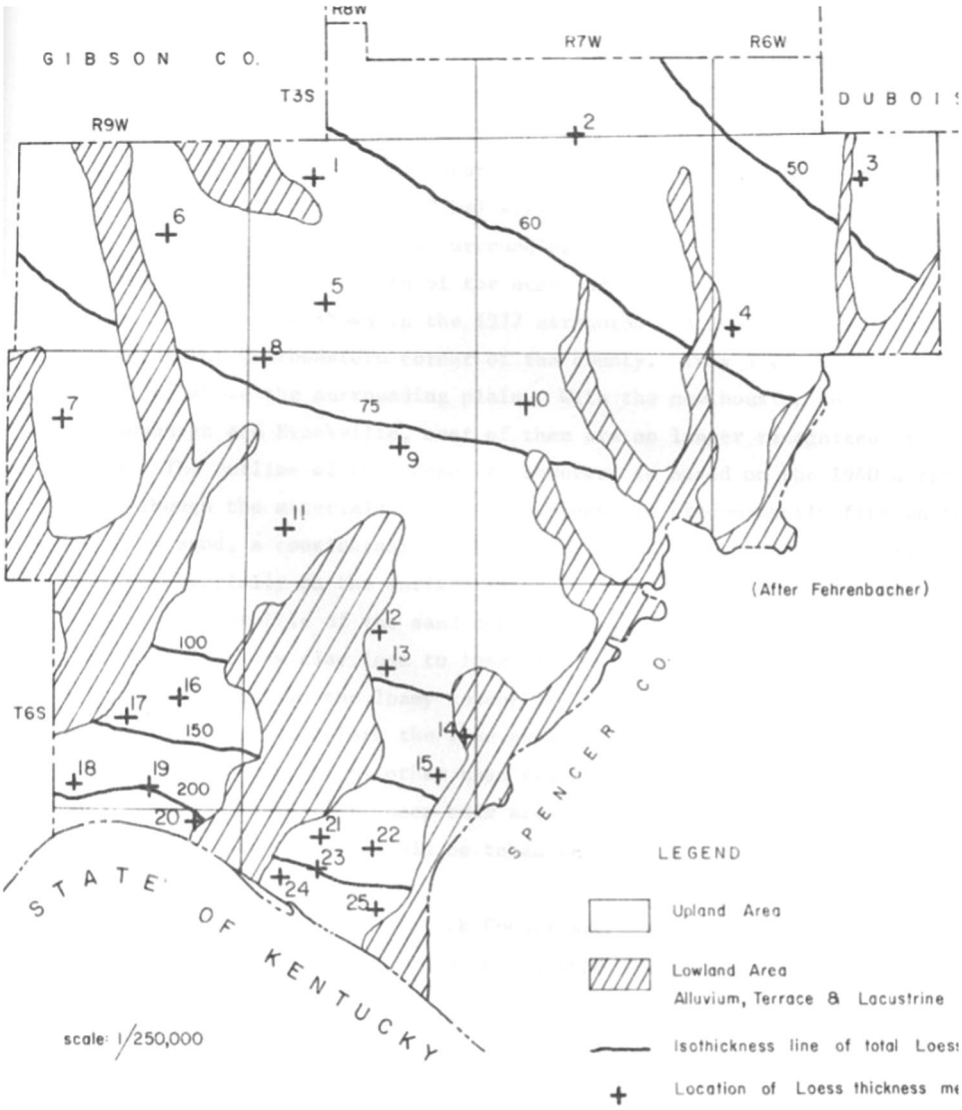

Figure 3.12 Isograms of loess thickness in Warrick County (Yeh 1979)

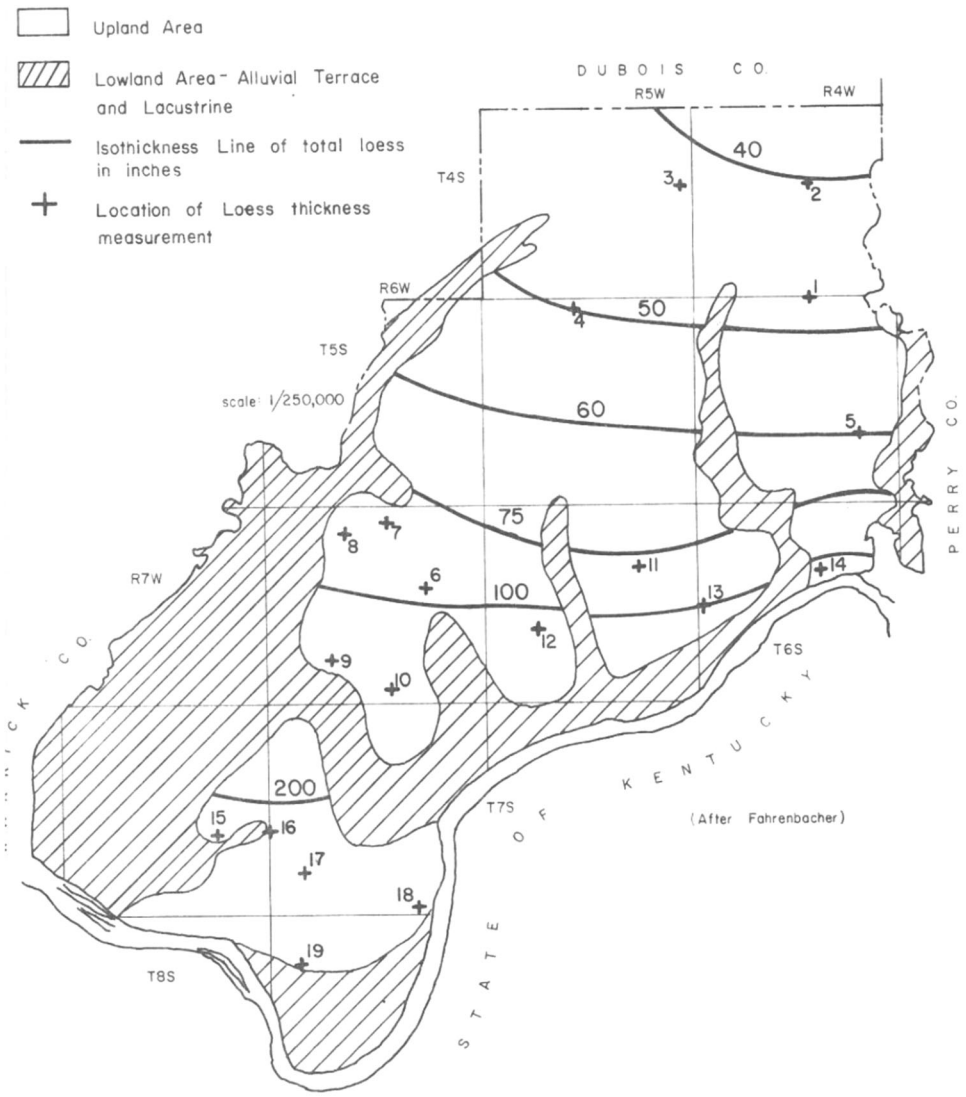

Figure 3.13 Isograms of loess thickness in Spencer County (Yeh 1978)

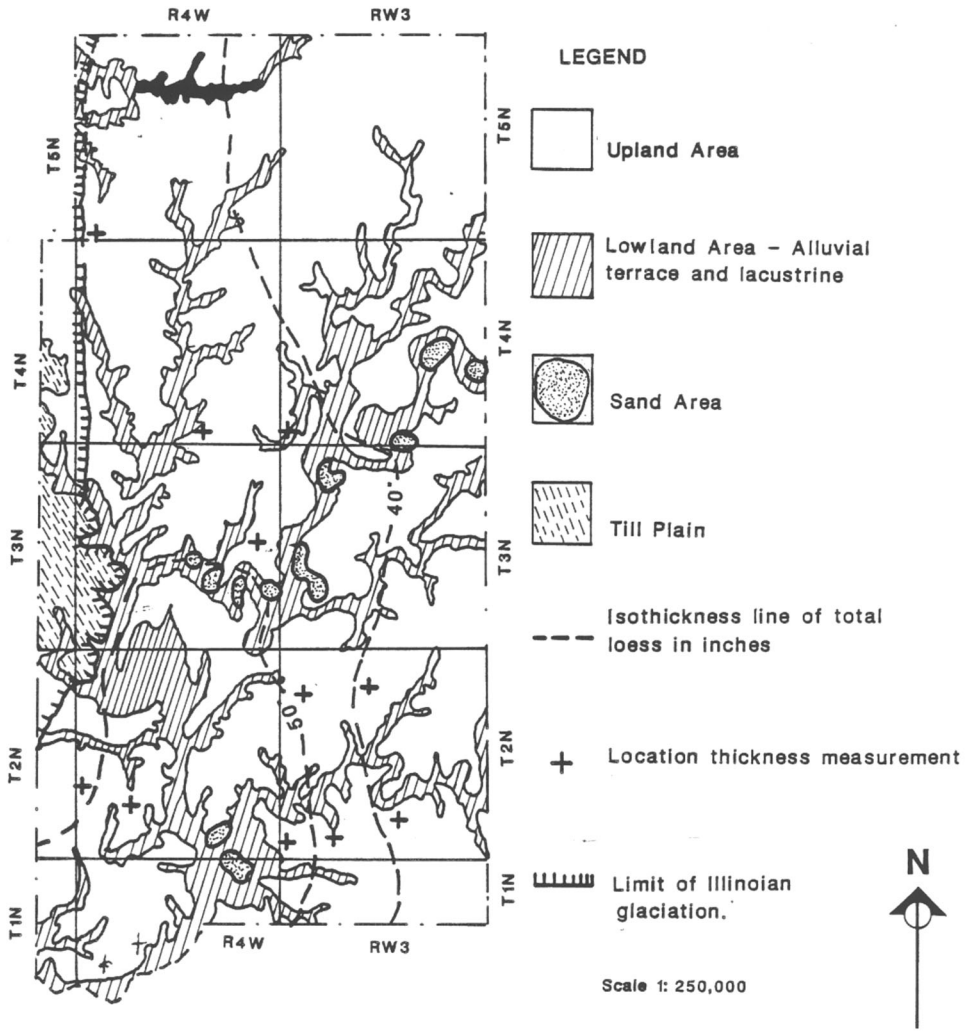

Figure 3.14 Isograms of loess thickness in Martin County (Okonkwo 1986)

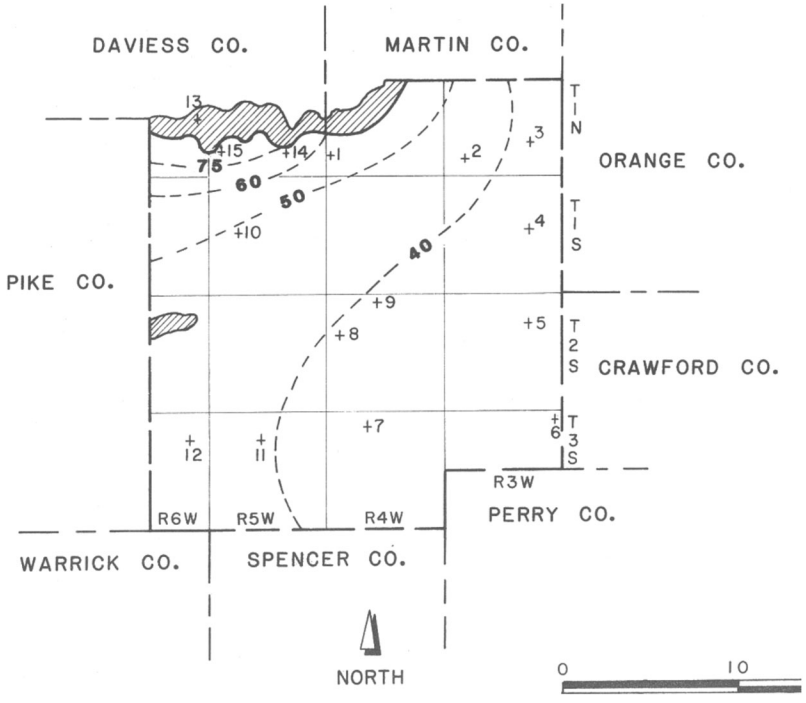

Figure 3.15 Isograms of loess thickness in Dubois County (Huang 1983)

Northeastern corner only has 40 inch deep loess deposits. The moderately deep loess deposits are confined along the narrow ridge tops.

3.4.7 Martin County

Figure 3.14 is the isogram map of loess thickness in Martin County showing extensive loess deposits covering nearly all the upland in the county. The average thickness of loess is about 50 inches, and it is distributed fairly evenly without any major variance in thickness. The thickest loess deposits are located near the valley of the East Fork White River, which flows through the southwest-central part of the county.

3.4.8 Dubois County

Figure 3.15 is the isogram map of loess thickness in Dubois County. It shows that the entire area of Dubois County is covered by thin loess deposits with thicknesses of 40 to 75 inches. The thickest loess deposits are at the Northwestern corner of this county, where the parent soil is leached loess underlain by glacial till. The loess tends to decrease in thickness toward the Southeastern corner of this county. Dubois County and Martin County are near the Eastern border of the main loess deposition area in Southwest Indiana. Discontinuous and thin loess deposits appear in the East of these two counties.

CHAPTER 4 MATERIALS AND METHODS

4.1 Introduction

This chapter presents the materials and methods employed for the experimental program. The chapter is organized in three main sections. Section 4.2 summarizes relevant information for the two soils used for the tests, including index properties, particle size distribution, classification and compaction behavior. Section 4.3 illustrates the equipment and methods used to prepare the test specimens and conduct the double oedometer tests. Finally, Section 4.4 summarizes the experimental program.

4.2 Soil Samples

4.2.1 Site Selection and Sampling Procedures

Samples obtained from two different sites were used for the experimental program presented in this report. One sample was obtained in Washington, IN (Daviess county) on US150, in proximity to the I69 corridor (Figure 4.1a). The second sample was obtained from the Purdue owned Throckmorton Farm in Tippecanoe County (Figure 4.1b).

The Washington site was selected as it is located in Daviess county, which is one of the areas in Indiana with the thickest deposits of loess (e.g. see Figure 3.6 and Figure 3.7). Soil from this site is herein referred to as Soil A.

The Tippecanoe site was selected for its proximity to Purdue, its accessibility, and the relative ease of sampling. The site was identified through a search of the USDA-National Soil Survey Center Laboratory Research Database (http://ssldata.nrcs.usda.gov) conducted with the assistance of Professor Phillip Owens of the Purdue Department of Agronomy. The USDA site contains physical and chemical data for approximately 10,000 soils in Indiana alone. Using the database, sampling sites were identified in Tippecanoe County, by searching through the Pedons for silty and loamy soils near the surface with less than 20% sand. The lower boundary of the loess layer was generally found by the Horizon indicator of "2Btg"; above this horizon the soil has a low sand content. Appendix A contains a sample print-out of the results of a query conducted using the USDA database.

Shallow loess deposits were identified at a Purdue Agriculture research farm in southern Tippecanoe County approximately 10 miles south of Purdue's West Lafayette campus. Figure 4.1b shows the location of the Throckmorton Farm site and sampling pit. This soil is herein referred to as Soil B.

Disturbed samples were collected at both sites. At the Tippecanoe site six five-gallon buckets of soil were gathered within on meter of the surface from an existing test pit. The soil from the buckets was mixed together in the lab to reduce the effects of spatial variability, and air-dried prior to storage. At this site high quality undisturbed block samples of loess were also obtained from the existing pit. These block samples were taken from within 1 meter of the surface using a method adapted from Galvao et al. (2003). Specifically, after constructing a shelf, and excavating the sample by hand using a sharp knife, a plastic cylinder was placed around the sample, and insulating foam was injected into the space between the soil and the cylinder to provide confinement, permit undercutting of the sample, and ensure safe handling, transportation and storage of this very brittle soil. Figure 4.2a shows the constructed shelf, carved sample (top), and a protected sample ready to be undercut (bottom). Figure 4.2b shows the expanded foam protecting the soil inside the plastic cylinder.

4.2.2 Daviess County Soil Sample (SOIL A)

Tests were performed to determine Atterberg limits, particle size distribution, specific gravity and compaction behavior of Soil A. Atterberg limits and particle size analysis are essential for soil classification, while an accurate estimate of the specific gravity is required for calculation of the phase relations. Table 4.1 summarizes the results of these tests, and indicates the standard followed in determining each property. Figure 4.3 presents the particle size distribution curve obtained by averaging data from two independent hydrometer tests. As seen in Table 4.1, Soil A can be

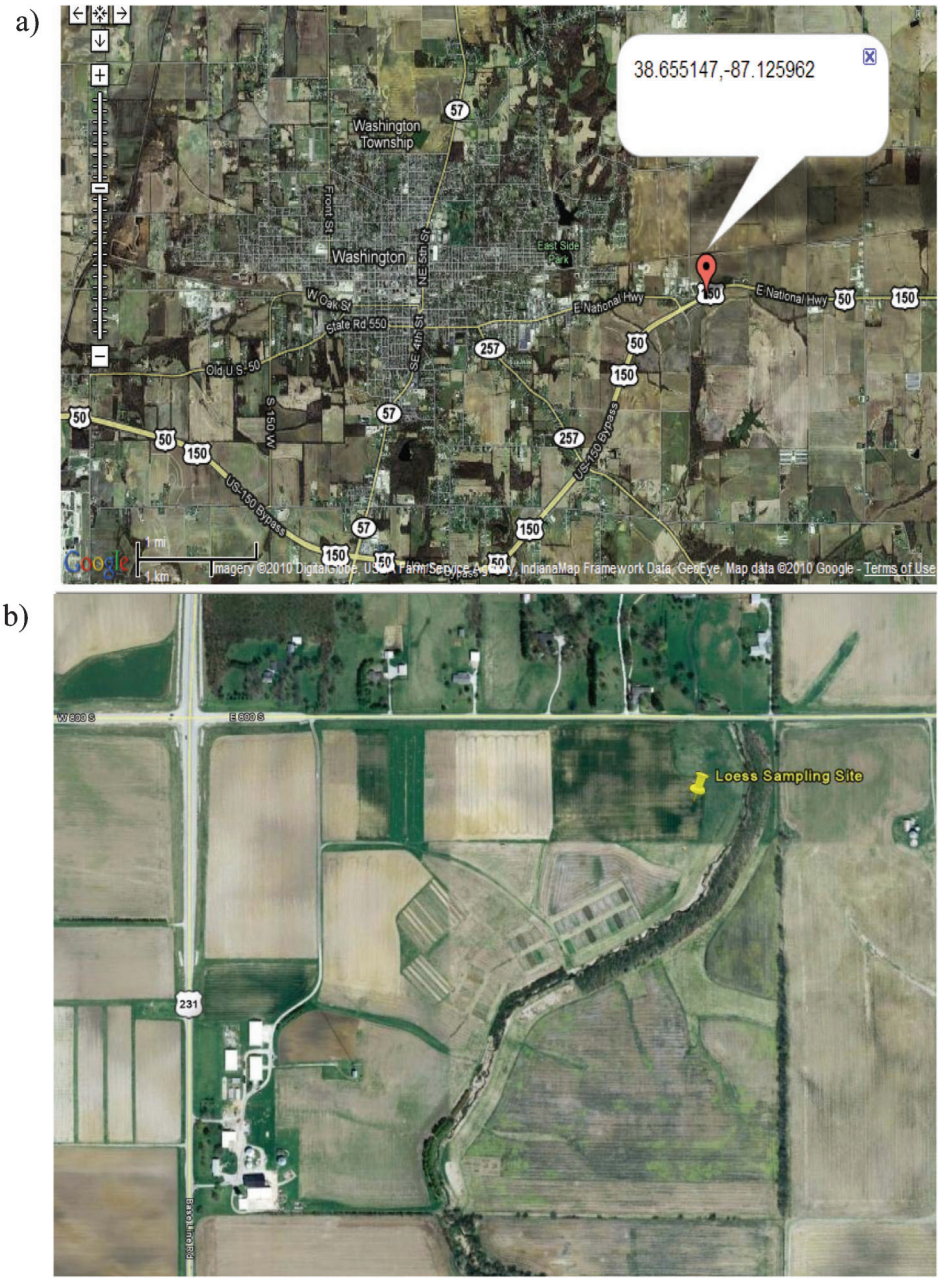

Figure 4.1 Loess Sampling Sites: a) US 150 in Washington, Daviess County (Soil A); and b) Throckmorton Farm in Tippecanoe County (Soil B)

classified as a low plasticity clay (CL) according to the USCS and falls within the A-6 category, based on AASHTO. It is termed a silty clay loam according to INDOT's classification and a silt loam according to the USDA's NRCS classification system.

Particle size distribution and Atterberg limits are consistent with typical data for loess, as can be seen in Figure 4.4 and Figure 4.5, which plot the data for Soil A alongside results collected from the literature. In particular, the particle size distribution falls within the range reported for clayey loess, falling at the "finer" end of the range for this soil.

Figure 4.6 shows the compaction curve of Soil A, obtained performing Standard Proctor tests (ASTM D698). The soil exhibits optimum moisture content of 18% and maximum dry density of 16.7 kN/m^3 (106.3 lb/ft^3).

4.2.3 Tippecanoe County Soil Sample (SOIL B)

Tests were performed to determine Atterberg limits, particle size distribution and specific gravity and compaction behavior of the soil sampled from the Purdue Agriculture Research farm, which is herein

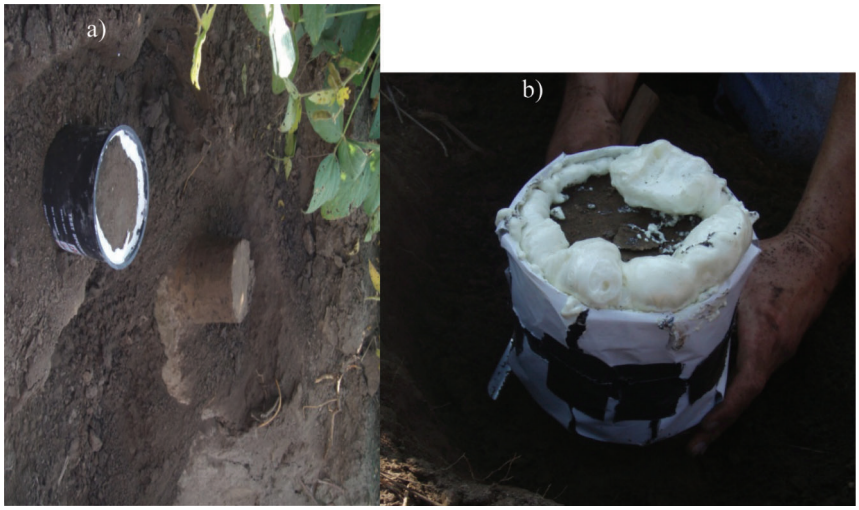

Figure 4.2 a) Sampling pit with sampling of Soil B underway; b) undisturbed sample of Soil B ready for transportation

TABLE 4.1
Summary of index test results for Soil A

Test	Result	Standard
Liquid Limit	37.3 %	ASTM D4318
Plastic Limit	19.5%	ASTM D4318
Plasticity Index	17.8%	ASTM D4318
Specific Gravity	2.691	ASTM D854
Sand	5.5 %	ASTM D422
Silt	69.5%	ASTM D422
Clay	25%	ASTM D422
ASTM Classification	CL	ASTM D2487
AASHTO Classification	A-6	AASHTO M145
INDOT Classification	Silty Clay Loam	Section 903.02 Standard Specifications
USDA Classification	Silt Loam	USDA NRCS

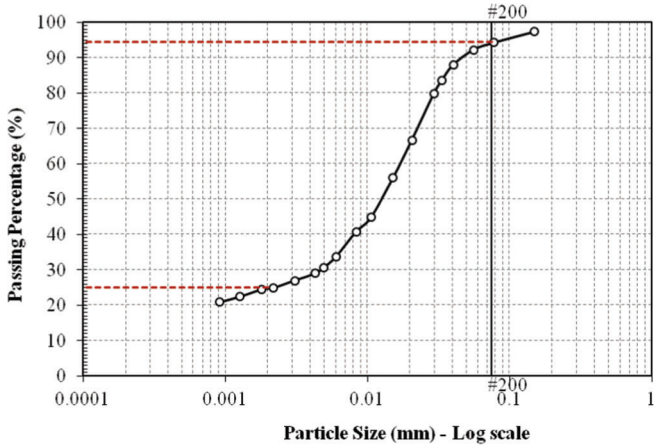

Figure 4.3 Particle size distribution of Soil A

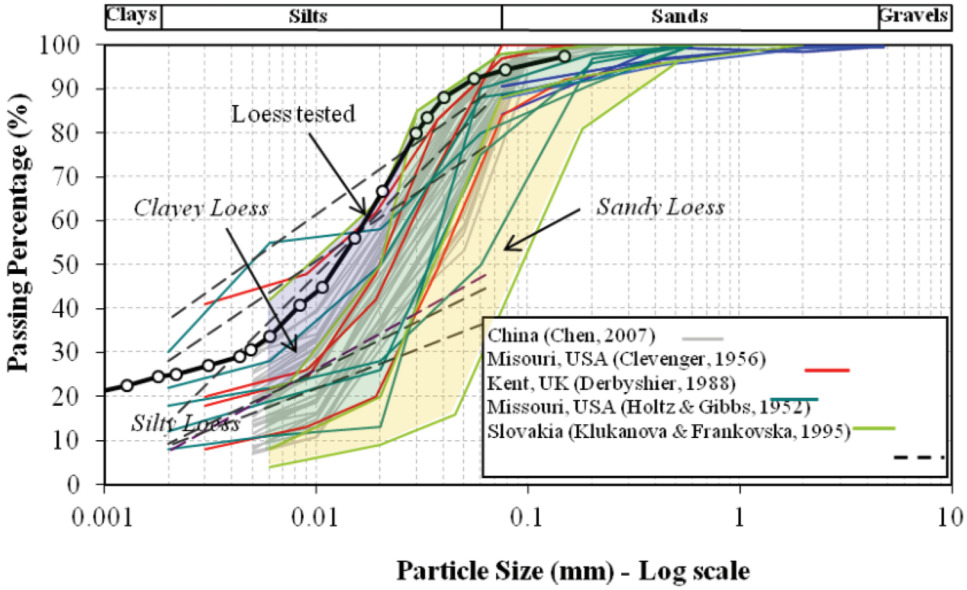

Figure 4.4 Comparison of particle size distribution of Soil A to literature data

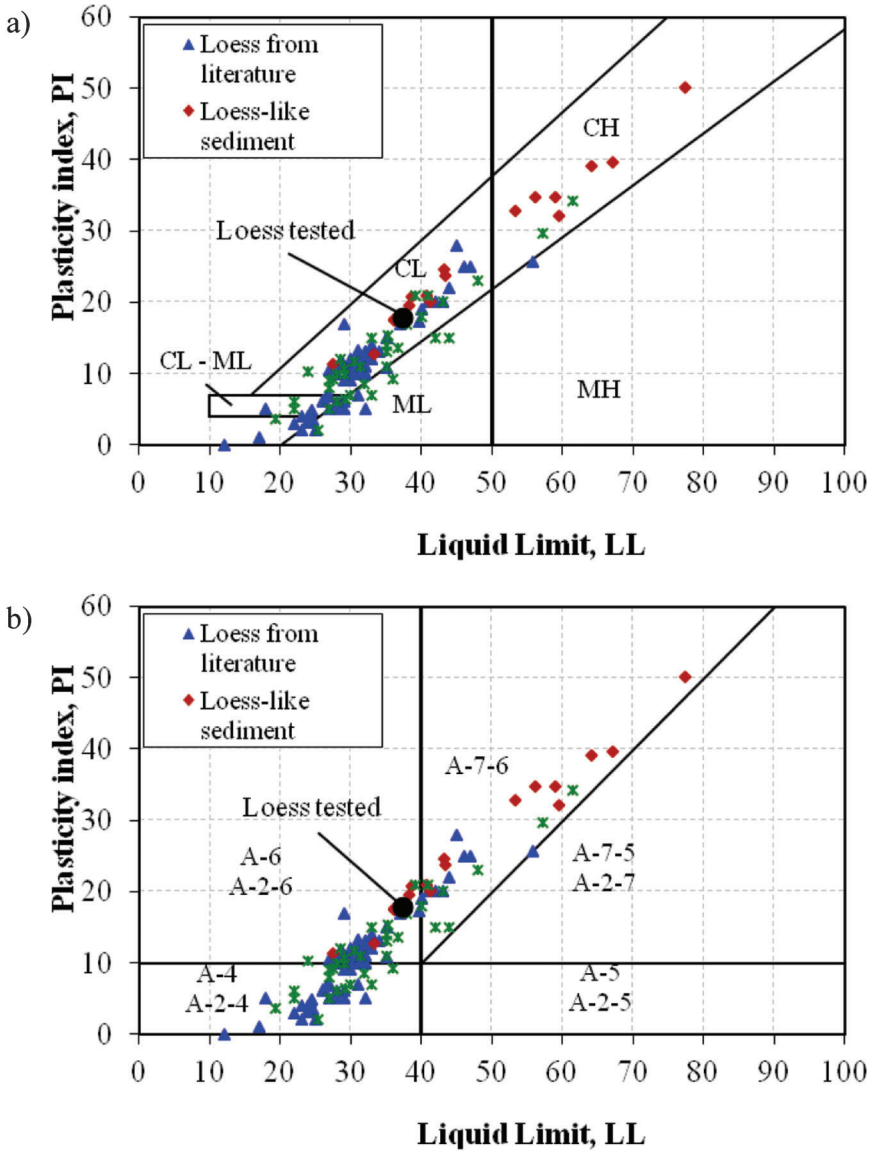

Figure 4.5 Comparison of plasticity characteristics of Soil A to literature data based on a) USCS and b) AASHTO

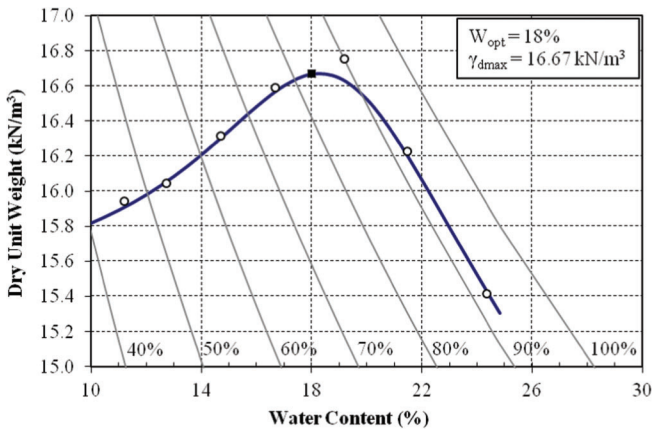

Figure 4.6 Standard Proctor compaction curve for Soil A

referred to as Soil B. Table 4.2 summarizes the results of these tests, and indicates the standard followed in determining each property. Figure 4.7 presents the particle size distribution curve obtained by averaging data from two independent hydrometer tests. Table 4.2 also includes USCS and AASHTO classification of the soil, which is the same as for Soil A. As seen in the table, the soil can be termed a silty loam according to INDOT's classification and a silt loam according to the USDA's NRCS classification system.

Particle size distribution and Atterberg limits are consistent with typical data for loess, as can be seen in Figure 4.8 and Figure 4.9 which plot the data for Soil B alongside results collected from the literature. In particular, as seen for Soil A, the particle size distribution falls within the range reported for clayey loess.

TABLE 4.2
Summary of index test results for Soil B

Test	Result	Standard
Liquid Limit	38.6 %	ASTM D4318
Plastic Limit	23.7%	ASTM D4318
Plasticity Index	14.9%	ASTM D4318
Specific Gravity	2.648	ASTM D854
Sand	14 %	ASTM D422
Silt	72.5%	ASTM D422
Clay	13.5%	ASTM D422
ASTM Classification	CL	ASTM D2487
AASHTO Classification	A-6	AASHTO M145
INDOT Classification	Silty Loam	Section 903.02 Standard Specifications
USDA Classification	Silt Loam	USDA NRCS

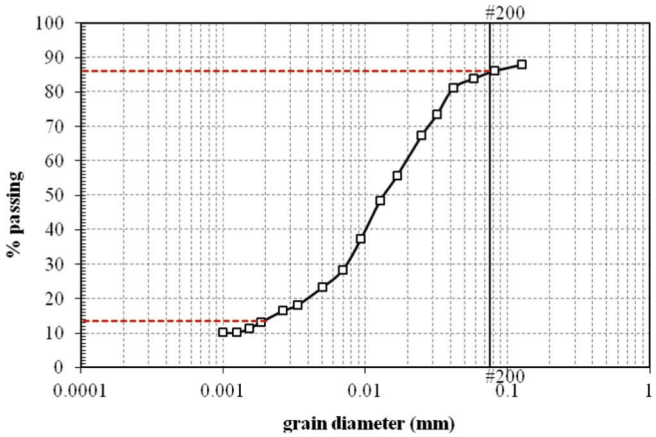

Figure 4.7 Particle size distribution of Soil B

Figure 4.10 shows the compaction curve of Soil B, obtained performing Standard Proctor tests (ASTM D698). The two figures present the data using SI units (Figure 4.10a) and English units (Figure 4.10a), respectively. The soil exhibits optimum moisture content of 21% and maximum dry density of 15.4 kN/m^3 (98 lb/ft^3).

4.3 Methods

4.3.1 Preparation of Specimens for Double Oedometer Tests

As discussed above, the compaction behavior of soils A and B was determined based on the Standard Proctor procedure outlined in ASTM D698 (see compaction curves in Figure 4.6 and Figure 4.10 for soil A and soil B, respectively). Specimens for the double oedometer tests were prepared targeting a range of values of relative compaction (RC=γ_d/γ_{dmax}) and water content, using the values of w_{opt} and γ_{dmax} obtained from the Standard Proctor tests as a reference. For preparation of these specimens two methods were considered.

The first, tested exclusively on Soil B, involved compaction of the soil inside a Proctor mold, and subsequent trimming of specimens from the top and the bottom of the Proctor specimen. A significant difference between the void ratios of these two specimens was observed, with the bottom specimen consistently exhibiting a smaller void ratio than the top one. This complicated the interpretation of the double oedometer tests, as the dry and wet specimens consistently had different initial conditions. Additionally, difficulties were encountered in trimming specimens on the dry side of optimum. As a result, use of this method was discontinued. The second method involved compaction

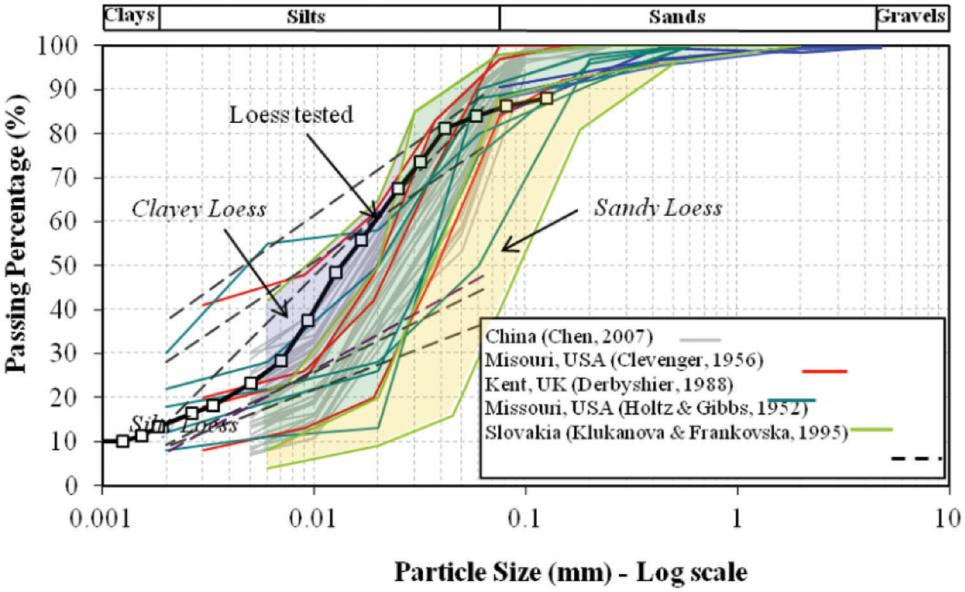

Figure 4.8 Comparison of particle size distribution of Soil B to literature data

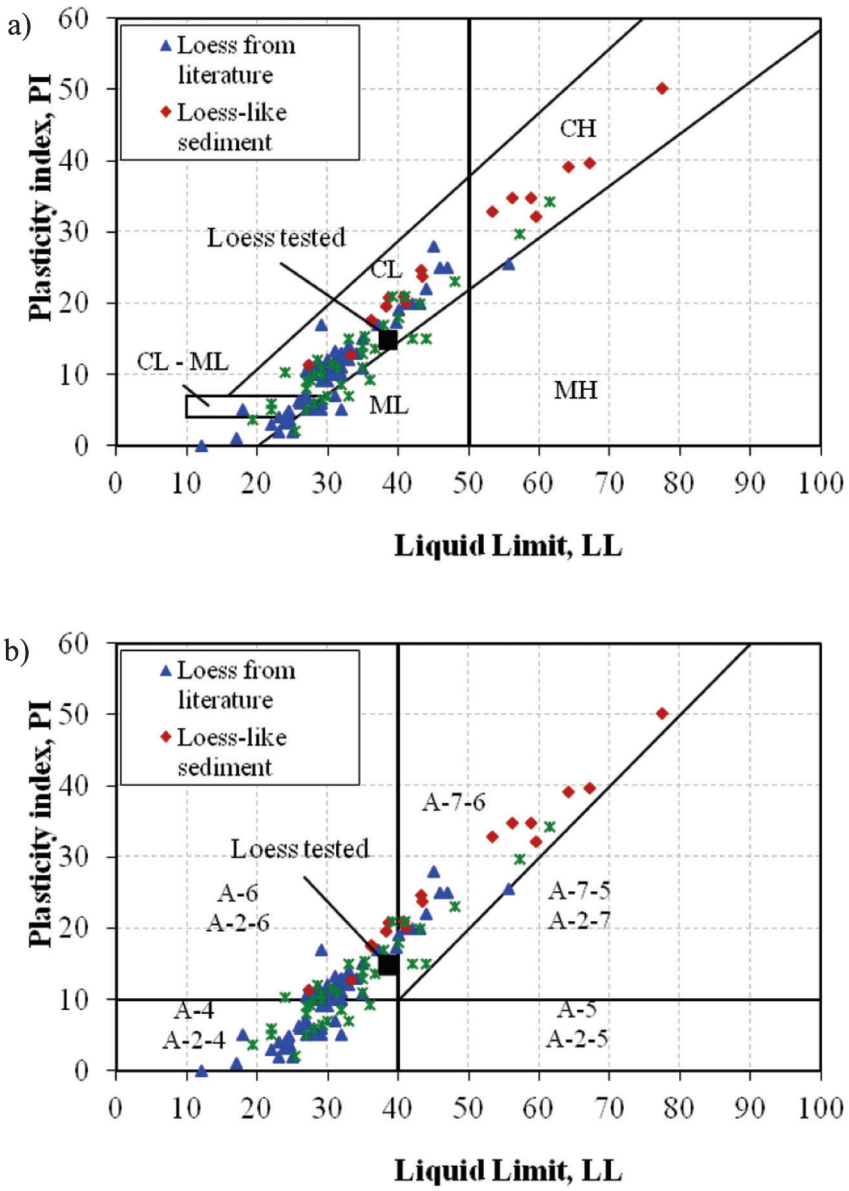

Figure 4.9 Comparison of plasticity characteristics of Soil B to literature data based on a) USCS and b) AASHTO

of the soil directly into the oedometer ring, following a procedure that mimicked the Standard Proctor test. Specifically, the soil was compacted in three layers with equal blows per layer by a known mass free-falling from a known height. A mass of 230.5 g with a circular impact surface and diameter approximately half that of the 2.5 in diameter of an oedometer ring (2.5in) was used (i.e. with relative dimensions similar to those of Proctor hammer and Proctor mold). Figure 4.11 shows the setup for the in-ring compaction.

All collapse data on compacted specimens presented in this report pertain to specimens compacted in the oedometer ring. Varying levels of compactive energy, and therefore initial dry density, were achieved by changing the number of blows per layer and the drop height. A trial and error procedure was employed to identify the appropriate parameters for any target value of relative compaction and water content.

Table 4.3 and Table 4.4 summarize the outcome of this trial and error procedure for Soil A and B, respectively. Specifically, each table presents the compactive energy required to obtain target values of relative compaction at a given water content and the means (number of drops and drop height) by which each was applied. Note that for a given value of relative compaction the required compactive energy varies with water content. For example, for Soil A 20% of the Standard Proctor energy is required to compact the soil prepared at a water content of 18% to a dry density corresponding to 80% relative compaction. This compactive effort was achieved dropping the circular mass from a 8 in drop height, using 7 blows for each of the three layers.

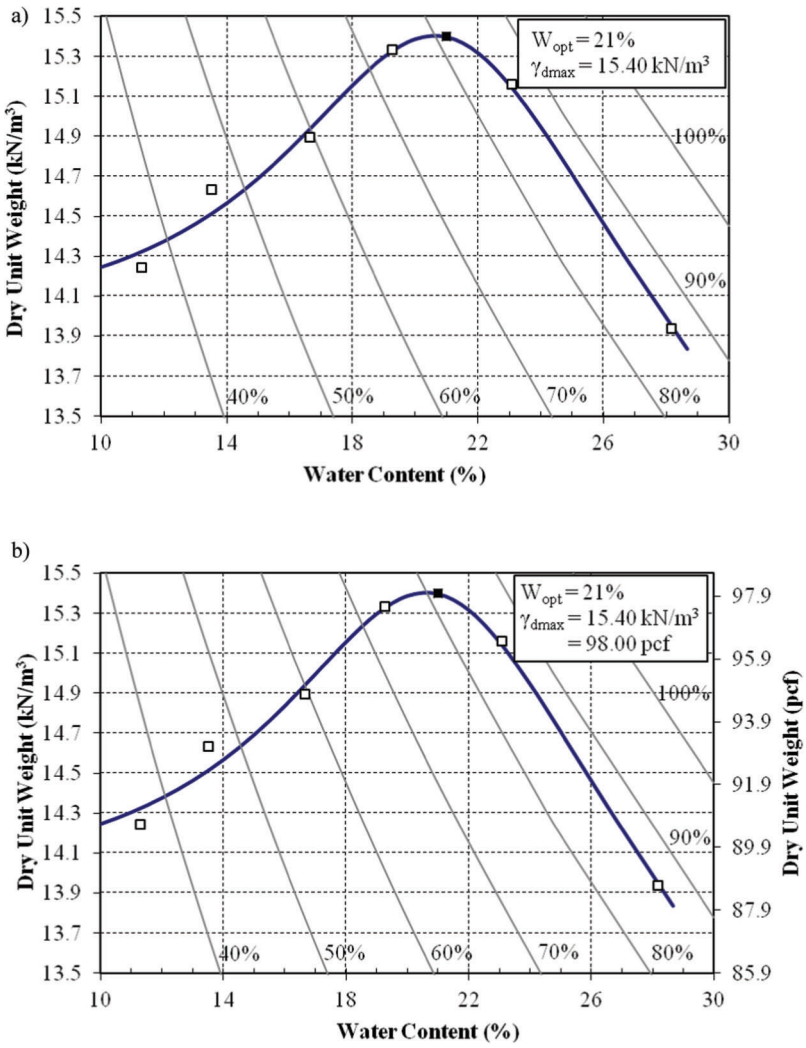

Figure 4.10 Standard Proctor compaction curve for Soil B: a) SI units; b) English units.

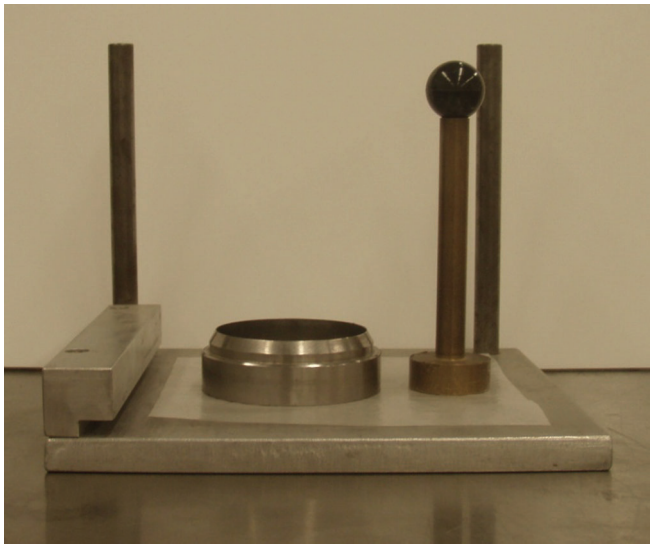

Figure 4.11 Compaction-in-Ring Set-Up

4.3.2 One-Dimensional Collapse Measurement

One-dimensional collapse measurements of the specimens were performed using the double oedometer method. This procedure requires two identical soil specimens, which are both loaded one-dimensionally. All tests in this research were conducted using two computer controlled CRS consolidation apparatuses available in the Purdue geotechnical. Figure 4.12 shows one of the CRS apparatuses. Note that the tests were performed under load control, using the load frame's computer controlled feedback system.

One specimen (Dry) was loaded starting from as-compacted conditions, and the other specimen was inundated with water at a low stress level (which varied slightly from test to test) and allowed to come to equilibrium. Flushing of the specimen occurred from the bottom up. Load increments were applied through the load frame computer interface, following a standard sequence (see Table 4.5). During each increment, load

TABLE 4.3
Results of trial and error procedure to determine compactive effort to achieve desired relative compaction for Soil A

w (%)	Desired RC (%)	Achieved RC (%)	Drop Height (in)	Blows per layer	Comp. Energy (ft-lb/ft^3)	Percent of Standard Proctor Compactive Energy (%)
18	80	81	8	7	2535	20
18	75	76	8	5	1811	15
17	90	89	8	15	5433	44
17	80	82	8	10	3622	29
16	80	80	8	8	2897	23
14	85	86	8	14	5070	41
14	80	80	8	8	2897	23
14	70	71	8	3	1087	9
13	80	80	8	8	2897	23

TABLE 4.4
Results of trial and error procedure to determine compactive effort to achieve desired relative compaction for for Soil B

w (%)	Desired RC (%)	Drop Height (in)	Blows per layer	Comp. Energy (ft-lb/ft^3)	Percent of Standard Proctor Compactive Energy (%)
21	90	5	17	3848	31
21	85	5.5	10	2490	20
21	80	4	10	1811	15
21	75	3	10	1358	11
18	95	6	15	4074	33
18	85	4	10	1811	15
15	85	6	15	4074	33

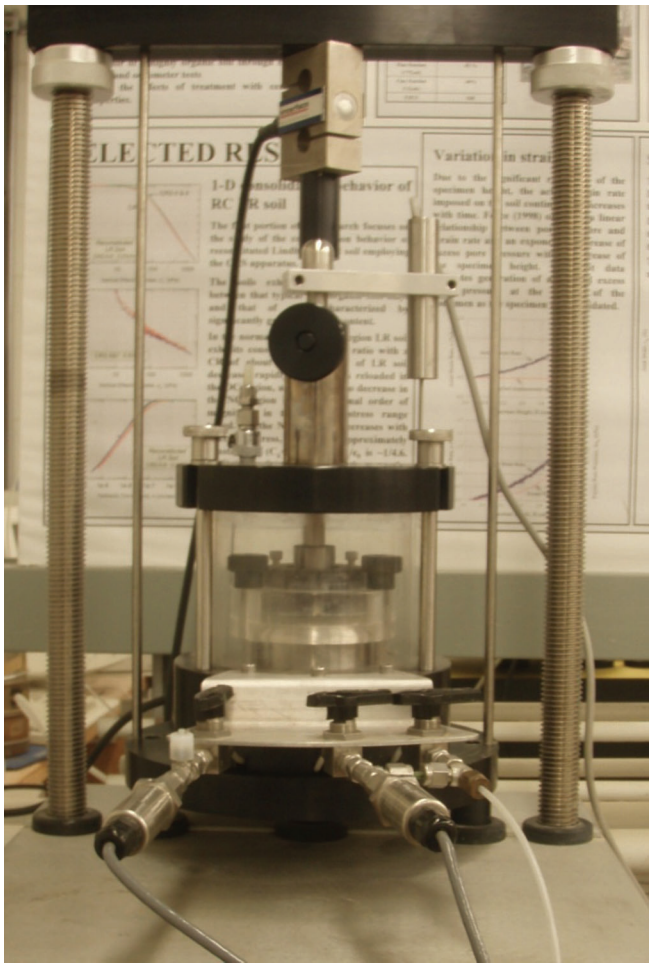

Figure 4.12 CRS Apparatus

and vertical deformation measured through a LVDT were recorded using the data acquisition system.

In the tests on Soil B the duration of the increments varied from test to test and from increment to increment covering a relatively wide range (7–30 hours). For these tests in general the load was increased when the deformation rate under the previous increment became slower than 0.0005%/h, as recommended by Jotisankasa (2005). For Soil A the duration of the increments what shortened to 1 hour in an effort to increase testing productivity. For these tests the rate of deformation after one our does not meet the criterion above. However, as seen in Figure 4.13 and Figure 4.14, which present examples of the curves of deformation versus time obtained under constant load for Soil A, the deformation of the specimen has reached

TABLE 4.5
Loading schedule

Target Stress (kPa)	
Seating (~5–8kPa)	Load (kg)
12.5	8.8
25	17.7
50	35.3
100	70.6
200	141.3
400	282.5
800	565.1
1600	1130.2
2760	1950

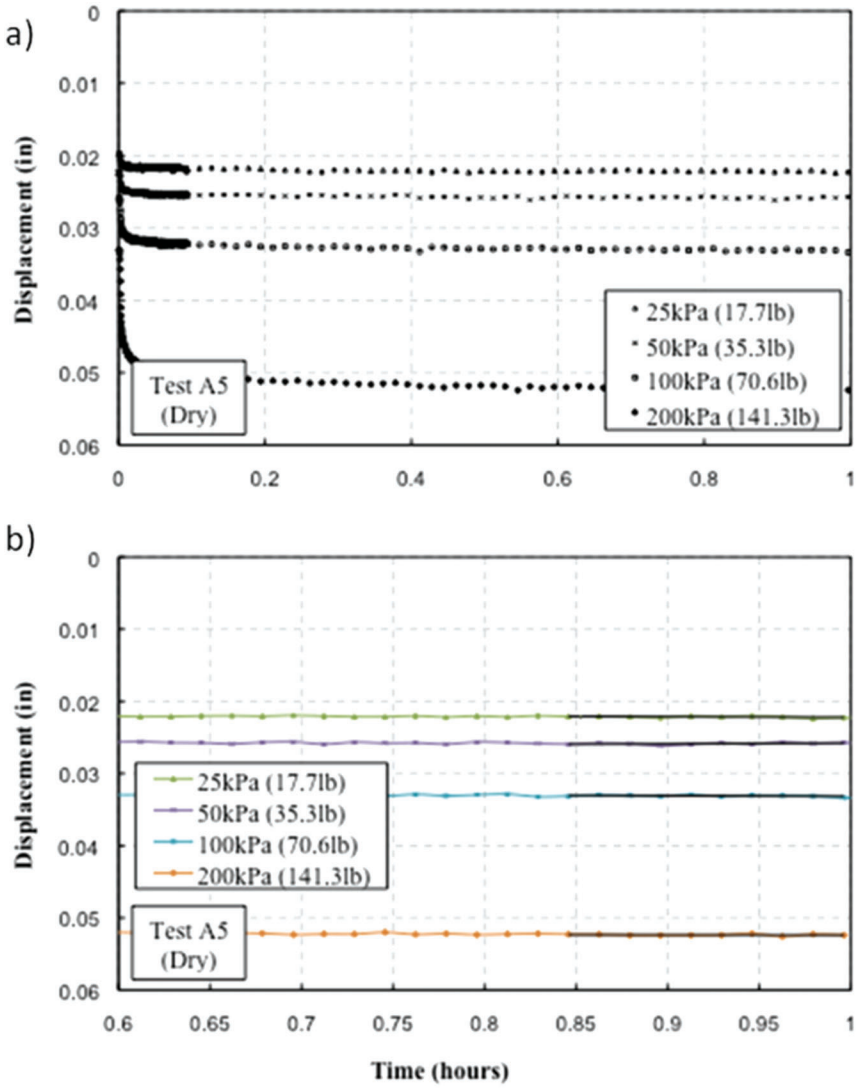

Figure 4.13 Examples of curves of deformation versus time under constant load for Soil A: a)–b) Test A5 – Dry Specimen

TABLE 4.6
Summary of double oedometer tests - Initial conditions (Soil A)

Test	Dry/wet	w_0 (%)	γ_d (kN/m^3) [γ_d (lb/ft^3)]	γ (kN/m^3) [γ (lb/ft^3)]	RC (%)	S_0 (%)	e_0
A1	Dry	15.5	13.6 [86.6]	15.7 [99.9]	81.5	44.1	0.94
	Wet	15.5	13.3 [84.7]	15.3 [97.4]	79.5	42.0	0.99
A2	Dry	12.8	13.2 [84.0]	14.9 [94.8]	79.2	34.5	1.00
	Wet	12.8	13.3 [84.7]	15.1 [96.1]	80.1	35.3	0.98
A3	Dry	17.4	13.7 [87.2]	16.0 [101.8]	81.9	50.1	0.93
	Wet	17.3	13.8 [87.8]	16.2 [103.1]	82.7	51.1	0.91
A4	Dry	16.9	14.8 [94.2]	17.4 [110.8]	89.0	58.5	0.78
	Wet	16.9	14.7 [93.6]	17.2 [109.5]	88.5	57.8	0.79
A5	Dry	14.1	13.5 [85.9]	15.4 [98.0]	81.2	40.0	0.95
	Wet	14.2	13.2 [84.0]	15.1 [96.1]	79.3	38.3	1.00
A6	Dry	15.5	13.6 [86.6]	15.7 [99.9]	81.4	44.0	0.95
	Wet	15.8	13.5 [85.9]	15.6 [99.3]	80.8	44.2	0.96
A7	Dry	17.3	12.6 [80.2]	14.8 [94.2]	75.7	42.7	1.09
	Wet	17.7	12.5 [79.6]	14.7 [93.6]	75.1	43.1	1.11
A8	Dry	14.3	14.5 [92.3]	16.6 [105.7]	87.1	47.2	0.82
	Wet	14.5	14.3 [91.0]	16.4 [104.4]	85.8	46.1	0.84

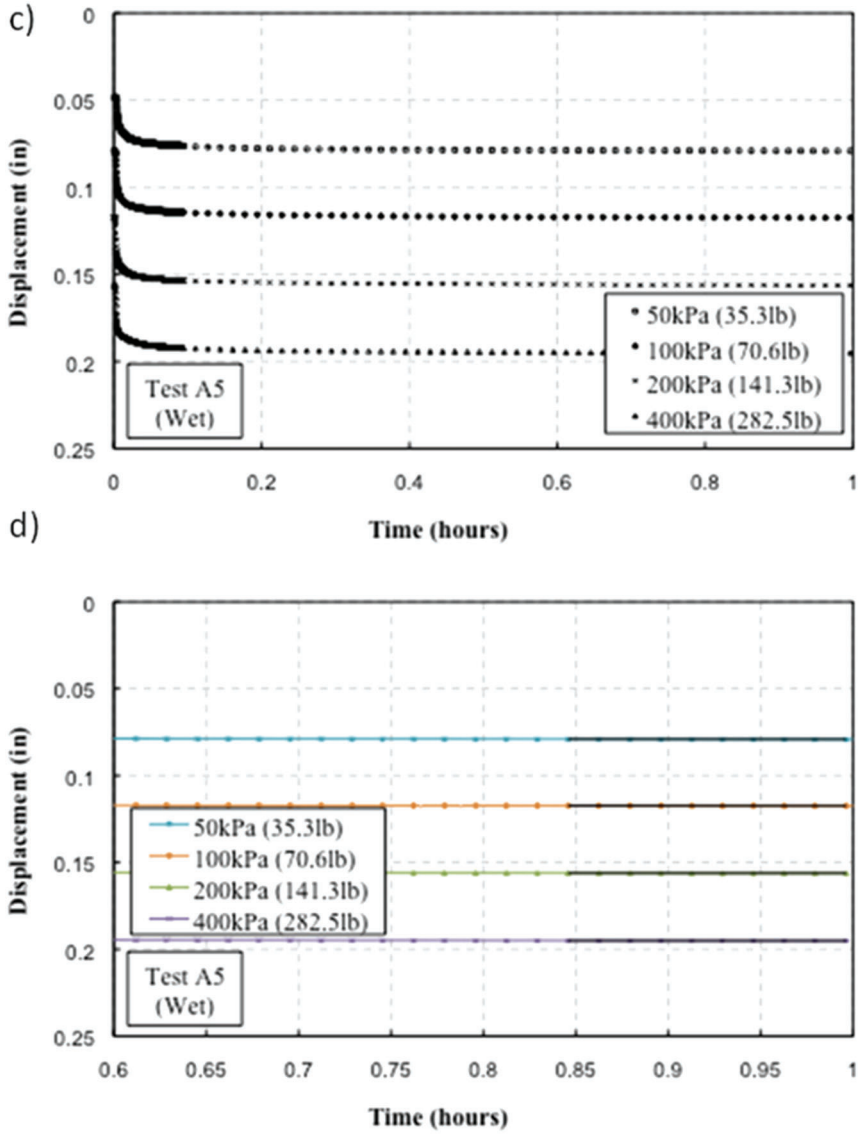

Figure 4.14 Examples of curves of deformation versus time under constant load for Soil A: c)–d) Test A5 – Wet Specimen

a relatively constant value after this short duration. This suggests indicating that the shortened duration of the constant load period does not impact the collapse measurements.

For each specimen, the data collected through the data acquisition system was reduced and summarized. Compression curves for the dry and wet specimen were obtained plotting the vertical stress values versus the end of increment deformations. Figure 4.15 shows an example of a pair of curves obtained testing soil A.

As discussed in Chapter 2, collapse potential is defined as the difference in volumetric (equal to axial strain in the case of 1D tests) strain between the "Dry,"

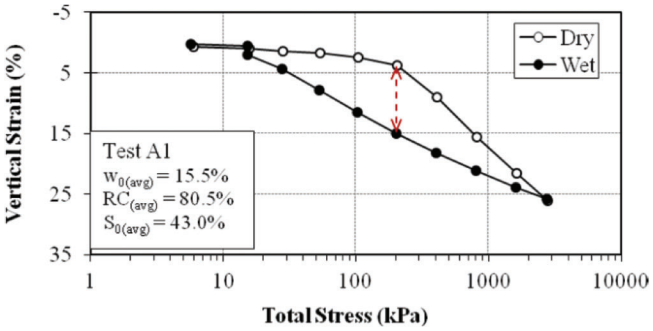

Figure 4.15 Example of compression curves obtained from double oedometer test (test A1 on soil A)

TABLE 4.7
Summary of double oedometer tests - Initial conditions (Soil B)

Test	Dry/wet	w_0 (%)	γ_d (kN/m^3) [γ_d (lb/ft^3)]	γ (kN/m^3) [γ (lb/ft^3)]	RC (%)	S_0 (%)	e_0
B1	Dry	14.8	15.3 [97.4]	17.6 [112.0]	99.6	56.6	0.69
	Wet	14.5	14.4 [91.7]	16.4 [104.4]	93.3	47.6	0.80
B2	Dry	19.7	15.3 [97.4]	18.3 [116.5]	99.4	74.8	0.69
	Wet	20.6	15.0 [95.5]	18.0 [114.6]	97.2	74.4	0.73
B3	Dry	21.4	13.2 [84.0]	16.0 [101.8]	85.5	58.3	0.97
	Wet	21.1	12.7 [80.8]	15.4 [98.0]	82.5	53.5	1.04
B4	Dry	20.9	14.2 [90.4]	17.1 [108.8]	91.9	66.6	0.83
	Wet	21.0	13.2 [84.0]	16.0 []101.8	85.6	57.5	0.97
B5	Dry	20.1	11.9 [75.7]	14.3 [91.0]	77.6	45.5	1.17
	Wet	20.7	11.4 [72.6]	13.7 [87.2]	74.0	42.9	1.27
B6	Dry	15.4	12.7 [80.8]	14.7 [93.6]	82.5	39.0	1.04
	Wet	15.0	12.5 [79.6]	14.3 [91.0]	81.0	36.7	1.08
B7	Dry	22.3	12.3 [78.3]	15.0 [95.5]	79.8	53.1	1.11
	Wet	22.6	12.4 [78.9]	15.2 [96.8]	80.4	54.7	1.09
B8	Dry	16.9	11.8 [75.1]	13.8 [87.8]	76.8	37.4	1.19
	Wet	17.6	11.6 [73.8]	13.7 [87.2]	75.4	37.9	1.23
B9	Dry	19.3	12.5 [79.6]	14.9 [94.8]	81.3	47.8	1.07
	Wet	19.6	12.4 [78.9]	14.8 [94.2]	80.6	47.6	1.09
B10	Dry	19.7	11.6 [73.8]	13.9 [88.5]	75.3	42.2	1.23
	Wet	19.8	11.2 [71.3]	13.4 [85.3]	72.6	39.6	1.32
B11	Dry	19.9	11.6 [73.8]	13.9 [88.5]	75.4	42.7	1.23
	Wet	19.3	11.5 [73.2]	13.8 [87.8]	75.0	41.0	1.24

Shaded cells indicate tests not considered in analysis.

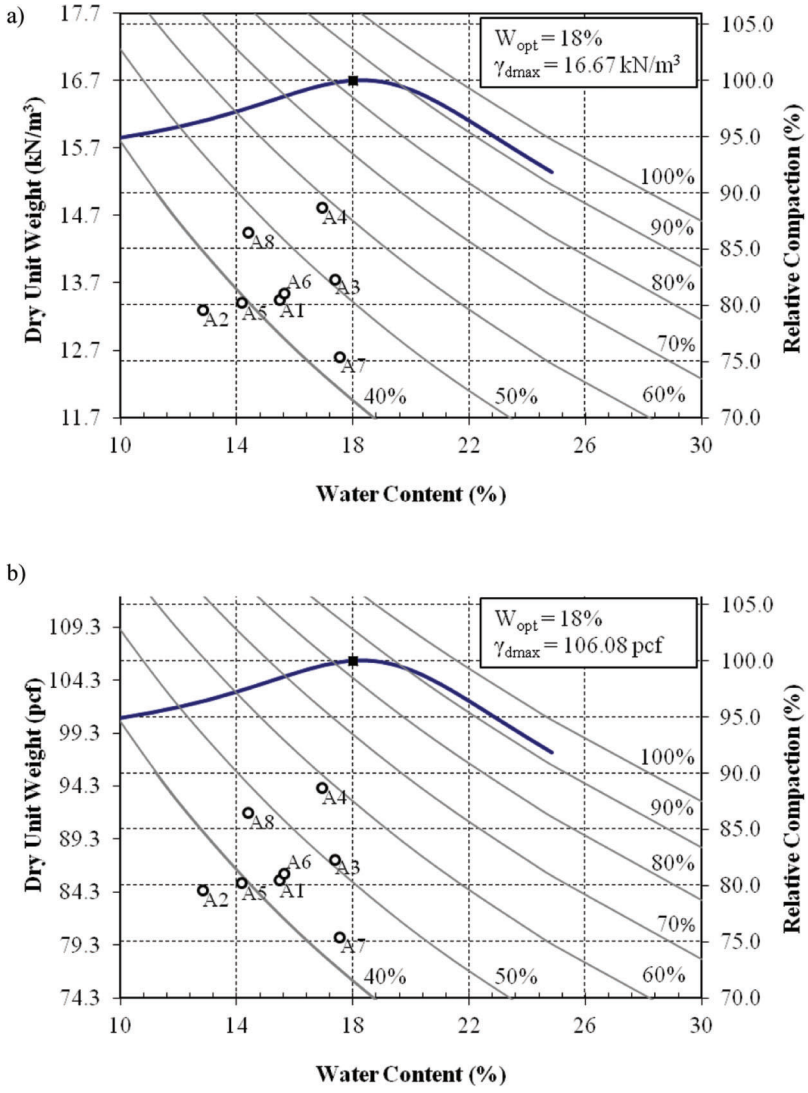

Figure 4.16 Standard Proctor curve and testing conditions for double oedometer tests (Soil A): a) SI units; b) English units.

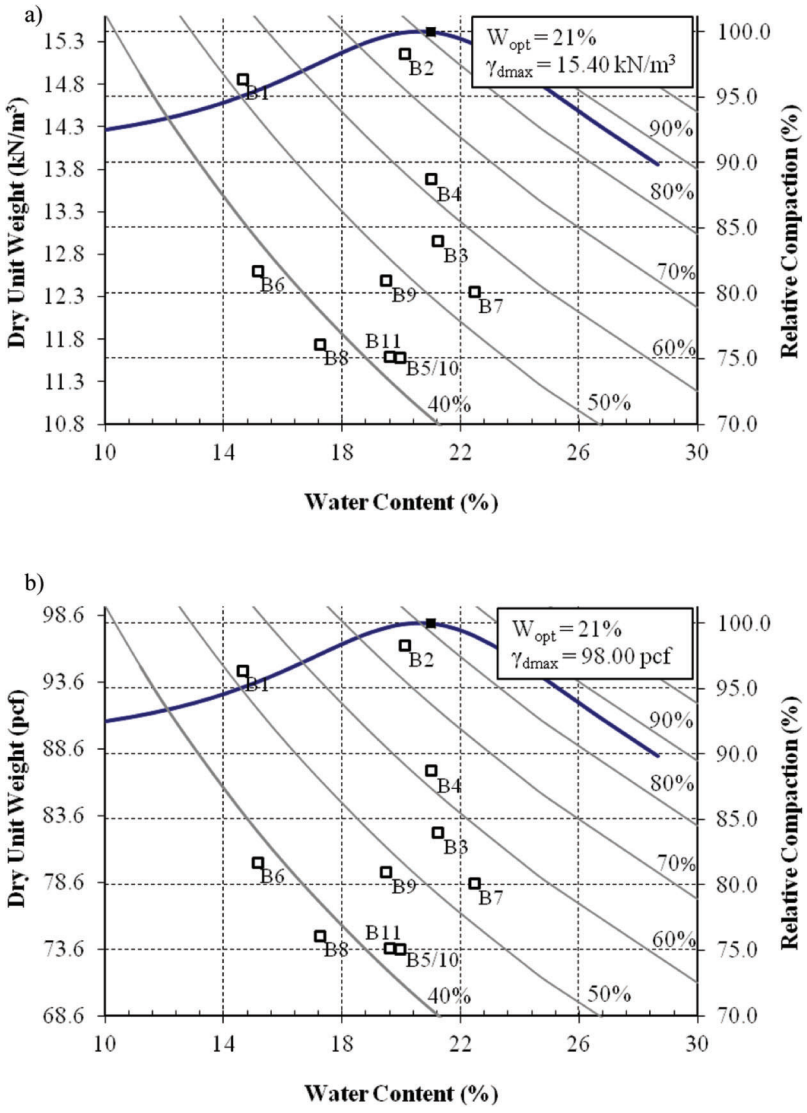

Figure 4.17 Standard proctor curve and testing conditions for double oedometer tests (Soil B): a) SI units; b) English units.

curve and the "Wet" curve, and the criterion outlined in ASTM D5333 is generally adopted to quantify the collapse potential

For Soil B only, wetting-induced collapse results from the double oedometer tests were confirmed by running select single oedometer tests in which the specimens were inundated with water under different overburden stress levels. Again, the soil was allowed to achieve equilibrium under the load before flushing occurred and 12 hours were allowed after flushing before application of the subsequent load increment.

4.4 Testing Program

Double oedometer tests were performed on both Soil A and Soil B. Table 4.6 summarizes the testing conditions examined using Soil A. Eight pairs of tests were performed (referred to as test A1 through A8). For each specimen tested, the table provides the initial (as compacted) conditions: water content, dry unit weight, total unit weight, relative compaction, degree of saturation and void ratio. In general, for each pair of test, the initial conditions are found to be consistent.

Figure 4.16 summarizes the average initial conditions for tests A1–A8 on a plot of dry unit weight versus water content, alongside the Proctor compaction data again using both SI and English units.

Table 4.7 and Figure 4.17 provide similar data for Soil B. Note that for this soil, some discrepancy between the initial conditions of the dry and wet specimen is observed in some of the tests. Note also that the results for the wet specimen of test B5 and the dry specimen of test B10 (shaded cells in Table 4.7) were considered unreliable, and are not used in the analysis presented in the following chapter. Given the fact that the initial conditions for tests B5 and B10 are relatively

close, in the following the data for the dry specimen of test B5 are compared to those for the wet specimen of test B10.

CHAPTER 5 RESULTS

5.1 Introduction

This chapter presents the results of the collapse measurements conducted on compacted specimens of soils A and B. The chapter is organized in two main parts. Section 5.2 presents the results of the tests on Soil A (Section 5.2.1) and Soil B (Section 5.2.2), highlighting the effect of water content, degree of saturation and relative compaction on the measured collapse deformation. Contour plots summarizing the measured collapse strains are also presented for each soil at the end of each subsection. The second part of the chapter (Section 5.3) compares the results obtained in this research to data available in the literature for similar soils.

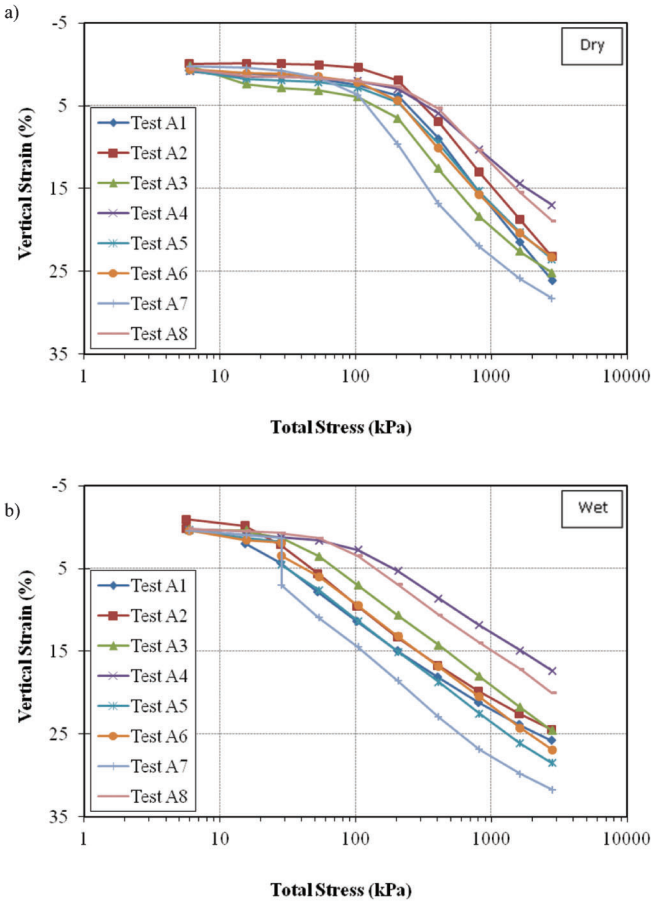

Figure 5.1 Compression curves from oedometer tests on Soil A: a) "dry" specimens, and b) "wet" specimens

5.2 Introduction

5.2.1 Soil A

As discussed in Chapter 4, eight pairs of oedometer tests were conducted on specimens of Soil A compacted over a range of water contents and values of relative compaction. Table 4.6 summarized the initial conditions for such tests. Note that all tests were conducted on specimens compacted dry of optimum, with values of relative compaction (RC) smaller than 90% (all values of RC are referenced to the Standard proctor results reported in Chapter 4). The compression curves from all tests performed without wetting ("dry" specimens) are shown in Figure 5.1a, while Figure 5.1b reports the curves for all the "wet" specimens. Note that all compression curves are reported in terms of strain versus total vertical stress as no measurements of suction and/or pore pressure were conducted. It is observed that the compression curves all break in correspondence to a different value of the preconsolidation stress. For the tests conducted on the "dry" specimens the range in values of σ'_p, reflects the energy applied to the specimens during compaction, with the tests conducted at the highest and lowest values of RC(%) providing the upperbound and lowerbound of σ'_p, respectively. The compression curves for each pair of oedometer tests are shown in Figure 5.2a–h. In these plots the vertical offset between the dry and the wet curves reflects the susceptibility of the soil specimen to wetting induced collapse at different stress levels. Each of the plots shown in Figure 5.2 reports the average water content, degree of saturation and relative compaction for the dry and wet specimen. These values are also included in Table 5.1, which also reports the difference in strain between each pair of curves at each stress levels. Note that for several of the tests Table 5.1 reports negative wetting induced strains at lower values of the stress level. These negative values reflect the fact that in such cases wetting produces swelling and not collapse.

As shown in Table 5.1 and in Figure 5.2a–h, for any pair of specimens, the wetting induced strain varies as a function of the stress level. For all the tests the same trend is observed: the wetting induced strain first increases, reaches a maximum and then decreases once again. Both the magnitude of the strains and the stress level at which the maximum wetting induced strain is measured vary as a function of the compaction conditions.

Table 5.1 highlights the strain measured at 200 kPa, as this value is used to define the collapsibility index, I_e. While for all pairs of tests, wetting ultimately leads to some degree of collapse, the collapsibility varies greatly. As indicated in the table, for the compaction conditions examined, I_e varies between 2.27% (moderate collapsibility) and 11.35% (severe collapsibility). In some of the tests significant straining is observed also under much smaller stress levels (e.g. Tests A1, A2, A6, A7). This suggests that collapse may be a concern also for

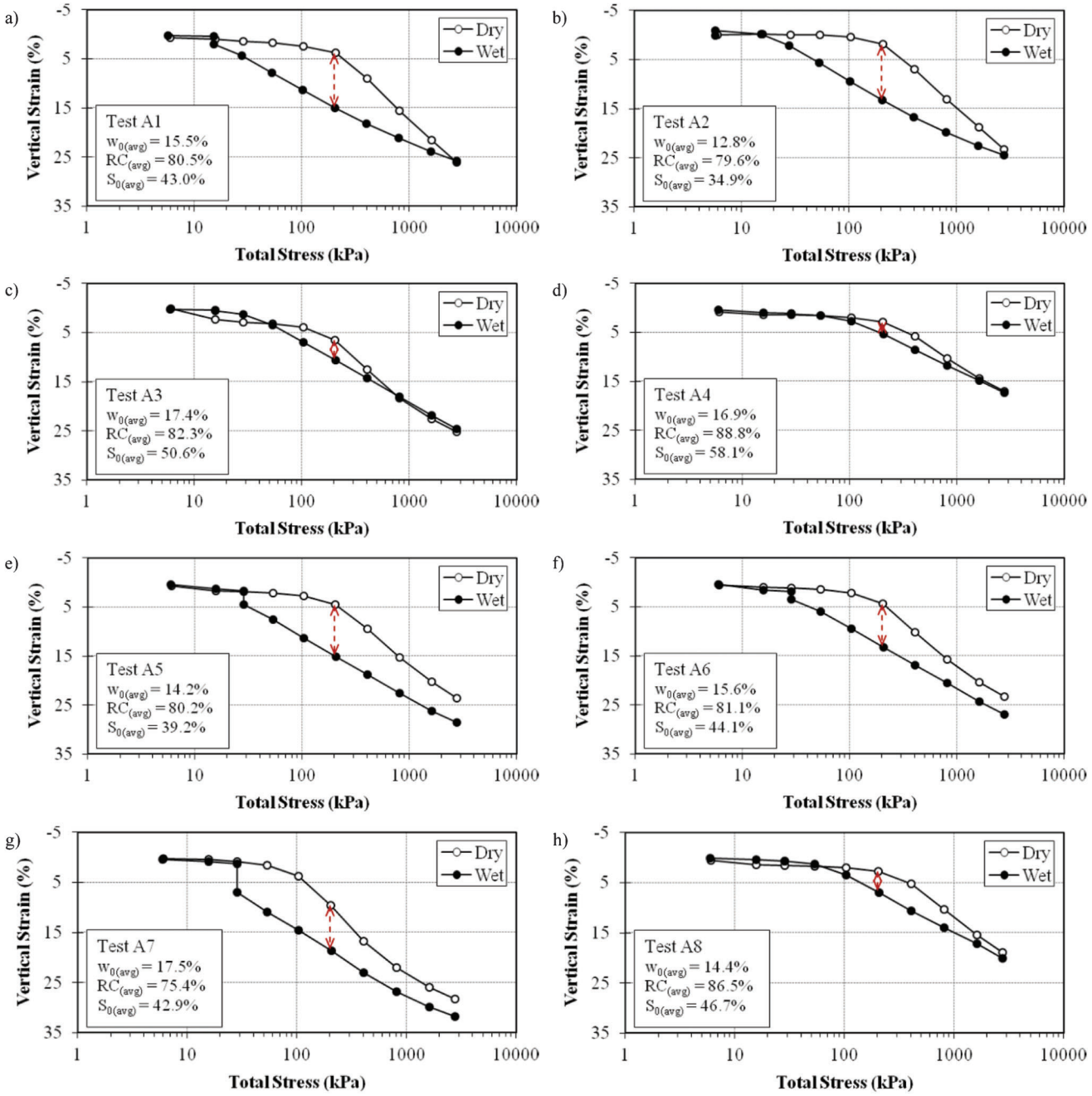

Figure 5.2 Compression curves from double oedometer tests: a) Test A1; b) Test A2; c) Test A3; d) Test A4; e) Test A5; f) Test A6; g) Test A7; h) Test A8

relatively shallow fills (e.g. 50 kPa corresponds to approximately 3 m of fill).

Table 5.1 also reports the maximum value of the collapse strain (I_{emax}), and the stress level at which it is measured. In all but three cases (tests A4, A7 and A8) the collapse strain measured at 200 kPa is greater than at any other stress level. This is shown more clearly in Figure 5.3, which highlights three subsets of the data: tests in which the maximum collapse strain (I_{emax}) occurs at σ'_v<200 kPa (test A7), tests in which the maximum collapse strain (I_{emax}) occurs at σ'_v=200 kPa (tests A1, A2, A3, A5, A6), and tests in which the maximum collapse strain (I_{emax}) occurs at σ'_v>200 kPa (tests A4 and A8). The last occurrence appears to be limited to specimens compacted at the higher values of RC(%) (~89% and ~87% for tests A4 and A8, respectively). In contrast, for the test compacted at the lower relative compaction (test A7: RC(%)~75%) the stress level at which the maximum collapse strain is measured decreases to 100 kPa. The effect of relative compaction and water content on the curve of wetting induced strain versus stress level is further illustrated

TABLE 5.1
Summary of double oedometer test results for Soil A

Test		A1	A2	A3	A4	A5	A6	A7	A8
$w_{0(avg)}$ (%)		15.5	12.8	17.4	16.9	14.2	15.6	17.5	14.4
Offset from w_{opt} (%)		−2.5	−5.2	−0.6	−1.1	−3.8	−2.4	−0.5	−3.6
$\gamma'_{d(avg)}$ (kN/m^3) [$\gamma'_{d(avg)}$ (lb/ft^3)]		13.4 [85.3]	13.3 [84.7]	13.7 [87.2]	14.8 [94.2]	13.4 [85.3]	13.5 [85.9]	12.6 [80.2]	14.4 [91.7]
$\gamma_{(avg)}$ (kN/m^3) [$\gamma_{(avg)}$ (lb/ft^3)]		15.5 [98.7]	15.0 [95.5]	16.1 [102.5]	17.3 [110.1]	15.3 [97.4]	15.6 [99.3]	14.8 [94.2]	16.5 [105.0]
$RC_{(avg)}$ (%)		80.5	79.6	82.3	88.8	80.2	81.1	75.4	86.5
$S_{0(avg)}$ (%)		43.0	34.9	50.6	58.1	39.2	44.1	42.9	46.7
$e_{0(avg)}$		0.97	0.99	0.92	0.78	0.97	0.95	1.10	0.83
Nominal Stress Level at Saturation (kPa)		12.5	2.8	12.5	25	25	25	25	25
Wetting induced strain (%)	12.5 kPa	−0.52	0.12	−1.33	−0.49	−0.41	0.30	0.40	−0.76
	25 kPa	2.49	1.68	−1.62	−0.34	−0.25	0.66	0.52	−0.87
	50 kPa	5.72	5.19	0.11	−0.08	5.04	4.21	8.91	−0.41
	100 kPa	8.83	8.99	2.85	0.65	8.29	7.08	10.66	1.32
	200 kPa	11.15	11.35	4.06	2.27	10.40	8.73	8.96	4.11
	400 kPa	9.31	9.95	1.68	2.70	9.23	6.77	6.20	5.27
	800 kPa	5.81	6.91	−0.30	1.56	7.24	4.77	4.87	3.59
	1600 kPa	2.52	3.92	−0.82	0.52	5.85	3.84	3.93	1.72
	2760 kPa	−0.15	1.34	−0.64	0.34	4.94	3.62	3.44	1.11
Ie (%)		11.15	11.35	4.06	2.27	10.40	8.73	8.96	4.11
$Ie_{(max)}$ (%) Stress level at $Ie_{(max)}$		11.15 (200 kPa)	11.35 (200 kPa)	4.06 (200 kPa)	2.70 (400 kPa)	10.40 (200 kPa)	8.73 (200 kPa)	10.66 (100 kPa)	5.27 (400 kPa)
Collapse Potential (ASTM D5333)		Severe	Severe	Moder.	Moder.	Severe	Mod. Severe	Mod. Severe	Moder.

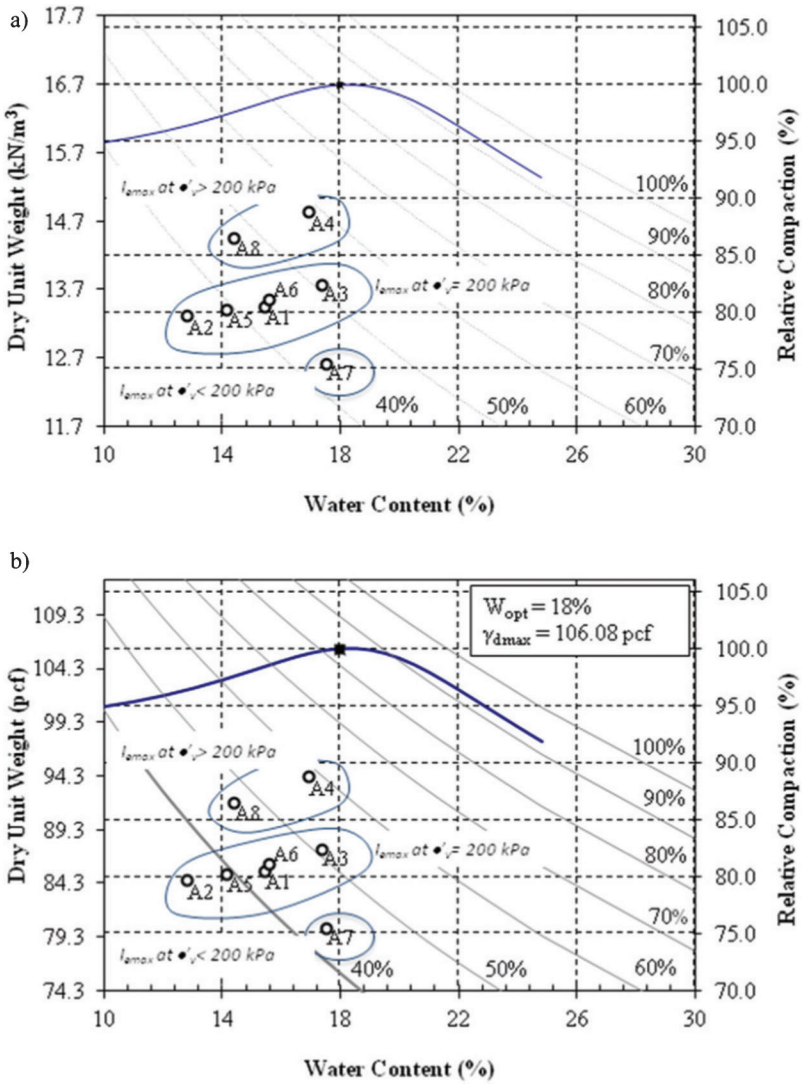

Figure 5.3 Effect of relative compaction and water content on stress level at which maximum collapse strain is observed (Soil A): a) SI units; b) English units

in Figure 5.4a and Figure 5.4b. In particular, Figure 5.4a shows how for soil specimens compacted at approximately the same water content, with decreasing values of RC(%), not only does the maximum collapse strain increase (from 2.7%, to 4.1% to over 10%), but also the stress level at which this value occurs decreases (from 400, to 200, to 100 kPa). This indicates that poor compaction is more likely lead to collapse susceptibility even for relatively small values of the overburden. This trend is consistent with previous data published in the literature (e.g. Lawton et al. 1989).

Figure 5.4b shows similar curves of wetting induced strain versus stress level, this time highlighting the effect of differences in the compaction water content, for specimens compacted at essentially the same RC(%). While decreasing values of the water content tend to be associated with increasing values of the wetting strains at almost all stress levels, the tests considered show no effect on the stress level at which the maximum collapse strain occurs (200 kPa for all tests).

Focusing on the strain measured at 200 kPa which is used in ASTM D5333 to quantify the collapsibility index, I_e, it is observed that, consistent with data available in the literature, the most significant collapse is observed in the specimens with the lower degree of saturation, water content and relative compaction. The trends of collapse strain with these three parameters are better illustrated in Figure 5.5a–c. Figure 5.5a plots the collapse strain versus the relative compaction for specimens compacted at approximately the same water content (17.3%), less than 1% point below the optimum moisture content (w_{opt}=18%). As expected, there is a clear trend of decreasing collapsibility with increasing RC (%). A marked reduction in collapsibility is observed when the relative compaction exceeds 82%.

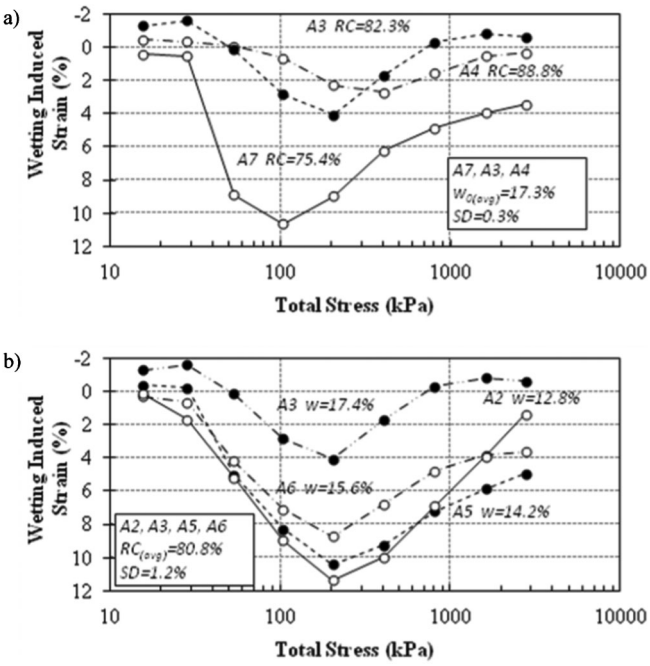

Figure 5.4 Effect of a) relative compaction and b) compaction water content on wetting induced strain as a function of stress level (Soil A).

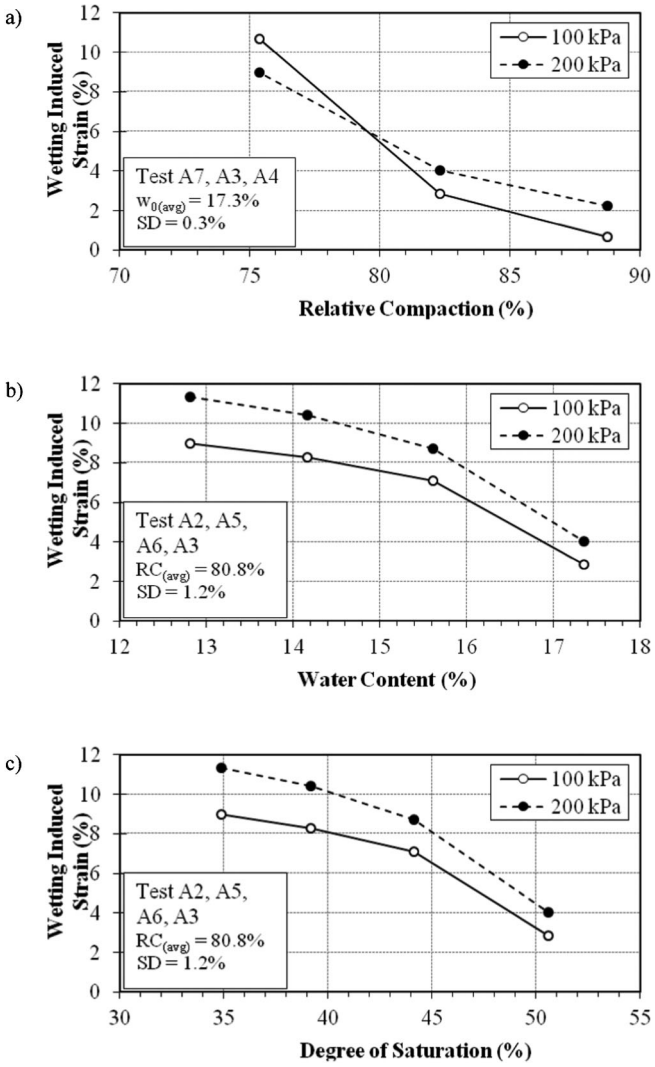

Figure 5.5 Variation of degree of collapsibility of Soil A as a function of: a) relative compaction, b) water content and, c) degree of saturation.

Note that the tests shown in Figure 5.5a also differ in the degree of saturation, with the degree of saturation being the lowest in the test with the lowest RC; hence the trend shown in the figure reflects changes in both relative compaction and degree of saturation.

Figure 5.5b and Figure 5.5c present the variation in collapsibility as a function of water content and degree of saturation, respectively, for specimens compacted at approximately the same relative compaction (~80%). Figure 5.5b shows that below a value of the water content equal to ~ 15.5% (2.5% points below optimum) the collapsibility is severe (see also Table 5.1), with no significant effect of the water content; for values of the water content higher than this threshold the degree of collapsibility decreases rapidly. Similar considerations apply to Figure 5.5c; in this case a threshold of the degree of saturation of 43% beyond which the collapsibility decreases significantly is observed.

Finally, Figure 5.6 presents contours of the degree of collapsibility in the γ_d-w plane (shown in SI units in Figure 5.6a and in English units in Figure 5.6b). Four different regions – none to slight, moderate, moderately severe, and severe – are identified based on the threshold strain values contained in ASTM D5333. In this figure the solid lines are contours drawn through areas where data are available, while dashed lines reflect extrapolations beyond the data set. Such extrapolations relied on observations of similar plots proposed by other authors (e.g. Lawton et al. 1989). Note that by definition of collapse potential these contours reflect the strains measured at 200 kPa. Different contours would be drawn based on data at a different stress level.

A few conclusions can be drawn from Figure 5.6. First, it can be expected that for this soil compaction to RC greater than 95% may greatly reduce, and possibly eliminate concerns about wetting induced collapse. Between 85% and 92–95% RC, the degree of collapsibility is moderate even in close proximity to the optimum moisture content, with no significant impact of the water content. Below 85% RC the degree of collapsibility increases, and for small reductions in the water content it can quickly go from moderate, to moderately severe to severe. While for this soil no data were gathered on the wet side of optimum, the trend in the data collected indicate that collapse issues are likely to be significantly reduced or eliminated for compaction to values of the water content beyond the line of optimum.

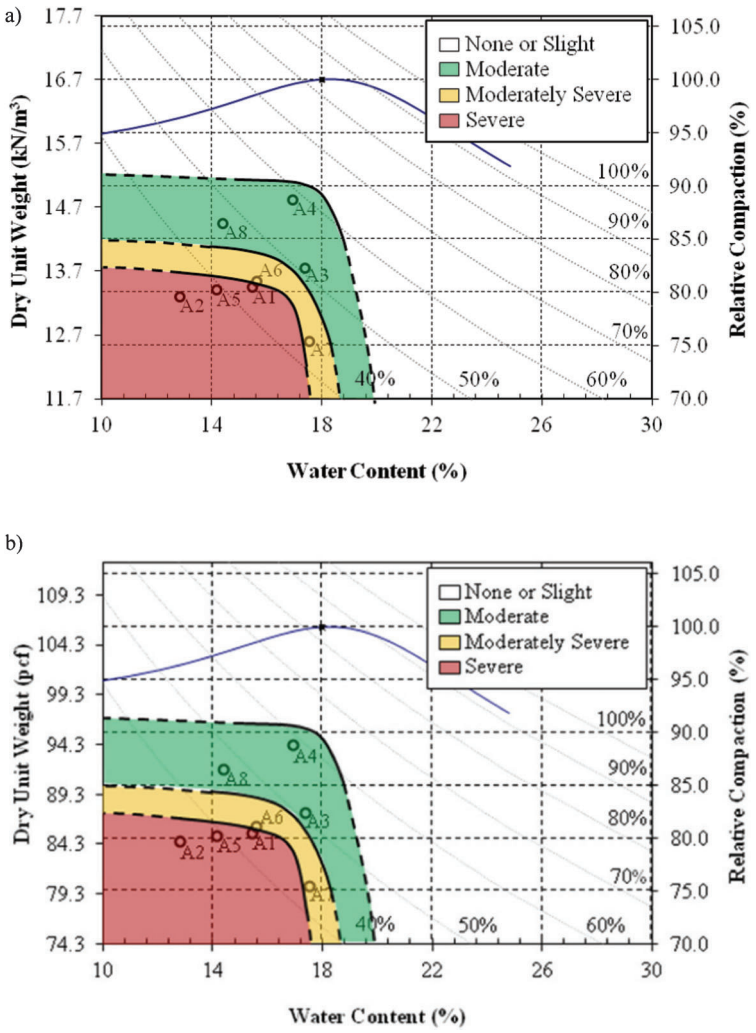

Figure 5.6 Contours of collapse potential on γ_d – w plane (Soil A): a) SI units; b) English units.

5.2.2 Soil B

As discussed in Chapter 4, eleven pairs of oedometer tests were conducted on specimens of Soil B compacted over a range of water contents ($w_{opt}-6.5\%$ to $w_{opt}+1.5\%$, although the majority of the tests were performed dry of optimum) and values of relative compaction (~74% to greater than 98%). Table 4.7 summarizes the initial conditions for such tests. The compression curves from all tests performed without wetting ("dry" specimens) are shown in Figure 5.7a, while Figure 5.7b reports the curves for all the "wet" specimens. As for Soil A, all compression curves are reported in terms of strain versus total vertical stress. As expected, a significant range in the compression behavior of the dry soil is observed depending on the compaction conditions. In particular, the greater the relative compaction, the larger the value of stress level (σ'_p) at which the compression curve breaks. For the tests in which loading in the oedometer sufficiently exceeded σ'_p, it is observed that the compression curves of the dry specimens exhibit a slight S-shape, with the slope of the virgin compression line slightly decreasing at higher stress levels. In contrast, the majority of the wet curves show an essentially constant value of the slope in the normally consolidated region.

Figures 5.8a–j present the pair of compression curves for each pair of tests (one "dry", one "wet") conducted on specimens compacted similarly. The average values of water content, relative compaction (RC%), and initial degree of saturation for each pair of specimens are presented in each figure. As discussed for Soil A, the vertical offset between each pair of curves represents the collapse potential as a function of stress level. All these values of the strain differential measured between the wet curve and the dry curve are summarized in Table 5.2.

As for Soil A, the negative values of the wetting induced strains reflect cases in which the effects of the swelling induced by wetting of the soil override any

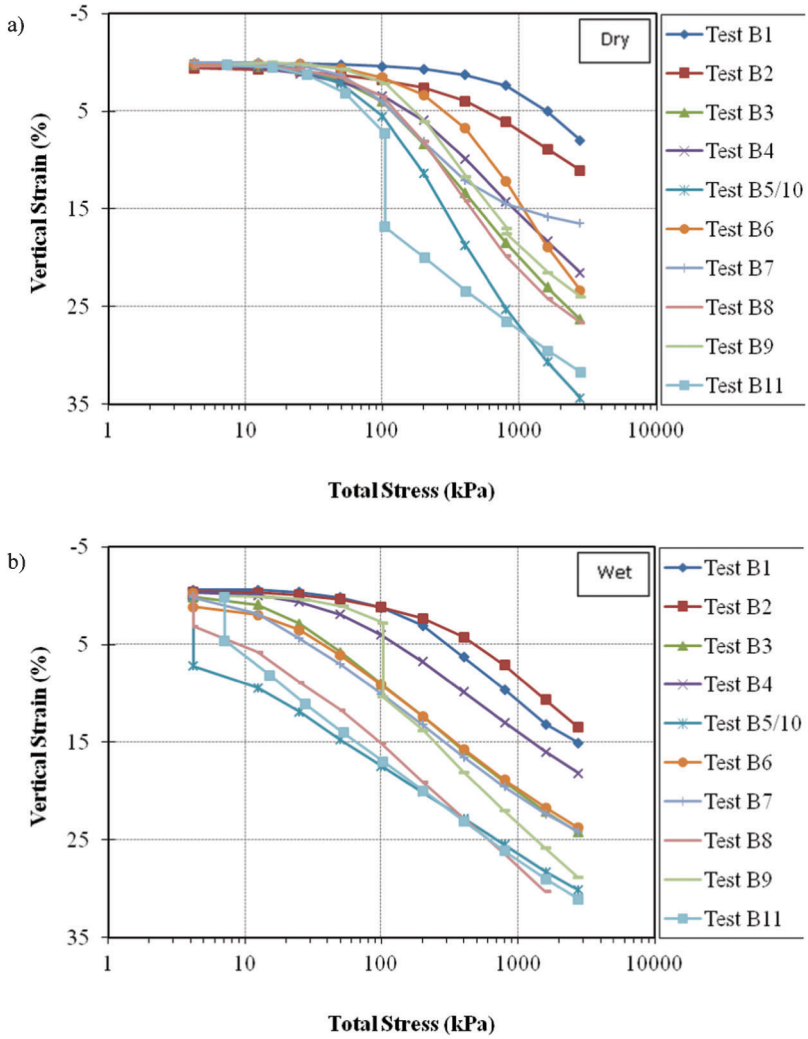

Figure 5.7 Compression curves from oedometer tests on Soil B: a) "dry" specimens, and b) "wet" specimens

wetting induced collapse. In this case the compression curve for the wet specimen falls above that for the dry one. As seen in Table 5.2, negative values of the differential strains are measured at low stress levels in the specimens compacted close to γ_{dmax} (tests B1 and B2), which are likely to exhibit slight to no collapse. The same trend of wetting induced strain versus stress level, described for Soil A is observed for Soil B: the wetting induced strain first increases with stress level, reaches a maximum value, and then decreases once again (see Figure 5.10a–b). The only exception to this trend is test B7. However, as highlighted in the note at the bottom of Table 5.2, data from this test at stress levels >400 kPa may not be considered completely reliable, due to the fact that the LVDT used to measure the vertical displacement in the dry specimen exceeded its linear range at this stress level. While corrections were made to account for this the data remains in question. Note also that for three of the tests (B3, B4, B5/10) Table 5.2 reports negative values of wetting induced strains over the last couple of stress increments. This indicates that at these stress levels the compression curve for the dry specimen has "fallen below" that for the wet specimen. This is a result of the S-shape of the compression curve of the dry specimens.

As shown in Table 5.2 and in Figure 5.8a–i, for any pair of specimens, the wetting induced strain varies as a function of the stress level. Table 5.2 highlights two values of the collapse strain: the strain measured at 200 kPa, which is used to define the collapsibility index, I_e, and the maximum value of the collapse strain termed $I_{e(max)}$. Given the wide range of compaction conditions examined for Soil B, both I_e and $I_{e(max)}$ vary greatly, from less than 1% (test compacted at close to optimum conditions - no collapse potential) to over 11% (severe collapse potential). Compared to Soil A, the stress level at which the maximum collapse strain is observed also varies significantly: from 50 kPa to 2760 kPa, depending on the compaction conditions. This is shown in Figures 5.9a–b, which highlights how the tests

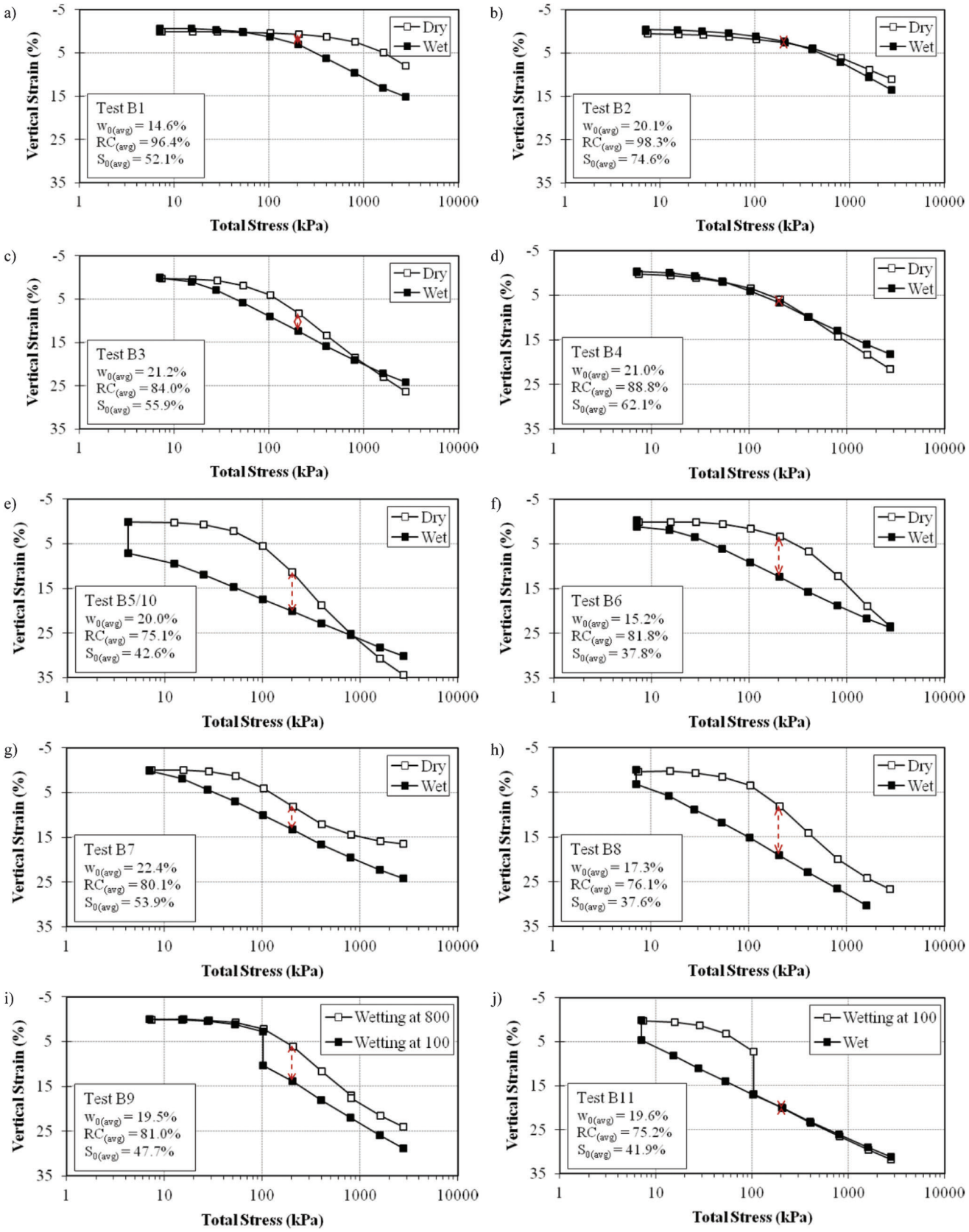

Figure 5.8 Compression curves from double oedometer tests: a) Test B1; b) Test B2; c) Test B3; d) Test B1; e) Tests B5/B10; f) Test B6; g) Test B7; h) Test B8; i) Test B9; j) Test B11

TABLE 5.2
Summary of double oedometer test results for Soil B

Test		B1	B2	B3	B4	B5/10	B6	B7	B8	B9	B11
$w_{0(avg)}$ (%)		14.6	20.1	21.2	21.0	20.0	15.2	22.4	17.3	19.5	19.6
Offset from w_{opt} (%)		−6.4	−0.9	0.2	0	−1	−5.8	+1.4	−3.7	−1.5	−1.4
$\gamma_{d(avg)}$ (kN/m^3) [$\gamma_{d(avg)}$ (lb/ft^3)]		14.8 [94.2]	15.1 [96.1]	12.9 [82.1]	13.7 [87.2]	11.6 [73.8]	12.6 [80.2]	12.3 [78.3]	11.7 [74.5]	12.5 [79.6]	11.6 [73.8]
$\gamma_{(avg)}$ (kN/m^3) [$\gamma_{(avg)}$ (lb/ft^3)]		17.0 [108.2]	18.2 [115.9]	15.7 [99.9]	16.5 [105.0]	13.9 [88.5]	14.5 [92.3]	15.1 [96.1]	13.7 [87.2]	14.9 [94.8]	13.8 [87.8]
$RC_{(avg)}$ (%)		96.4	98.3	84.0	88.8	75.1	81.8	80.1	76.1	81.0	75.2
$S_{0(avg)}$ (%)		52.1	74.6	55.9	62.1	42.6	37.8	53.9	37.6	47.7	41.9
$e_{0(avg)}$		0.75	0.71	1.00	0.90	1.24	1.06	1.10	1.21	1.08	1.24
Nominal Stress at Saturation (kPa)		4.2	4.2	4.2	4.2	4.2	4.2	4.2	4.2	100 & 800	4.2 & 100
Wetting induced strain (%)	12.5 kPa	−0.70	−1.04	0.52	−0.60	9.21	1.81	1.85	5.52	- [a]	7.66
	25 kPa	−0.53	−1.02	2.09	−0.47	11.22	3.32	4.08	8.18	- [a]	9.83
	50 kPa	−0.07	−0.91	3.98	−0.08	12.59	5.53	5.74	10.19	- [a]	10.87
	100 kPa	0.80	−0.64	5.06	0.61	11.94	7.55	6.06	11.63	8.24	9.74
	200 kPa	2.35	−0.27	4.01	0.81	8.77	8.99	5.09	11.02	7.73	- [b]
	400 kPa	5.00	0.28	2.46	−0.01	4.10	8.96	4.42	8.63	6.36	- [b]
	800 kPa	7.23	1.02	0.57	−1.30	0.23	6.65	5.10 [c]	6.59	5.05	- [b]
	1600 kPa	8.16	1.78	−0.91	−2.34	−2.42	2.83	6.54 [c]	6.15	- [a]	- [b]
	2760 kPa	7.10	2.38	−2.11	−3.39	−4.23	0.37	7.70 [c]	-	- [a]	- [b]
Ie (%)		2.35	−0.27	4.01	0.81	8.77	8.99	5.09 [c]	11.02	7.73	9.74[b]
$Ie_{(max)}$ (%)(stress at $Ie_{(max)}$)		8.16 (1600 kPa)	2.38 (2760kPa)	5.06 (100 kPa)	0.81 (200kPa)	12.59 (100 kPa)	8.99 (200 kPa)	6.06 [c] (100 kPa)	11.63 (100 kPa)	8.24 (100 kPa)	10.87 (50 kPa)
Collapse Potential		Moderate	None	Moderate	Slight	Mod. Severe	Mod. Severe	Moderate	Severe	Mod. Severe	Mod. Severe

[a]For this pair of tests no data are available below 100 kPa as both specimens were maintained dry up to that stress level. No data are available beyond 800 kPa, because both specimens have been flushed with water.

[b]For this pair of tests only, Ie was determined at 100 kPa because both specimens were flushed with water before reaching 200 kPa. Hence no wet induced strains are reported for stresses greater than 100 kPa.

[c]For test B7 there are questions on the reliability of the data for the dry specimen above 400 kPa, as the LVDT used to measure the vertical displacement exceeded its linear range. While corrections were made to account for this the data remains in question.

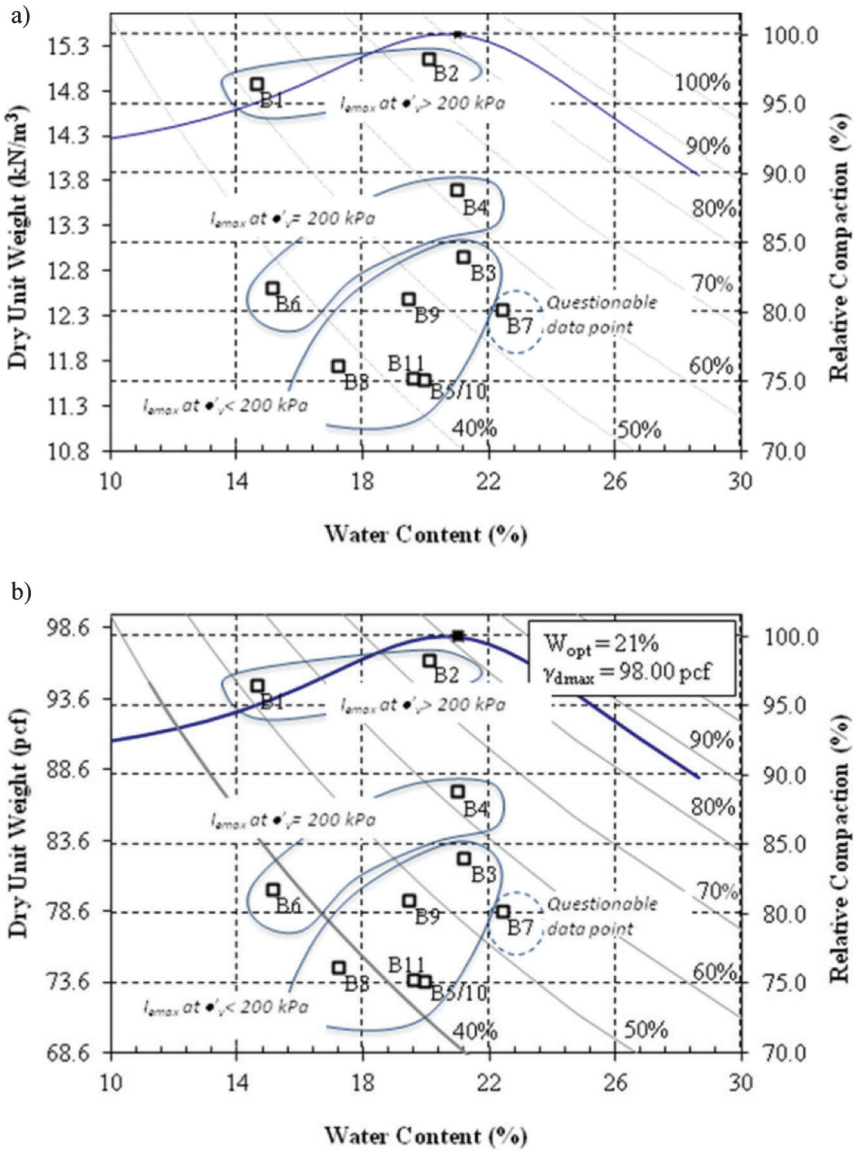

Figure 5.9 Effect of relative compaction and compaction water content on stress level at which maximum collapse strain is observed (Soil B): a) SI units; b) English units.

conducted can be grouped in three sub-sets: the tests in which the maximum collapse strain (I_{emax}) occurs at $\sigma'_v > 200$ kPa (tests B1 and B2); the tests in which (I_{emax}) occurs at $\sigma'_v = 200$ kPa (tests B4, B6), and the tests in which I_{emax} occurs at $\sigma'_v < 200$ kPa (tests B3, B5/10, B7, B8, B9, B11). The figure illustrates that as the relative compaction and the water content decrease, the stress level at which the measured collapse strain reaches the maximum value decreases. With inadequate compaction collapse may become a concern even for relatively small values of the overburden (e.g. see test B5/10). The dependence of the stress level at which collapse is maximized is further illustrated in Figure 5.10a–b. Figure 5.10 plots the wetting induced strain as a function of stress level for four tests all compacted at similar water content, but at different values of relative compaction (from 88.8% for test B4 to 75.1% for test B5/10. The figure shows that as the relative compaction decreases not only do the collapse strains increase, but the stress level at which the maximum collapse strain is measured also decreases. This trend is consistent with previous observations reported in the literature (e.g. Lawton 1986).

A similar plot is shown in Figure 5.10b, this time showing the effect of compaction water content. Consistent with the results for Soil A, the figure shows that all specimens reach the maximum collapse strain at stresses in the 100–200 kPa range, with no clear trend with water content. In contrast, previous work by Lawton (1986) and Lawton et al. (1989) indicated an

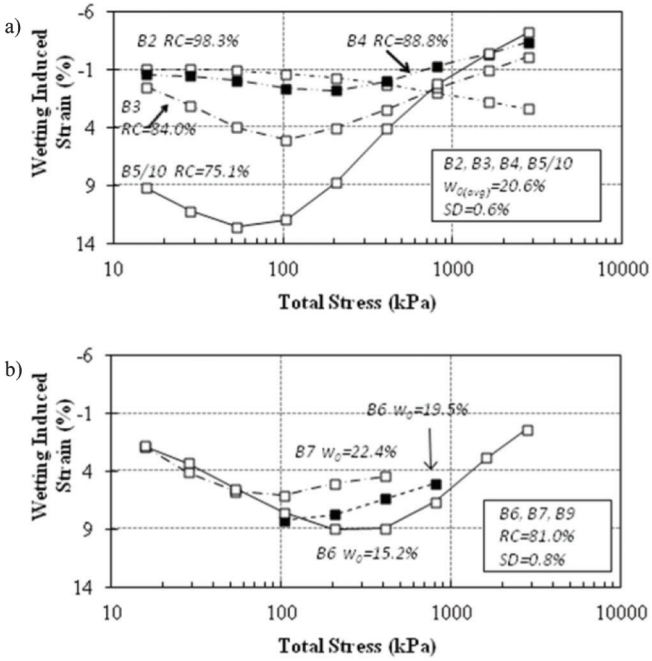

Figure 5.10 Effect of a) relative compaction and b) compaction water content on wetting induced strain as a function of stress level (Soil B).

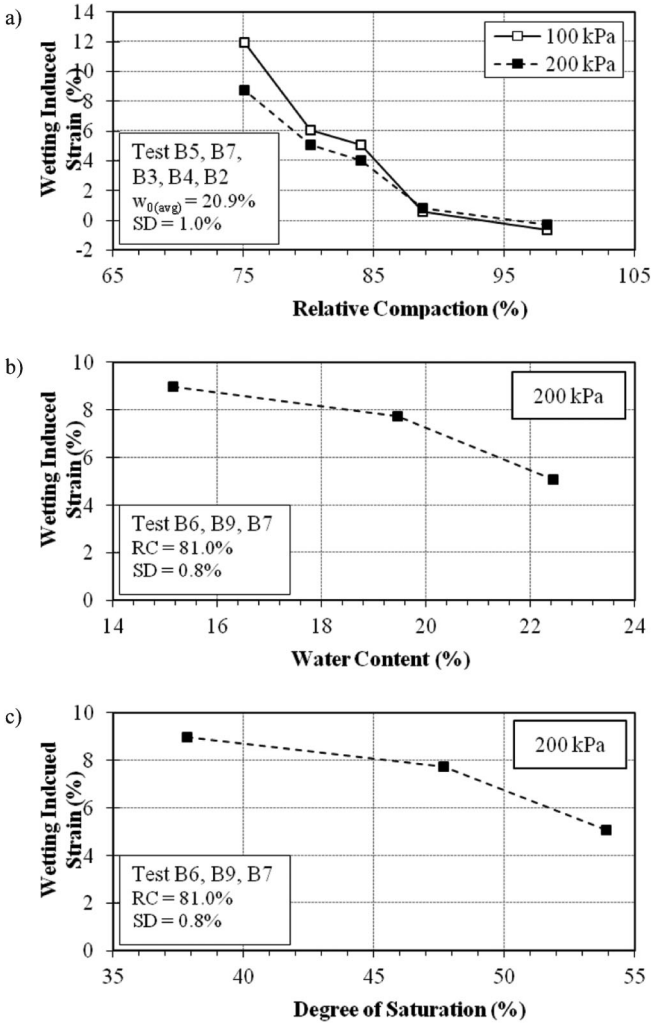

Figure 5.11 Variation of collapsibility of Soil B as a function of: a) relative compaction, b) water content and, c) degree of saturation.

increase in the stress level at which the maximum collapse strain is observed with decreasing compaction water content.

Focusing on the I_e data, trends of collapse versus relative compaction, water content and degree of saturation are illustrated in the plots shown in Figure 5.11a–c. Figure 5.11a shows the variation in the wetting induced strain for 4 tests conducted on specimens compacted at water content very close to the optimum value. It is seen that as the RC decreases the degree of collapsibility increases greatly, with the collapse potential going from none (test B2, RC~98%), to slight (test B4, RC~89 %), to moderately severe (test B3, RC~ 84%), to severe (test B5, RC~75 %). Note that this increase in collapse potential also reflects the reduction in the initial degree of saturation of the specimens, with S_0 going from ~75% for test B2 to ~43% for test B5. A similar trend is observed in the variation of the collapse strain measured at 100 kPa.

Figure 5.11b–c show similar plots illustrating the effects of compaction water content and degree of saturation on the collapse strain at 200 kPa measured on specimens compacted at approximately the same relative compaction (~81%).

Finally, Figures 5.12a–b compile all the data for Soil B to show regions of different collapse potential plotted on the w-γ_d plane (in solid lines the contours through the experimental data; in dashed lines the contours extrapolated beyond the present data set). Consistent with ASTM D5333, five regions of collapse potential are identified in the plot: none, slight, moderate, moderately severe and severe. Note that, by definition of collapse potential, these contours reflect the strains measured at 200 kPa. Slightly different contours would be drawn based on data at a different stress level. Because of the wider range of compaction conditions

TABLE 5.3
Summary of index properties for soils A and B

Test	Soil A	Soil B
Liquid Limit	37.3 %	38.6 %
Plastic Limit	19.5%	23.7%
Plasticity Index	17.8%	14.9%
Specific Gravity	2.691	2.648
Sand	5.5 %	14 %
Silt	69.5%	72.5%
Clay	25%	13.5%
ASTM Classification	CL	CL
AASHTO Classification	A-6	A-6

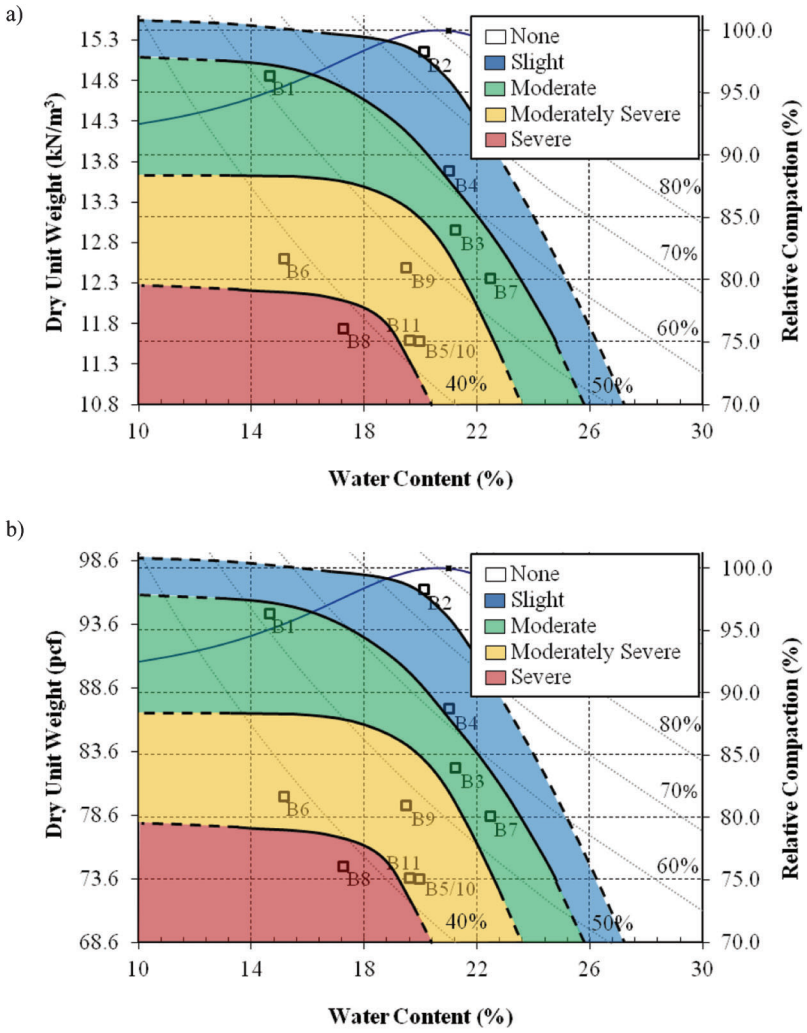

Figure 5.12 Contours of collapse potential on γ_d – w plane (Soil B): a) SI units; b) English units.

examined for Soil B, compared to Soil A, it is possible to determine the critical RC value above which there is no collapse potential, irrespective of water content. For Soil B, this critical value is equal to approximately 105%. Below this value of RC(%), the collapse potential increases rapidly. Between 105% and 98% RC, the collapse potential is 'slight' essentially irrespective of the compaction water content (unless the soil is compacted wet of optimum). Between 98% and 88% RC, and between 88% and ~79% RC, the collapse potential is 'moderate' and 'moderately severe', respectively, for most values of the compaction water content. Below 79% RC the collapse potential is 'severe' although it reduces to moderately severe if the compaction water content falls in the $w_{opt}\pm1\%$ range. For all values of RC(%), the collapse potential decreases provided that the soil is compacted sufficiently on the wet side of optimum. Compaction at $w_{opt}\pm1\%$ appears in most cases to push the collapse potential to the lower category of collapse potential. Finally, the trend in the data collected indicate that for this soil collapse issues are likely to be eliminated for compaction to values of the degree of saturation beyond 80% (the degree of saturation corresponding for this soil to the optimum conditions).

5.2.3 Comparison of Results from Two Datasets

It is of interest to compare the results gathered for Soil A and Soil B. The index properties of the two soils, which were presented in Chapter 4, are summarized in Table 5.3. It is shown that the two soils are similar in many respects, and in particular in their plasticity characteristics, their classification, and their silt content. One difference is in the sand and clay content: Soil A as higher clay content (25% compared to 13.5%) and lower sand content (5.5% versus 14%), compared to Soil B. Despite this difference, as shown in Figure 4.4 and Figure 4.8, the particle size distributions for both soils fall in the same region of clayey loess. Note that no information is available regarding the shape and angularity of the silt fraction in the two soils.

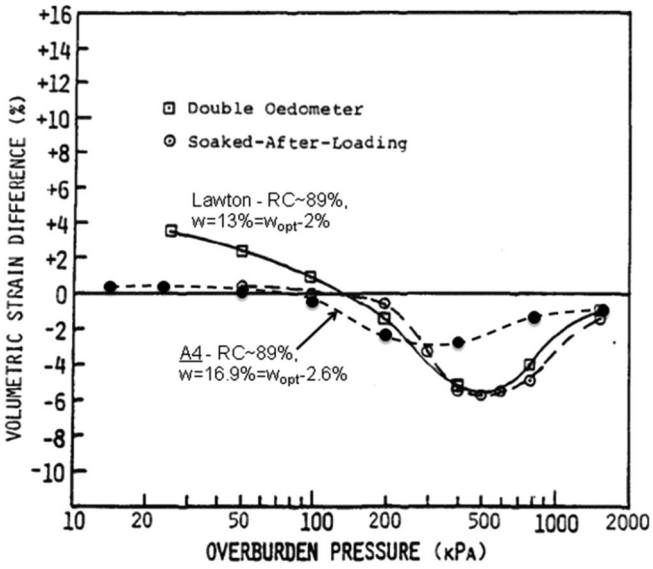

Figure 5.13 Wetting induced strain versus overburden stress for specimens comcpated at ~ 89% relative compaction (adapted from Lawton et al. 1992).

Note: the graph above uses a strain sign convention opposite to that employed in this research

Previous research indicates that this factor, along with clay and sand fraction, can have significant effect on the collapsibility of the soil.

Overall, the trends in the data for soils A and B are consistent, in terms of the influence of compaction water content, degree of saturation, and relative compaction on the collapse strains, as well as on the stress at which the maximum collapse strain is measured. Additionally, comparable values of the collapse strain are measured for the two soils for specimens compacted to similar values of relative compaction ad degree of saturation (the compaction water content does not appear as useful of a reference parameter, due to differences in the optimum moisture content determined for the two soils). For example, a comparison can be made between the data of: tests A7 (RC=75.4%, S_0=42.9%) and B5/10 (RC=75.1%, S_0=42.6%), which display values of I_e equal to 8.96% and 8.77%, respectively (moderately severe collapse potential); tests A6 (RC=81.1%, S_0=44.1%) and B9 (RC=81.0%, S_0=47.7%), which display values of I_e equal to 8.73% and 7.73%, respectively (moderately severe collapse potential); and tests A4 (RC=88.8%, S_0=58.1%) and B4 (RC=88.8%, S_0=62.1%), which display values of I_e equal to 2.7% (moderate collapse potential) and 0.81% (slight collapse potential), respectively. Comparison of the contour plots presented in Figure 5.6 and Figure 5.12 shows some differences in the collapse potential for the two soils. The most notable are: the greater extension of the region of moderate collapsibility for Soil B (which extends to RC values as high as 98% for Soil B, compared to ~92% for Soil A); the more limited extension of the regions of moderate collapsibility for Soil A compared to Soil B; and the slight increase in the threshold value of RC(%) below which severe collapse potential is observed increases (from approximately 79% for Soil B to 82% for Soil A).

The results for soils A and B are further analyzed in Section 5.2, where they are compared to data published in the literature for similar soils.

5.3 Comparison of Collapse Measurements to Data from Literature

This section is organized in two sub-sections. Section 5.3.1 compares the collapse data presented in Section

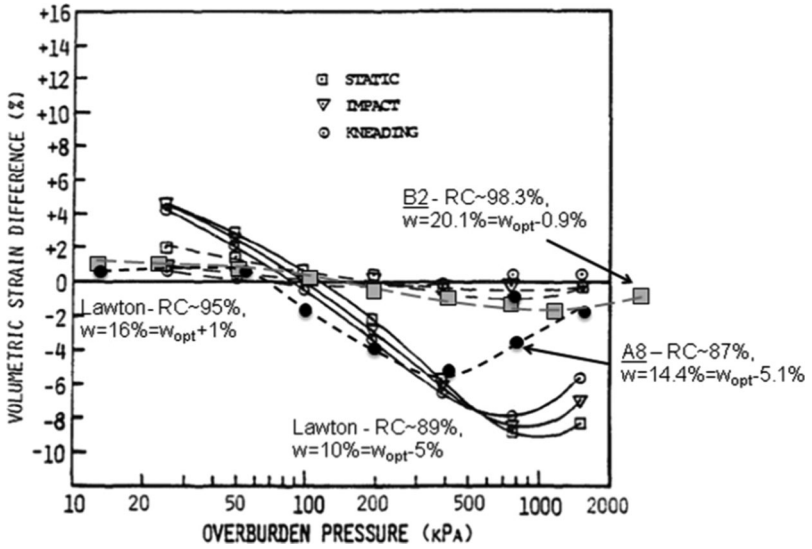

Figure 5.14 Wetting induced strain versus overburden stress (adapted from Lawton et al. 1992)

Note: the graph above uses a strain sign convention opposite to that employed in this research

5.2 to published data collected for similar soils. Section 5.3.2 examines the applicability of the collapse criteria presented in Table 2.1 to the soils and compaction conditions examined in this research.

5.3.1 Comparison of Collapse Results to Literature Data

As discussed in Chapter 2, several researchers have studied the problem of wetting induced collapse in compacted soils. This section aims at comparing the data gathered in this study to selected results documented in the literature. The following five studies have been selected for this purpose, as they pertain to soils that have similarities to the two examined in this research, are based on similar experimental procedures (single and/or double oedometer tests), and they provide sufficient detail that allows quantitative comparisons to the data collected for soils A and B.

a) the work by Lawton and co-workers documented in Lawton (1986), Lawton et al. (1989), and Lawton et al. (1992).
b) the study by Basma et al. (1992);
c) the study by Alwail et al. (1994);
d) the study by Kim et al. (2008).

The work by Lawton and co-workers is probably the most extensive study of the collapse behavior of a given soil. The soil studied by these authors has the following characteristics: 62% sand, 23% silt, 15% clay, LL = 34%, PI=15%. The most notable difference from the soils examined in this research is in the sand and silt content (compare values above to data in Table 4.3) and the silt to sand ratio (0.37 vs. 12.6 and 5.2 for soils A and B, respectively).

Despite these differences, the data provided by Lawton (1989, 1992) show many similarities in the trends linking the collapse measurements to the influencing parameters (stress level, water content, relative compaction). For example, Figure 5.13 and Figure 5.14 shows the change in wetting induced strain as a function of stress level for soil specimens of different values of relative compaction and water content. It is observed that all curves display the same trend displayed by the data for soils A and B (see Figure 5.4 and Figure 5.10), where the strain first increases, reaches a maximum and then decreases once again. Note that the values of RC reported for the soil tested by Lawton have been corrected in Figure 5.13to express them relative to the standard Proctor parameters rather than to the modified ones, as done in the original publication. Figure 5.14 also shows the same trend of increasing maximum collapse strain with decreasing value of relative compaction. Moreover, it is observed that the curves for specimens of soils A and B with similar values of RC(%) and water content (not in absolute value but in terms of offset from optimum conditions), which are overlain on the original plots, show values of the maximum collapse of the same order, with the specimens tested by Lawton et al. (1992) exhibiting marginally greater collapse.

The data by Lawton et al. (1992) also support another trend observed in this research, i.e. the increase in the stress level at which the maximum collapse strain occurs with increasing relative compaction (see Figure 5.4a and Figure 5.10a). The data by Lawton et al. (1992) highlighting this trend are shown in Figure 5.15a. Again the values of RC reported for the soil tested by Lawton have been corrected to express them relative to the standard Proctor parameters. For reference data for two tests on Soil A compacted at similar water contents and different values of RC(%) are overlain on this plot. Again the collapse strain measurements are comparable, although consistently the curves for the soil tested by Lawton et al. (1992) reach the maximum collapse strain at a vertical stress level greater than that typically observed for soils A and B.

Figure 5.15b shows a trend, which, instead, was not observed in this research (see Figure 5.4b and Figure 5.10b), i.e. the increase in the stress level at which the maximum collapse strain is measured with decreasing compaction water content (at same relative compaction).

Finally, Lawton (1989) and Lawton et al. (1992) report contours of wetting induced stain on the relative compaction – water content plot. One such plot, determined for a stress level of 200 kPa is shown in Figure 5.16 (again the values of RC% have been corrected from the original plot so that they are referenced to the standard Proctor results). This plot can be compared to those shown in Figure 5.6 and Figure 5.12 for soils A and B, respectively, to compare the collapse potential of the three soils. One first observation pertains to the value of the relative compaction above which collapse does not occur independent of the water content. For the soil tested by Lawton et al. (1992) this critical value is equal to approximately 96%. For Soil B this value is equal to 105% (see Figure 5.12) indicating the greater susceptibility of this soil to collapse. Note that this critical value could not be determined for Soil A (see Figure 5.6) due to the lack of data at high values of relative compaction.

It is instead possible to compare for all three soils the value of relative above which the collapse strain at 200 kPa is less than 2% (slight degree of collapsibility). This value is equal to approximately 92% for the soil tested by Lawton et al. (1992), compared to 91% and 97% for soils A and B, respectively. Again this demonstrates the higher collapse potential of Soil B.

Finally, it can be observed that the contour map presented in Figure 5.16 has similar features to those presented earlier for soils A and B. One difference that might be noted is the steeper slope of the contours on the very dry side of optimum. This indicates a more rapid mitigation of the collapsibility of the soils with an increase in compaction water content, compared to what was observed in Figure 5.6 and Figure 5.12 for soils A and B.

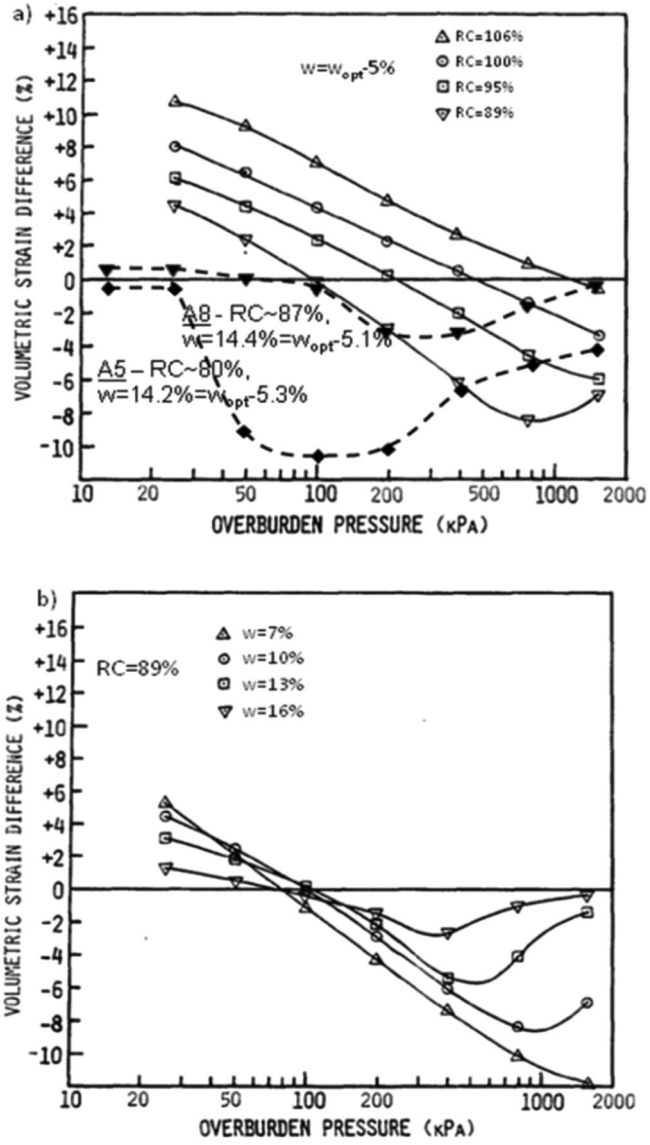

Figure 5.15 Effect of a) relative compaction and b) water content on wetting induced collapse (adapted from Lawton et al. 1992)

Note: the graphs above use a strain sign convention opposite to that employed in this research

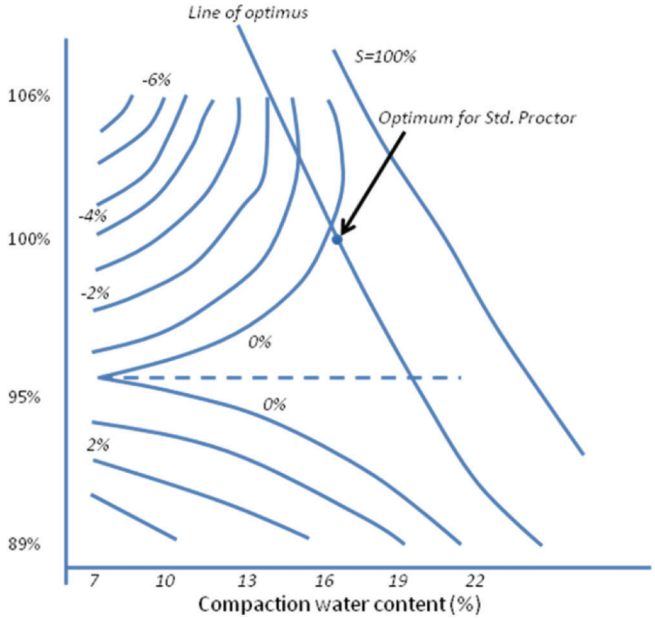

Figure 5.16 Contours of equal wetting induced strain at 200 kPa (adapted from Lawton et al. 1992)

As discussed in Chapter 2, by study by Basma et al. (1992) examined the collapse behavior of eight different soils by performing single oedometer tests. The properties of these soils are summarized in Table 5.4. Note that soils S7 and S8 are granular soils, and their data cannot be directly compared to the results obtained in this research.

Figure 5.17 shows data obtained measured on specimens of the eight soils tested by Basma et al. (1992) compacted at a relative compaction of 80% and at a water content of 6% (significantly on the dry side of optimum). Collapse strains are plotted as a function of stress level and the difference between the sand and clay content. Superimposed on this plot are the collapse strain values measured at 200 kPa in tests A2 and B6. These two tests were compacted at RC close to 80% and at water contents on the dry side of optimum (see Table 5.1 and Table 5.2). From Table 5.3, it is found that the difference in sand and clay fractions is −19.5%

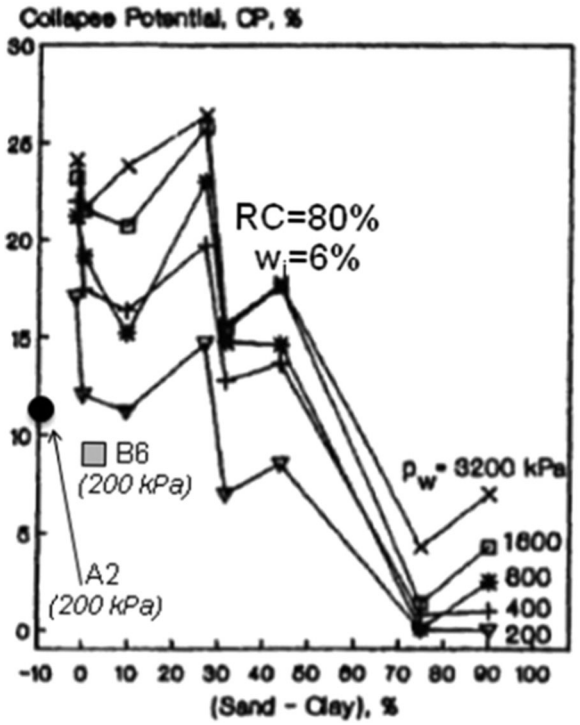

Figure 5.17 Comparison of data for soils A and B to database by Basma et al. (1992): collapse strain vs. (sand-clay)%

TABLE 5.4
Properties of soils tested by Basma et al.1992

	PROPERTIES														
	Grain-Size Characteristics					Consistency Limits		Compaction Characteristics		Packing Characteristics					
Soil series(1)	Sand (4.75 mm–75 μm) (%)(2)	Silt (75–2 μm) (%)(3)	Clay (<2 μm) (%)(4)	Coefficient of uniformity C_u(5)	Coefficient of concavity C_c(6)	Liquid limit LL(%)(7)	Plasticity index Pl(%)(8)	Maximum dry unit wei ght γd_{max} (KN/m^3)(9)	Optimum water content OWC (%)(10)	Maximum packing dry unit weight γp_{dmax}(KN/ m^3(11)	Minimum packing dry unit weight $\gamma p_{d\max}$ (KN/m^3(12)	Maximum void ratio $e_{\max}$(13)	Minimum void ratio $e_{\min}$(14)	Specific gravity G_S(15)	Unified soil classification (16)
S1	40.6	50.5	8.9	17.5	7.2	36.6	12.7	18.7	14.5	–	–	–	–	2.74	CL
S2	47.8	47.2	5.0	25.0	1.1	29.1	11.2	19.3	13.5	–	–	–	–	2.72	CL
S3	13.3	73.5	13.2	60.0	15.0	57.2	28.9	17.0	19.3	–	–	–	–	2.69	CH
S4	19.6	70.4	10.0	11.5	2.9	28.0	7.0	17.2	14.3	–	–	–	–	2.77	ML-CL
S5	24.4	49.6	26.0	35.0	0.5	36.0	11.1	16.3	21.0	–	–	–	–	2.66	ML
S6	42.1	42.9	15.0	100.0	0.9	28.2	10.6	18.3	13.7	–	–	–	–	2.69	CL
S7	84.0	7.0	9.0	6.4	1.6	30.0	3.0	–	–	19.2	15.5	0.70	0.37	2.63	SM
S8	92.2	5.8	2.0	3.4	1.1	25.0	5.0	–	–	17.8	14.5	0.83	0.49	2.65	SP-SC

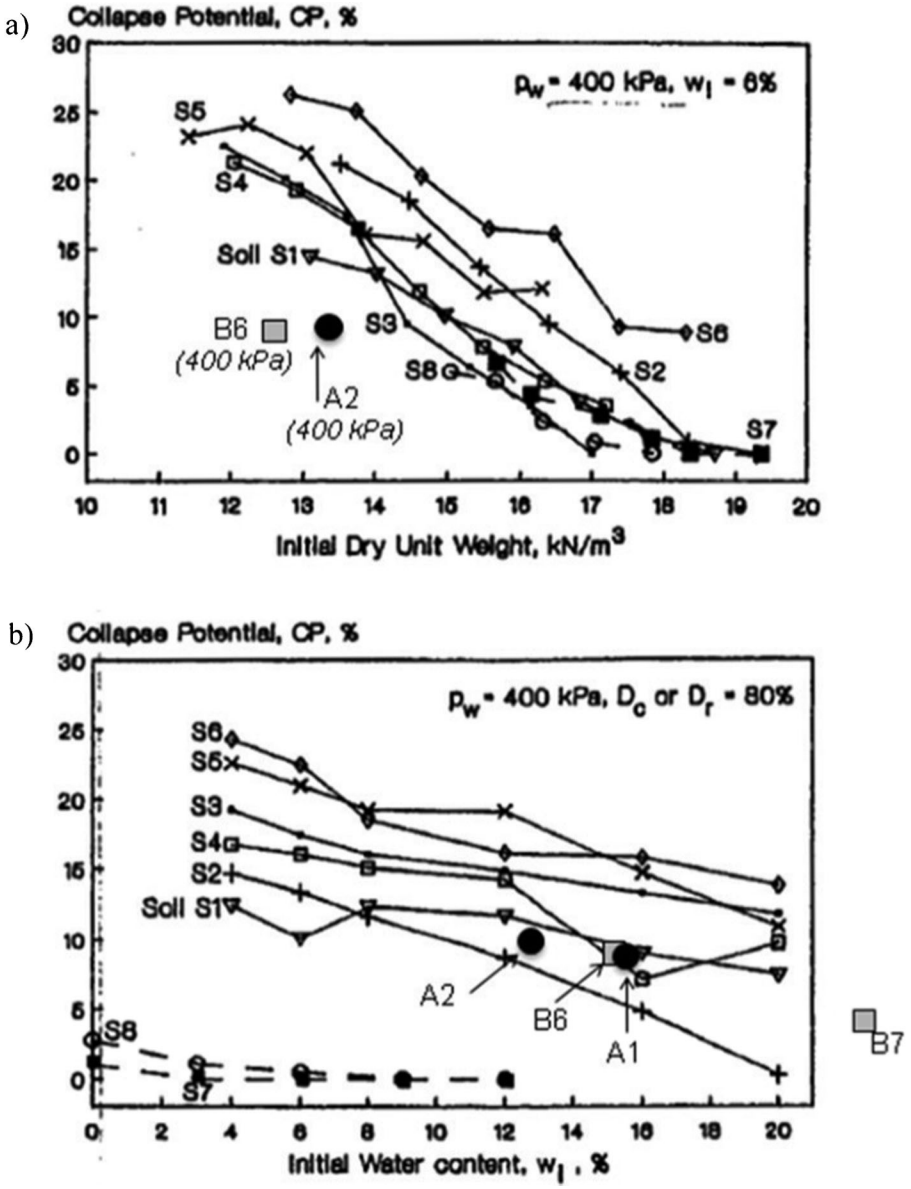

Figure 5.18 Comparison of data for soils A and B to database by Basma et al. (1992): collapse strain at 400 kPa vs. a) initial dry unit weight and b) compaction water content.

for Soil A (plotted in correspondence to −10% in Figure 5.13) and +0.5% for Soil B. The 200 kPa collapse strains for tests A2 and B6 are found to fall relatively close to the data band presented by Basma et al. (1992). One significant difference lies in the fact that Basma et al. report increasing values of the collapse strains at higher stresses, while in this research it was found that typically the collapse strains tended to reach their maximum value at strains below 400 kPa (see Table 5.1 and Table 5.2 and Figure 5.3 and Figure 5.9).

The collapse strain data for specimens A2 and B6 (this time measured at 400 kPa) are further compared to the database provided by Basma et al. in Figure 5.18a–b. Here collapse strains are plotted as a function of the compaction dry unit weight (Figure 5.18a) or compaction water content (Figure 5.18b). In Figure 5.18a the data for soils A and B again fall slightly below the data for the soils presented by Basma et al., which however were compacted at a much lower water content. Instead, when plotted versus water content in Figure 5.18b, the data for specimens A1, A2, B6 and B7 (chosen to have the same relative compaction as the data presented in the original plot) fall within the band of the dataset provided by Basma et al. (1992), in close proximity to the results for the two CL soils included in the database. It is somewhat surprising that water content can be used effectively as a reference parameter as soils differ in the range of water contents in which they can be compacted, the optimum moisture content, as well as the degree of saturation at any given water content.

Basma et al. (1992) also propose an equation for predicting the collapse potential from (sand-clay)%,

compaction water content and compaction dry density, and stress level. The authors demonstrate that predictions made using this equation fit well with data measured on their eight soils, as well as with data from previous studies (e.g. Lawton et al. 1989). However, it is found that the equation significantly overpredicts the collapsibility of soils A and B, especially for increasing values of the stress level. One possible explanation is that the equation was derived from data for soils containing significant sand % (>10%) and more sand than clay.

Alwail et al. (1994) address the effects of soil composition on wetting induced collapse, by performing double oedometer tests on soils fabricated in the laboratory by mixing different quantities of sand, silt and clay. Alwail et al. (1994) conclude that the quantity of clay plays a key role in determining the magnitude of collapse, as demonstrated by the relationship between percent clay and maximum collapse shown in Figure 5.19. Note that all data reported in this figure pertain to specimens compacted at 90% of the maximum dry density obtained from the Modified Proctor test, and 3% dry of optimum. Comparison of collapse strains measured on soils A and B to the data shown in Figure 5.19 is not straightforward as the modified proctor γ_{dmax} or w_{opt} are not known. Despite this data from two of the tests performed in this research are included over the plot by Alwail et al. (1994) in Figure 5.19. The two tests are: test B1, compacted at RC~ 96% (referenced to the standard Proctor) and at a water content over 6% points dry of the standard Proctor optimum moisture content; and test A4 compacted at RC~ 90% (referenced to the standard Proctor) and at a water content approximately 2.5% points dry of the standard Proctor optimum moisture content. Note that it is not expected that the data for soils A and B necessarily fall in the band presented by the authors of Figure 5.19, as all the data points shown in the figure pertain to soils prepared using the same parent soils. As shown in Figure 5.19, not only do the data for soils A and B fall slightly off the band of the rest of the data, but they also display opposite trend. It is worth pointing out how the trend of increasing collapse with increasing clay percentage proposed by Alwail et al. (1994) contradicts some earlier studies on the role played by clay% on collapse potential. For example Handy (1973) suggested that for Iowa loess the highest degree of collapsibility was associated with clay contents below 16%, and that further increases in clay content above this threshold led to continued decrease in the collapsibility. Data collated from the literature by Lawton et al. (1989) indicated instead that there is a critical value of the clay content in correspondence to which the collapse strain is maximized. These authors indicated that for sand-clay mixes this critical value is around 40%, while it reduces to approximately 15% for silt-clay mixes. This observation is consistent with the greater collapsibility of Soil B relative to Soil A observed under similar compaction conditions (e.g. see Figure 5.19).

Finally, it is of interest to try to compare the data for Soils A and B to the results presented by Kim et al. (2008), as these authors also tested a CL loess sample obtained in Indiana. As already mentioned in Chapter 2, this soil has the following characteristics: LL=32.2% PI=9.3%, clay=20%, silt~80%, γ_{dmax}= 17.1 kN/m^3 (108.8 lb/ft^3), w_{opt}=16.2%. Three test results are reported for this soil: a) test 1 - RC=100%, $w=w_{opt}$=16.2%, I_e=0.16%; b) test 2 - RC=90%, $w=w_{opt}-6.7\%=9.5\%$, I_e=0.19%; c) test 3 - RC=80%, $w=w_{opt}-9\%=7.2\%$, I_e=3.83%. Comparison of these data to the contour plots presented in Figures 5.6 and 5.12 for soils A and B indicates that these soils tend to exhibit greater collapse strains than that tested by Kim et al. 2008), especially as the relative compaction decreases (compare for example test B6 which has RC~82~, $w=w_{opt}-5.8\%=15.2\%$, and I_e~9%; to test 3 above).

5.3.2 Applicability of Existing Collapsibility Criteria to Data for Soils A and B

Criteria for judging the collapse potential of a soil introduced in the literature were discussed in Chapter 2 and summarized in Table 2.1. Table 5.5 and Table 5.6 examine the applicability of a few of these criteria to the data collected for soils A and B, respectively.

In general, it is found that none of the criteria examined are able to fully capture the behavior of these soils. For some this is to be expected. For example, the criteria by Clevenger (1958) and Brink (1958) are based on fixed threshold values of the dry unit weight, with no consideration of soil type or water content variation. The first provides two threshold values: 12.6 kN/m^3 (80.2 lb/ft^3) and 14 kN/m^3 (89.1 lb/ft^3). For values of the dry unit weight below 12.6 kN/m^3 the criterion indicates that large collapse settlements are to be expected, and that for values below 14 kN/m^3 that small settlements are to be expected. Note that the term "medium settlement" has been used in Table 5.5 and Table 5.6 for values of the dry unit weight falling in between these values. The criterion by Brink (1958) has instead a unique threshold value of the dry unit weight. The criterion by Gibbs (1961) is a step ahead in this regard in that it is based on a threshold value of the dry unit weight that varies depending on the liquid limit of the soil. In its original form it provides a yes/no answer and therefore cannot reflect the differences in collapse potential that are to be expected at the same dry unit weight for different compaction water contents. Note that in the tables below the criterion was slightly adapted in that two values of the threshold dry unit weight were used, one (~ 13 kN/m^3 = 82.8 lb/ft^3) determined in correspondence to the liquid limit, the second determined assuming a slightly lower LL (to reflect the uncertainty in determining this parameter). The slightly modified classification presented in Table 5.5 and Table 5.6 uses the term "high collapse potential" if the dry unit weight is lower than the first threshold, "collapse potential" if it falls between the two thresholds, and "no collapse" if it falls above the second

TABLE 5.5
Application of select collapsibility criteria to data for Soil A

	Gibbs (1961)		*Denisov (1951)*		*Clevenger (1958)*		*Soviet Building Code (1962)*		*Handy (1973)*		*S. Africa Criteria (Brink 1958)*	
Test [a]	γ_d (kN/m^3) [γ_d (lb/ft^3)]	Classification	K	Classification	γ_d (kN/m^3) γ_d (lb/ft^3)	Classification	L	Classification	Clay	Classification	CP	Classification
A1 High	13.42 [85.4]	No collapse	1.038	Medium	13.42 [85.4]	Medium Settlement	−0.019	Collapsible	25%	<50% probability of collapse	83.42	Collapsible
A2 High	13.28 [84.5]	Collapse potential	1.016	Medium	13.28 [84.5]	Medium Settlement	−0.008	Collapsible		(24–32% clay)	83.42	Collapsible
A3 Med	13.72 [87.3]	No collapse	1.087	Medium	13.72 [87.3]	Medium Settlement	−0.042	Collapsible			83.40	Collapsible
A4 Med	14.80 [94.2]	No collapse	1.281	Non collapsible	14.80 [94.2]	Small Settlement	−0.123	Noncollapsible			83.34	Collapsible
A5 High	13.38 [85.2]	No collapse	1.032	Medium	13.38 [85.2]	Medium Settlement	−0.016	Collapsible			83.42	Collapsible
A6 High	13.52 [86.1]	No collapse	1.054	Medium	13.52 [86.1]	Medium Settlement	−0.027	Collapsible			83.41	Collapsible
A7 High	12.57 [80.0]	High collapse potential	0.913	Medium	12.57 [80.0]	Medium to Large Settlement	0.046	Collapsible			83.46	Collapsible
A8 Med	14.42 [91.8]	No collapse	1.209	Medium	14.42 [91.8]	Small Settlement	−0.095	Collapsible			83.36	Collapsible

[a]Data from experimental results. Collapse termed none if I_e<0.1%, medium if I_e<6%, high if I_e>6%.

TABLE 5.6
Application of select collapsibility criteria to data for Soil B

	Gibbs (1961)		*Denisov (1951)*		*Clevenger (1958)*		*Soviet Building Code (1962)*		*Handy (1973)*		*S. Africa Criteria (Brink 1958)*	
Test[a]	γ_d (kN/m^3) [γ_d (lb/ft^3)]		K	Classification	γ_d (kN/m^3) γ_d (lb/ft^3)	Classification	L	Classification	Clay	Classification	CP	Classification
B1 Med	14.84 [94.5]	No collapse	1.369	Noncollapsible	14.84 [94.5]	Small Settlement	−0.158	Non collapsible	13.5%	high probability of collapse	83.34	Collapsible
B2 None	15.13 [96.3]	No collapse	1.410	Noncollapsible	15.13 [96.3]	Small Settlement	−0.181	N/A		(<16% clay)	83.33	Collapsible
B3 Med	12.93 [82.3]	High collapse potential	1.000	Medium	12.93 [82.3]	Medium Settlement	−0.009	Collapsible			83.44	Collapsible
B4 Med	13.67 [87.0]	No collapse	1.119	Medium	13.67 [87.0]	Medium Settlement	−0.066	N/A			83.40	Collapsible
B5/10 High	11.56 [73.6]	High collapse potential	0.807	Medium	11.56 [73.6]	Large Settlement	0.098	Collapsible			83.52	Collapsible
B6 High	12.59 [80.1]	High collapse potential	0.949	Medium	12.59 [80.1]	Medium to Large Settlement	0.017	Collapsible			83.46	Collapsible
B7 Med	12.33 [78.5]	High collapse potential	0.913	Medium	12.33 [78.5]	Large Settlement	0.037	Collapsible			83.47	Collapsible
B8 High	11.72 [74.6]	High collapse potential	0.829	Medium	11.72 [74.6]	Large Settlement	0.085	Collapsible			83.51	Collapsible
B9 High	12.47 [79.4]	High collapse potential	0.932	Medium	12.47 [79.4]	Large Settlement	0.027	Collapsible			83.47	Collapsible
B11 High	11.58 [73.7]	High collapse potential	0.811	Medium	11.58 [73.7]	Large Settlement	0.096	Collapsible			83.51	Collapsible

[a]Data from experimental results. Collapse termed none if I_e<0.1%, medium if I_e<6%, high if I_e>6%.

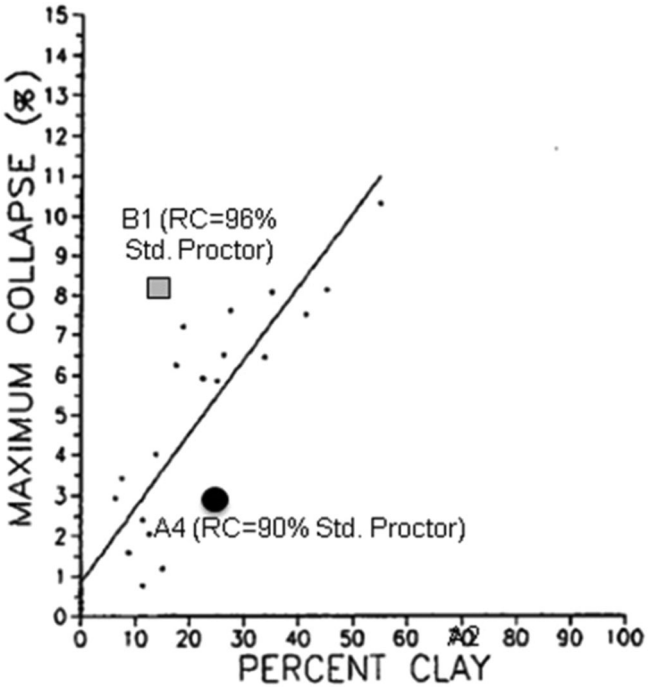

Figure 5.19 Comparison of data for soils A and B to relationship proposed by Alwail et al. (1994) to relate maximum collapse strain to percent clay.

value. Finally, the criteria by Denisov (1951) and the Soviet Building code (1962) are based on consideration of how close the soil's void ratio is to that corresponding to the liquid limit state.

While none of the criteria alone can describe the variability in collapse potential observed in this experimental program, it appears that insights can be gathered from the use of two or more of these methods in combination. For example, Handy's (1973) criterion could be used to screen soils with potential for soil collapse, while the criterion by Clevenger (1958) or the one by Gibbs (1961) could be used to get a preliminary assessment of the degree of collapsibility, prior to conducting laboratory tests.

CHAPTER 6 CONCLUSIONS AND RECOMMENDATIONS

6.1 Conclusions

This section is a summary of the most important conclusions reached with this research. It is divided into five sub-sections. The first four summarize the most significant observations derived from the literature review work and address: the characteristics of loess (6.1.1), the significance of this soil deposit in Indiana (6.1.2), the methods for measuring the collapsibility of compacted soils in the laboratory (6.1.3), and the current knowledge on the collapse behavior of compacted soils (6.1.4). The last one (6.1.5) summarizes the key conclusions of the experimental work.

6.1.1 Loess Characteristics

Loess, a wind-deposited material mainly derived from the major valley train of glaciers, is the most well-known collapsible soil, covering approximately 10% of the land area of the world. In the United States, there are five major regions of significant loess deposits, including the central U.S. interior lowland that extends into Southwestern Indiana.

In general, loess is a silt-based soil commonly yellow to buff in color. Its particle size distribution falls in a wide range depending on composition and environment, but typically loess has quite uniform particle size predominantly in the range of 0.01–0.005 mm. It is usually accompanied by some clay and sand. Silt and sand particles are coated by clay particles, which form clay "bridges" or "buttresses" between the grains, and are the source of bonding between the particles. In the sand and silt fractions, quartz, feldspar, carbonate, mica, and gypsum are usually the most common minerals, while hydromica, montmorillonite, mixed layered kaolinite, and finely-dispersed quartz and calcite dolomite are the major minerals in the clay fraction. In addition to the minerals listed above, most loess contains some carbonates, gypsum, and humic substances, which can all play a role in the bonding system of loess and impact the soil's collapsibility. Interparticle bonds are either (e.g. cementation due to the calcium carbonates) or hydro-labile (e.g. from clay bridges and buttresses or from soluble salts). The latter are responsible for the wetting induced collapse strains measured in loess.

6.1.2 Loess Deposits in Indiana

Despite the predominance of silt-sized particles in loess, not all soils with silt size particles are loess. In addition to consultation of geological maps, the following can aid in the identification of loess: loess usually has a flour texture when touched; its color typically ranges from yellow to buff; in the field no stratifications and vertical cuts are often observed to be stable in a dry state. In the laboratory, loess can be identified through its index properties. Loess usually has sand content less than 15%, clay content not over 25%, dry unit weight less than 13.7 kN/m^3 (87.2 lb/ft^3), and low plasticity index with liquid limit usually less than 50%. Based on a review of the literature most loess soils are classified as CL according to the USCS and A-2-4 or A-2-6 based on AASHTO.

Indiana loess originated from glacial deposition and loess is distributed across most of Indiana, with the exception of the northeast part of the state. The thickest loess deposits (in some cases reaching 25 ft) are located in the southwest part of Indiana and in a small area in the southeast near the Ohio River. Central and southeast Indiana contain thin and moderately thick loess deposits, respectively. South-central Indiana is covered by some discontinuous loess.

In Indiana, loess underlies major highways such as I65, I64, I70, US31, US41, US50, US40, IN64, and the I69 extension.

Information on the presence and thickness of loess deposits can be obtained from the engineering soils maps developed since the 1970s by the Indiana Department of Transportation in conjunction with Purdue University. Counties in which loess deposits are found to be prevalent include: Knox County, with deposits as thick as 200 inches, but decreasing to only 25 inches moving north-east; Gibson County which is covered by moderately deep loess deposits (5–25 feet), again decreasing in thickness moving east-ward; Posey County where all the upland area is mantled by windblown silt or loess deposits as thick as 300 inches; Vanderburgh County, where half of the upland area is covered by moderately deep loess deposits (6–15 feet), while thicker loess deposits (~ 300 inches) are located in the southwest region; Warrick County, where thick loess deposits (~ 200 inches) are found in the Southwestern corner of the county, with decreasing values of thickness moving north-east; Spencer County, in which moderately deep loess deposits (3–15 feet) can be found in over one sixth of the county (from 200 inches to 40 inches, moving north-east); Martin County in which extensive loess deposits (~ 50 inches thick) cover nearly all the upland and thicker deposits are found near the valley of the East Fork White River; Dubois County, which is entirely covered by thin loess deposits with thicknesses of 40 to 75 inches, decreasing toward the Southeastern corner of this county.

Unfortunately soils maps are not available for all counties in Indiana. Other sources of information include the map produced by Purdue University, the USDA and the Indiana Soil Conservation Service. This map indicates that other counties where loess deposits are expected to be significant in extent and thickness include: Vigo County, Parke County, Clay County, Sullivan County, and Daviess County.

6.1.3 Laboratory Methods for Measuring Collapse Potential

Collapse potential is an indication of the degree of bulk volume change soils exhibit due to the combined effects of load and water infiltration. It is generally expressed as the volumetric strain associated with wetting. There are a variety of approaches to measure the collapse potential of soils including laboratory methods and field methods. The most common way is to conduct laboratory tests using the oedometer apparatus. The main advantage of this approach is that three most important factors which affect collapse potential: degree of saturation, dry density, and overburden stress, can be controlled and measured. Typically, results of oedometer tests are used for one-dimensional analysis. Similar measurements can be conducted in the triaxial apparatus, although it has been shown (Lawton 1989) that little additional information on collapse is gained from these tests.

Two types of oedometer tests can be employed to determine collapse potential: the single-oedometer test and the double-oedometer test. In the single-oedometer test a soil specimen is placed in the oedometer, and the desired overburden stress is gradually applied in increments until strain equilibrium is achieved. The soil specimen is then flushed with water under the applied stress. The collapse strain measured after water infiltration is termed collapse potential. ASTM standard D5333 describes the procedure for the single oedometer test. It also classifies the degree of specimen collapse based on the collapse index I_e, the wetting induced strain under a surcharge of 200 kPa. The criterion distinguishes between no (I_e=0%), slight (I_e=0.1%–2%), moderate (I_e=2.1%–6%), moderately severe (I_e=6.1%–10%), and severe (I_e>10%) degree of collapsibility, and can be applied also to the results of the double oedometer test.

The use of the double-oedometer test is based on an assumption that "the deformations induced by wetting are independent of the loading-wetting sequence" (Lawton et al. 1992). The test is conducted using two identical samples: one is tested as in a typical oedometer test at the original water content, while the other specimen is loaded after flushing with water at a low stress level. The difference in the deformations measured from the two tests is the collapse due to wetting at any given stress level. The advantage of the double-oedometer test is that through a single test one can obtain a large amount of data without repeating single oedometer tests at different stress levels.

6.1.4 Collapsibility of Compacted Soils

Four main factors affect the magnitude of wetting-induced subsidence in compacted fills: applied stress, clay content, dry density and as-compacted water content. Other influencing factors include compactive prestress, principal stress ratio, and sample disturbance. These topics have been studied by various researchers. The literature on these topics can be organized in three subsets: laboratory experimental studies; combined field-laboratory investigations; and case history documentation. The review below addresses the first group of studies as they are most relevant to the worked performed for this project.

In the area of laboratory studies, the main contribution has come from the work by Lawton and co-workers who performed over 150 single and double oedometer tests to characterize wetting-induced collapse in a compacted soil with 62% sand, 23% silt, 15% clay (note that this material would not be classified as a loess). The study found a negligible effect of the type of compaction (impact, kneading, and static compaction), and observed general consistency between the results of single and oedometer tests. Additionally several conclusions on the role played by the influencing parameters were drawn. Wetting-induced collapse was found to increase with decreasing values of relative compaction and compaction water content. For any test a stress level, termed "crossover pressure", above which collapse

is measured, was observed. With increased stress, the collapse strain was observed to increases up to a certain critical stress level, after which it decreased. Lawton (1986) this critical stress to the compactive prestress developed in the soil as a result of compaction and decreases as water content increases for a constant relative compaction. Testing under broader range of compaction conditions allowed Lawton (1986) to observe that no wetting induced collapse is observed in specimens compacted to the right of the line of optimum, regardless of the dry unit weight; and secondly, that there is a threshold value relative compaction above which little to no collapse will occur regardless of water content or degree of saturation.

Lawton et al. (1992) also provided a review of soil types susceptible to collapse, primarily focusing on the study of the effect of clay content on collapsibility by El Sohby and Rabbaa (1984). They observed that the greatest collapse potential was observed in correspondence to a critical clay content value, which was around 15% for silt-clay mixes, and 40% for sand-clay mixes.

Steadman (1987) followed the work of Lawton and highlighted the effect of the fines content on collapse potential. This work, which made use of laboratory fabricated soils with a predominant sand fraction, showed that for low fines contents (approx. 10%), the maximum collapse is small for all soils, but that for increasing percentages of fines, collapse increased substantially. The role played by the type of fines was also highlighted: soils containing equal parts of silt and clay were found to collapse more than the soil containing only clay or silt as the fine material. Further, soils containing only clay fines collapsed more than soils containing only silt fines.

Basma and Tuncer (1992) researched similar factors relating to collapse; they investigated the effect of initial dry unit weight and water content, then expanded the study to include the effects of soil type and the coefficient of uniformity, C_u. With regard to soil type, they found that a higher difference between percentage of sand and clay in the soil lowers the collapse potential at a specific stress level. Testing eight native soils from Jordan they develop a model for predicting collapse from the following properties: coefficient of uniformity, initial water content, compaction dry-unit weight, and pressure at wetting.

Alwail et al. (1994) further investigated the effect of clay fraction on collapse. These researchers created 25 soil combinations by preparing soils in the laboratory from the same sand, silt and clay materials. Their major finding was a linear relationship between maximum collapse and percentage of clay. These authors also observed that soils with a higher clay/silt ratio experienced greater magnitude of collapse than soils with a lower clay/silt ratio.

6.1.5 Experimental Work

The experimental work conducted for this research employed two loess samples. The first, referred to in this report as Soil A, was obtained in Washington, IN. This site is located in Daviess County, an area of the state characterized by the presence of medium to thick deposits of loess. The second sample, referred to as Soil B, was collected on the Purdue Agriculture Research farm in Tippecanoe County.

The two soils have significant similarities in that they have high silt content (~70%) and similar Atterberg limits. They are both classified as CL according to the USCS, and as A-6 according to AASHTO. Despite slight differences in sand (5.5% and 14% for soils A and B, respectively) and clay (25% and 13.5%, respectively) content, the particle size distributions for both soils fall within the region typical of clayey loess. Both soils are representative examples of loess typically found in Indiana.

The testing program conducted on the two soils included index tests (particle size analysis, Atterberg limits, and specific gravity determination), standard Proctor compaction tests, and an extensive program of double oedometer tests. The latter were conducted on specimens compacted at a variety of values of the relative compaction (from ~75% to close to optimum conditions), and of the water content (from 5–6% points on the dry side of optimum to optimum). The double oedometer tests provided data on the wetting induced collapse as a function of stress level (from 12.5 kPa to 2760). Based on these data the degree of collapsibility of each specimen was established using the criterion proposed in ASTM D5333, which is based on the collapse index I_c, the wetting induced strain under a surcharge of 200 kPa. The following are the main findings derived from this work:

Wetting induced collapse was observed in all but the one specimen of Soil B (B2) compacted at close to optimum conditions. For the other specimens the values of the collapse index varied from less than 1% (slight degree of collapsibility) to over 11% (severe degree of collapsibility).

The wetting induced collapse was found to increase with decreasing relative compaction, decreasing compaction water content and decreasing compaction degree of saturation. Significant wetting induced strains were observed even for specimens compacted at close to 88–96% RC, in the case of water contents significantly on the dry side of optimum.

For all compaction conditions the wetting induced strain was found to increase with stress level, reach a maximum value at a critical stress, and then decrease again. The lower the relative compaction, the lower the critical stress. In several specimens significant wetting induced strains were observed at relatively low stresses (25–100 kPa), indicating that wetting induced collapse may require consideration even for small fill thicknesses.

For Soil B a threshold value of the relative compaction of ~100% was identified above which wetting induced collapse was greatly reduced or eliminated, irrespective of the compaction water content (a similar threshold may be expected for Soil A). This value is greater than that reported for other soils in

the literature. Based on this result it is suggested that a minimum relative compaction of 105% be specified for the compaction of loess in the field.

Compaction on the wet side of optimum eliminates the issue of wetting induced collapse. However, the collapsibility of the soil is very sensitive to small reductions in compaction water content. It is suggested that compaction specifications for this soil do not allow for compaction at water contents lower than $w_{opt}-1.5\%$.

The behavioral trends observed in this study are generally consistent with the data presented in the literature. On the other hand, the measured values of the collapse strains greatly exceed previous data collected on loess from Indiana (Kim et al. 2008).

Existing criteria for estimating collapse potential do not completely capture the collapse behavior of the soils examined in this research. They may be used to gain an initial assessment of the degree of collapsibility of a soil but cannot be considered a substitute for laboratory determination of the collapse potential. The collapse prediction model developed by Basma et al. (1992) was found to significantly overestimate the collapsibility of soils A and B.

The double oedometer test is an effective method for measuring the collapse potential of compacted soils, and it is recommended that a battery of such tests be required whenever a loess soil is being considered for use in a fill or embankment.

6.2 Recommendations for Future Work

This research has focused on reviewing the literature on several topics relevant to the collapsibility of soils, in particular the characteristics, genesis, mineralogy and collapse mechanisms of loess, existing methods for measuring collapse potential of soils in the laboratory and the field, the collapse behavior of compacted soils, and the significance of loess deposits in Indiana. Additionally experimental work involving a series of double oedometer tests on compacted specimens was conducted. This work has led to the collection of high quality data on the collapse behavior of two soils representative of typical loess deposits existing in Indiana that may be used as a reference when utilizing similar soils for fills and embankments, recommendations for laboratory procedures to be employed for assessing the degree of collapsibility of a soil, and recommendations for compaction specifications to be used in the field.

The scope of the work has been ultimately limited by time and resource availability, and there are undoubtedly issues that would require further consideration. The recommendations for future studies can be summarized as follows:

(1) This research focused on two soils with relatively similar characteristics, in particular a silt content of approximately 70%, and clay % between 13 and 25%. Future work should extend the experimental program to a broader set of soil, evaluating for example the impact of smaller silt contents, and the presence of more plastic fines.

(2) This research was aimed at studying the wetting induced collapse behavior of compacted loess. Hence, the testing focused on specimens compacted on the dry side of optimum, and a lower bound threshold for the compaction water content was proposed. It is known, however, that compaction on the wet side of optimum can cause problems related to loss of shear strength and stiffness. Future work should include CBR and/or resilient modulus tests to establish water content compaction limits not only on the dry side but also on the wet side of optimum.

(3) This work has focused on assessments of the degree of collapsibility of compacted loess at the laboratory scale. Despite the value of these tests, the volume of soil tested, is necessarily small. Hence, future work should include field experimentation on large volumes of soil.

(4) From a scientific perspective the mechanisms responsible at the microscale for wetting induced collapse of soils are still not completely understood. Currently available microscopy techniques, including SEM's equipped with loading stages, and capable of controlling the relative humidity and temperature of the sample appear promising for gaining an increased understanding in this area

6.3 Recommendations for Implementation

The work performed as part of this research has established that wetting induced deformations in compacted loess can be significant under some compaction conditions, and thus that the concerns over the use of these soils in compacted fills and embankments may be justified when compaction is not adequately controlled and/or when subsurface wetting is not prevented.

It is also clear that the problem of wetting induced collapse involves many uncertainties related not only to the soil variability, but also to the source of wetting (e.g. surface or subsurface introduction, rising groundwater table) and to the primary source of driving stress (overburden, structural, or both). As a result, the consensus is that there it is impossible to "standardize" solutions in terms of mitigation measures of compaction specifications.

Based on the review of the existing literature on the topic, and the analysis of the experimental data collected on two soil samples considered representative of loess deposits found in the State of Indiana, it is recommended that the following be implemented when a loess soil is being considered for use in a fill or embankment:

a) a series of double oedometer tests should be prescribed on specimens compacted at conditions close to those expected in the field to establish the soil-specific risk for wetting induced collapse and define compaction specifications; the oedometer tests should involve loading to stress levels representative of the overburden stresses expected in the field and the quantification of the collapse potential should rely on ASTM D5533.

b) where soil specific laboratory data are not available, compaction specifications should require that: [i] the field relative compaction should always exceed 105–110% of the optimum value derived from standard Proctor tests; and [ii] that the compaction water contents should be no lower than $w_{opt}-1.5\%$, where w_{opt} is the optimum water content derived from standard Proctor tests.
c) avoidance or minimization of subsurface wetting should be considered the primary approach to mitigating the problem of wetting induced collapse and provisions for ensuring this should be included in project specifications;
d) given that the degree and depth of wetting can never be known with certainty, and that the source of wetting may also not necessarily be clear, a risk-based approach must be taken in addressing the problem of wetting induced collapse.

APPENDIX A
Summary of conversations with engineers and geologists from Illinois, Iowa, Kansas, Minnesota and Ohio

TABLE A.1
Summary of conversations with engineers and geologists from Illinois, Iowa, Kansas, Minnesota and Ohio

STATE:	CONTACT(S):	Q1: Experience with wetting-induced collapse in compacted loess	Q2: Tests/methods to assess potential for wetting induced collapse	Q3: Specifications adopted for loess in compacted fills/ embankments	Q4: Mitigation methods employed	Other notes:
Illinois	Riyad Wahab	no experience with problems due to post-construction wetting collapse	None	Field compaction moisture content restricted to 105 or 110% of OMC (not related to collapse concerns)	Not applicable	Placement of silt restricted within the embankment core, and capping with 2 ft minimum of cohesive material required
Iowa	Bob Stanley, Steve Megivern	Problems of wetting induced collapse not seen/recognized.	No specialized lab investigation for collapsible soils	No specialized soil specification for loess (w% within $\pm$2% of OMC)	Not applicable	Significant loess deposits (up to 100 thick) present in Iowa. Almost 100% silt in west of State.
Kansas	Bob Henthorne	Few problems (e.g. US 36 in North of State) due to underdrains not working; problems with loess of intermediate gradation	Some assessment based on particle size distribution	Some project specific specifications	Underdrain techniques (with varying success); different ditch and backslope designs to limit access of water	In some cases clay or lime added to loess to provide binding effect.
Minnesota	John Siekmeier, Chris Dulian, Rich Lamb	Knowledge of problem, but no direct experience observing these problems	None	None	Not applicable	Loess not recommended as an embankment material. Silt loams and silty clay loams (loess) not re-used due to constcutability issues (problems in drying when wet) which cause construction delays.
Ohio	Gene Geiger	No experience with use of loess in embankments. If used in fills, probably in minor amounts and mixed with other soil types.	Not applicable	Not applicable	Not applicable	Limited presence of loess in Ohio. Restricted to Cincinnati area and possibly near Lake Erie

REFERENCES

AASHTO Standard M 145, 2003: Classification of Soils and Soil-Aggregate Mixtures for Highway Construction Purposes, American Association of State Highway and Transportation Officials, Washington D.C.

ASTM Standard D-422, 2007: Standard Test Methods for Particle-Size Analysis of Soils, *Annual Book of ASTM Standards*, ASTM International, West Conshohocken, PA

ASTM Standard D-698, 2007: Standard Test Methods for Laboratory Compaction characteristics of Soil Using Standard Effort (12 400 ft-lbf/ft^3 (600 kN-m/m^3), *Annual Book of ASTM Standards*, ASTM International, West Conshohocken, PA

ASTM Standard D-854, 2010: Standard Test Methods for Liquid Limit, Plastic Limit, and Plasticity Index of Soils, *Annual Book of ASTM Standards*, ASTM International, West Conshohocken, PA

ASTM Standard D-2487, 2010: Standard Test Methods for Standard Practice for Classification of Soils for Engineering Purposes (Unified Soil Classification System), *Annual Book of ASTM Standards*, ASTM International, West Conshohocken, PA

ASTM Standard D-4318, 2010: Standard Test Methods for Liquid Limit, Plastic Limit, and Plasticity Index of Soils, *Annual Book of ASTM Standards*, ASTM International, West Conshohocken, PA

ASTM Standard D-5333, 2003: Standard Test Methods for Measurement of Collapse Potential of Soils, *Annual Book of ASTM Standards*, ASTM International, West Conshohocken, PA

Alwail, T. A., Ho, C. L., and Fragaszy, R. J. (1994). "Collapse mechanism of compacted clayey and silty sands." *Geotechnical Special Publication*, 2(40), 1435–1446.

Arthur Bettis, E., Muhs, D. R., Roberts, H. M., and Wintle, A. G. (2003). "Last Glacial loess in the conterminous USA." *Quaternary Science Reviews*, 22(18–19), 1907–1946.

Basma, A. A., and Tuncer, E. R. (1992). "Evaluation and control of collasible soils." *Journal of Geotechnical Engineering*, Vol.118(No. 10), 1491–1504.

Benites, L. A. (1968). "Geotechnical properties of the soils affected by piping near the Beson area, Cochise County, Arizona," University of Arizona, Tucson.

Bettis, A. E., Muhs, D. R., Roberts, H. M., and Wintle, A. G. (2003). "Last Glacial loess in the conterminous USA." *Quaternary Science Reviews*, 22(18–19), 1907–1946.

Bishop, A. W. (1959). "The principle of effective stress." *Lecture delivered in Oslo, Norway, in 1955, published in Teknisk Ukeblad*, 106(39), 859–863.

Booth, A. R. (1977). "Collapse settlement in compacted soils." *CSIR Research Report 324*, Council for Scientific and Industrial Research, Pretoria, South Africa.

Brink, A. B. A. (1985). "Engineering geology of South Africa." *Silverton: Building Publication*, 4.

Camp, M. J., and Richardson, G. T. (1999). *Roadside Geology of Indiana*, Mountain Press Publishing Company, Missoula, Montana.

Chen, Z. H., Lin, Z. G., Huang, X. F., Shao, S. J., and Yang, D. Q. (2007). *Loess from China*, Taylor and Francis Group, London.

Clemence, S. P., and Finbarr, A. O. (1981). "Design Considerations for collapsible soils." *Journal of the Geotechnical Engineering Division*, Vol.107(No, GT3), 305–317.

Clevenger, W. A. (1956). "Experiences with loess as foundation materials." *Journal of Soil Mechanics and Foundation Division*, 82(3), 1025–1025–26.

Das, B. M. (2007). *Principles of foundation engineering*, PWS publishing company, Boston, MA.

Denisov, N. Y. (1951). The engineering properties of loess and loess loams, Gosstroiizdat, Moscow.

Derbyshire, E. (2001). "Geological hazards in loess terrain, wth particular reference to the loess region of China." *Earth-Science Reviews*, 54, 231–260.

Derbyshire, E., and Mellors, T. W. (1988). "Geological and geotechnical characteristics of some loess and loessic soils from China and Britain: A comparison." *Engineering Geology*, 25(2–4), 135–175.

Dudley, J. H. (1970). "Review of Collapsing Soils." *Journal of Soil Mechanics and Foundation Division*, 96, 925–947.

Eden, D. N., and Hammond, A. P. (2003). "Dust accumulation in the New Zealand region since the last glacial maximum." *Quaternary Science Reviews*, 22(18–19), 2037–2052.

Egri, G. (1972). "The physico-chemical properties and engineering problems of the loess soils." *Acta Gelo. Acad, Sci. Hung.*, 16, 337–345.

El-Sohby, M. A., and Rabbaa, A. A. "Deformation behavior of unsaturated soil upon wetting." *Proceedings of Eighth Regional Conference for African on Soil Mechanics and Foundation Engineering*, Harare 129–137.

Evstatiev, D. "Design and treatments of loess basin in Bulgaria." Proceesings of the NATO Advanced Research Workshop on Genesis and Propertoes of Collapsible Soils, Loughborough, U.K., 413.

Feda, J. (1964). "Colloidal activity, shrinking and swelling of come clays." *Proceedings Soil Mechanics Seminar*, 531–546.

Galvão, T. C., Drnevich, V. P., and Schulze, D. G. (2003). "A Technique for Cutting Brittle Undisturbed Lateritic Soil Block Samples." *Environmental Monitoring and Assesment*, 84(1–2), 178–181.

Gibbs, H. J. (1961). "Properties which divide loess and dense uncemented soils." *Earth laboratory report EM-658*, Bureau of Reclamation, U.S. Department of the Interior, Washington D.C.

Grabowska-Olszewska, B. (1988). "Engineering-geological problems of loess in Poland." *Engineering Geology*, 25(2–4), 177–199.

Handy, R. L. (1973). "Collasible loess in Iowa." *Proceedings, Soil Science Society of America*, 37, 281–284.

Hester, N. C. (1997). "Quaternary Geological Map of Idiana, Miscellaneous Map 59." Indiana Geological Survey and Indiana University.

Hodek, R. J., and Lovell, C. W. (1979). "A new look at compaction processes in fills." *Bull., Association of Engrg. Geol.*, 16(4), 487–499.

Holtz, W. G., and Gibbs, H. J. (1956). "Engineering properties of expansive clays." *Trans. ASCE*, 121, 641–677.

Holtz, W. G., and Hilf, J. W. "Settlements of soil foundations due to saturation." *Proc. 5th Internation Conference on Soil Mechanics and Foundation Engineering*, 673–679.

Houston, S. L., and Houston, W.N. (1997). "Collapsible soils engineering."

Houston, S. L., Houston, W. N., and Lawrence, C. A. (2002). "Collapsible soil engineering in highway infrastructure development." *Journal of Transportation Engineering*, Vol. 128(No. 3), 295–300.

Houston, S. L., Houston, W.N., and Spadola, D.J. (1988). "Prediction of field collapse of soils due to wetting." *Journal of Geotechnical Engineering*, Vol. 114(No. 1), 40–58.

Houston, S. L., Houston, W.N., Zapata, C.E., and Lawrence, C. . (2001). "Geotechnical engineering practice for collapsible soils." *Geotechnical and Geotechnical Engineering*, 19, 333–355.

Huang, C. T. (1983). "Engineering soils map of Dubois County, Indiana." *JHRP-83-7*, Indiana Department of Highways and School of Civil Engineering Purdue University.

Huang, C. T. (1984). "Engineering soils map of Gibson County, Indiana." *JHRP-84-2*, Indiana Department of Highways and School of Civil Engineering Purdue University.

Jackson, P. D., Northmore, K. J., Entwisle, D. C., Gunn, D. A., Milodowski, A. E., Boardman, D. I., Zourmpakis, A., Rogers, C. D. F., Jedderson, I., and Dixon, N. (2006). "Eletrical resistivity monitoring of a collapsing meta-stable soils." *Quarterly Journal of Engineering Geology and Hydrogeology*(39), 151–172.

Jemings, J. E., and Knight, K. "A Guide to construction on or with materials exhibiting additional settlement due to collpase of grain structure." *Proceedings Sixth Regional Conference for Africa on Soils Mechanics and Foundation Engineering*, Druban, South Africa.

Johnson, G. L. (1988). "Engineering soils map of Knox County, Indiana." *JHRP-88-16*, Indiana Department of Highways and School of Civil Engineering Purdue University.

Jotisankasa, A. (2005). "Collapse behaviour of a compacted silty clay," University of London.

Jotisankasa, A., Ridley, A., and Coop, M. (2007). "Collapse behavior of compacted silty clay in suction-monitored oedometer apparatus." *Journal of Geotechnical and Geoenvironmental Engineering*, 133(7), 867–877.

Kim, D., Chung, Y., Siddiki, N. Z., Shin, Y., and Kim, J. R. (2008). "Mechanical characteristics of Indiana loess soils for highway embankments." TRB 2008 Annual Meeting.

Klukanova, A., and Frankovaska, J. "The Slovak carpathians loess sediments, their fabric and properties." *Proceesings of the NATO Advanced Research Workshop on Genesis and Propertoes of Collapsible Soils*, Loughborough, U.K., 413.

Kropp, A. L., McMahon, D. J., and Houston, S. L. (1994). "Case history of a collapsible soil fill." In Vertical and horizontal deformations of foundations and embankments, A. T. Yeung and G. Y. Felio, eds., ASCE Special Publication 40.

Lawton, E. C. (1986). "Wetting-induced collapse in compacted soil," Washington State University, Pullman, Washington.

Lawton, E. C., Fragaszy, R. J., and Hardcastle, J. H. (1989). "Collapse if compacted clayey sand." *Journal of Geotechnical Engineering*, Vol. 115(No. 9), 1252–1267.

Lawton, E. C., Fragaszy, R. J., and Hardcastle, J. H. (1991). "Stress Ratio Effects on Collapse of Compacted Clayey Sand." *Journal of Geotechnical Engineering*, 117(5), 714–730.

Lawton, E. C., Fragaszy, R. J., and Hetherington, M. D. (1992). "Review of Wetting-Induced Collapse in Compacted Soil." *Journal of Geotechnical Engineering*, 118(9), 1376–1394.

Lutenegger, A. J. (1988). "Determination of collapse potential of soils." *Geotechnical Testing Journal*, 11(3), 173–178.

Lutenegger, A. J., and Hallberg, G. R. (1988). "Stability of loess." *Engineering Geology*, 25(2–4), 247–261.

Mahmoud, H., Houston, W. N., and Houston, S. L. (1995). "Apparatus and procedure for an in-situ collapse test " *ASTM Geotechnical Testing Journal*, 121(4).

Miller, G. A., Muraleetharan, K. K., and Lim, Y. Y. (2001). "Wetting-induced settlement of compacted-fill embankments." *Transportation Research Record*, 1755, 111–118.

Mitchell, J. K., and Soga, K. (2005). *Fundamentals of soil behavior*, John Wiley & Sons, Hoboken, N.J.

Muhs, D. R., and Bettis III, E. A. (2000). "Geochemical variations in Peoria loess of western Iowa indicate Last Glacial Paleowinds of mid-continental North America." *Quarternary Research*, 53, 49–61.

Muhs, D. R., Bettis III, E. A., MacGeehin, J., and Been, J. M. (2001). "Impact of climate and parent material on chemical weathering in loess derived soils of the Mississippi River Valley." *Soil Science Society of America Journal*, 65, 1761–1777.

Okonkwo, I. O. (1986). "Engineering soils map of Martin County, Indiana." *JHRP-86-22*, Indiana Department of Highways and School of Civil Engineering Purdue University.

Osipov, V. I., and Sokolov, V. N. "Factors and mechanism of loess collapsibility." *Proceesings of the NATO Advanced Research Workshop on Genesis and Propertoes of Collapsible Soils*, Loughborough, U.K., 413.

Peck, R. B., and Ireland, H. O. (1958). "Discussion of experiences of loess as foundation material." *Trans. ASCE*, 123, 171–179.

Pereira, J. H. F., and Fredlund, D. G. (2000). "Volume change behavior of collapsible compacted gneiss soil." *Journal of Geotechnical and Geoenvironmental Engineering*, 126(10), 907–916.

Popescu, M. E. (1986). "A comparison between the behaviour of swelling and of collapsing soils." *Engineering Geology*, 23(2), 145–163.

Priklonski, V. A. (1952). *Gruntoedenia-Vtroarid Chast*, Gosgeolzdat, Moscow.

Purdue University, USDA, and Indiana Soil Conservation Service. (1977). "Indiana Soil Regions." AY (Purdue University Cooperative Extension Service).

Pye, K., and Johnson, R. (1988). "Stratigraphy, geochemistry, and thermoluminescence ages of Lower Mississippi Valley loess." *Earth Surface Processes and Landforms*, 13, 103–124.

Rogers, C. D. F. "Types and distribution of collapsible soils." Proceesings of the NATO Advanced Research Workshop on Genesis and Propertoes of Collapsible Soils, Loughborough, U.K., 413.

Rogers, C. D. F., Dijkstra, T. A., and Smalley, I. J. (1994). "Hydroconsolidation and subsidence of loess: Studies from China, Russia, North America and Europe : In memory of Jan Sajgalik." *Engineering Geology*, 37(2), 83–113.

Rollins, K. M., and Rogers, G.W. (1994). "Mitigation measures for small structures on collapsible alluvial soils." *Journal of Geotechnical Engineering*, Vol. 120(No. 9), 1533–1553.

Rollins, K. M., Rollins, R. L., Smith, T. D., and Beckwith, G. H. (1994). "Identification and characterization of collapsible gravels." *Journal of Geotechnical Engineering*, Vol. 120(No. 3), 528–542.

Ruhe, R. V. (1984). "Clay-mineral regions in Peoria loess, Mississippi River basin." *Journal of Geology*, 92, 339–343.

Smith, J., Vance, D., Kemp, R. A., Archer, C., Toms, P., King, M., and Zarate, M. (2003). "Isotopic constraints on the source of Argentinian loess - with implications for atmospheric circulation and the provenance of Antarctic dust during recent glacial maxima." *Earth and Planetary Science Letters*, 212(1–2), 181–196.

Steadman, L. (1987). "Collapse settlement in compacted soils of variable fines content," Washington State University.

Sultan, H. A. "Collapseing Soils." Proceedings Seventh International Conference on Soil Mechanics and Foundation Engineering, Seciality Session No. 5, Mexico City.
West, T., R. (1995). *Geology: Applied to Engineering*, Prentice Hall, Inc.
Yang, Y. (1989). "Study of mechanism of loess collapse." *Science in China (Ser. B)*, 32(5), 604–617.
Yeh, P. T. (1975). "Engineering soils map of Vanderburgh County, Indiana." *JHRP-75-7*, Indiana Department of Highways and School of Civil Engineering Purdue University.
Yeh, P. T. (1978). "Engineering soils map of Spencer County, Indiana." *JHRP-78-22*, Indiana Department of Highways and School of Civil Engineering Purdue University.
Yeh, P. T. (1979). "Engineering soils map of Warrick County, Indiana." *JHRP-79-20*, Indiana Department of Highways and School of Civil Engineering Purdue University.
Yeh, P. T. (1982). "Engineering soils map of Posey County, Indiana." *JHRP-82-6*, Indiana Department of Highways and School of Civil Engineering Purdue University.